2022

Investigating the role of NLRP3 inflammasome in chemotherapy-induced peripheral neuropathy

Urszula O. Warncke
Virginia Commonwealth University

INVESTIGATING THE ROLE OF NLRP3 INFLAMMASOME IN CHEMOTHERAPY-INDUCED PERIPHERAL NEUROPATHY

A dissertation submitted in partial fulfillment of the requirements for the degree of

Doctor of Philosophy at Virginia Commonwealth University

By

Urszula Osinska Warncke

Associate of Arts, 2010, Sinclair Community College

Bachelor of Science, 2012, Wright State University

Master of Science, 2015, Wright State University

Director: M. Imad Damaj, Ph.D.

Professor, Department of Pharmacology & Toxicology

Virginia Commonwealth University

Richmond, Virginia

August 2022

ACKNOWELDGEMENTS

This endeavor would not have been possible without Dr. M. Imad Damaj, professor and chair of my committee. I am thankful for the opportunity to become a member of his lab where, in addition to working with amazing young scientists, I was able to form life-time friendships. I also could not have undertaken this journey without my defense committee, who kindly provided knowledge, expertise, and generous support.

I would like to express my gratitude to the VCU C. Kenneth and Dianne Wright Center for Clinical and Translational Research for accepting me into their program, providing financial and moral support. I would like to extend my sincere thanks to the Department of Pharmacology and Toxicology and Dr. William Dewey for accepting me into their departmental family.

Lastly, I would be remiss in not mentioning my family and friends. I am extremely grateful to Kimberly Strong, my American mom, for helping me achieve so many milestones in my life, her mentoring and endless support. I am so thankful for having my husband Jared by my side, for his belief in me and motivation during this process. I had the pleasure of working with/collaborating with many great people who will forever be dear to my heart. I would also like to thank Zoey, Boo and Charlie; my furry friends for all their entertainment and emotional support.

TABLE OF CONTENTS

LIST OF TABLES

LIST OF FIGURES

CHAPTER TWO

CHAPTER THREE

LIST OF ABBREVIATIONS

ANOVA	Analysis of Variance
ASC	Apoptosis-Associated Speck-like Protein containing a CARD
ATP	Adenosine Triphosphate
AUC	Area Under the Curve
BBB	Blood Brain Barrier
BNB	Blood Nerve Barrier
CaMKII	Ca^{2+}/calmodulin Dependent Protein Kinase II
CARD	C-terminal Caspase Activation and Recruitment Domain
Casp-1	Caspase-1
CCI	Chronic Constriction Injury
CFA	Complete Freund's Adjuvant
CGRP	Calcitonin Gene Related Peptide
CIA	Collagen-Induced Arthritis
CIPN	Chemotherapy-Induced Peripheral Neuropathy
CNS	Central Nervous System
DAMP	Danger Associated Molecular Pattern
DEG d	Differentially Expressed Genes
DH	Dorsal Horn
DRG	Dorsal Root Ganglia
Ds	Desensitized Sensitive
FST	Forced Swim Test
g	Gram
GABA	Gamma-aminobutyric Acid
GSDM	Gasdermin D
HCNs	Hyperpolarization-Activated Channels
HO-1	Heme Oxygenase-1
i.p.	Intraperitoneally
Iba1	Ionized Calcium Binding Adaptor Molecule 1
IENFs	Intra-Epidermal Nerve Fibers
IHC	Immunohistochemistry
IL-1β	Interleukin-1β
IL-10	Interleukin-10
IL-18	Interleukin-18
IL-4	Interleukin-4
IL-6	Interleukin-6
Iκ-B	Inhibitor Kappa B
IP3R1	Inositol 1,4,5-trisphosphate Receptor 1
Jak-2	Janus Kinase-2
Kg	Kilogram
KO	Knockout
LDB	Light/Dark Box
LPA	Lysophosphatidic Acid
LRR	Leucine-rich Repeat Domain
MCP1	Monocyte Chemoattractant Protein-1

mg	Milligram
mPTP	Mitochondrial Permeability Transition Pore
NEK7	NIMA-related Kinase 7
NF- κB	Nuclear Factor-kappa B
NGF	Nerve Growth Factor
NLRP3	NACHT, LRR, and PYD domains-containing protein 3
NMDA	N-methyl-D-aspartate
NMDAR	*N*-methyl-D -aspartate receptor
NOD	Nucleotide-binding Oligomerization Domain
Nrf2	Nuclear Factor-Erythroid-2-Related Factor 2
NSCLC	Non–Small Cell Lung Cancer
OATP1B2	Organic Anion-Transporting Polypeptide 1B2
OCT	Optimum Cutting Temperature
OCT2	Organic Cation Transporter 2
OCTN1	Organic Cation/Carnitine Transporters
OIPN	Oxaliplatin-Induced Peripheral Neuropathy
Oxa	Oxaliplatin
Pac	Paclitaxel
PAM	Positive Allosteric Modulators
PAMP	Pathogen Associated Molecular Patterns
PBS	Phosphate-Buffered Saline
PDA	Dynamic Plantar Aesthesiometer
PE2	Prostaglandin E2
PGP 9.5	Protein Gene Product 9.5
PI3K	Phosphatidylinositol 3 Kinase
PIPN	Paclitaxel-Induced Peripheral Neuropathy
PKC	Protein Kinase C
PNS	Peripheral Nervous System
PPARα	Peroxisome Proliferator-Activated Receptor-alpha
PRR	Pattern Recognition Receptor
Pt (DACH)Cl_2	dichloro (1,2-diaminocyclohexane)platinum (II)
PYCARD	Apoptosis-Associated Speck-like Protein containing a CARD
ROS	Reactive Oxygen Species
SCI	Spinal Cord Injury
S1P	Sphingosine 1-Phosphate
TNFα	Tumor Necrosis Factor alpha
TLR	*Toll*-like receptor
TRPA1	Transient Receptor Potential Ankyrin 1
TRPM8	Transient Receptor Potential Melastatin 8
WT	Wildtype

STATEMENT OF CONTRIBUTIONS

Chapter 2

Experimental design was planned by Dr. M. Imad Damaj and Urszula Warncke. Breeding of NLRP3 and ASC mice was managed by Bryan McKiever, Jared Mann and Abigail Park. Dr. Wisam Toma performed selected von Frey tests. Urszula Warncke conducted data analyses and the remaining studies and wrote the manuscript. The completed manuscript was reviewed by Dr. M. Imad Damaj.

Chapter 3

Oxaliplatin-Induced Peripheral Neuropathy in Mice: Impact of Dose, Sex, and Strain on Sensory and Affective-like Behaviors was published in Frontiers in Pain Research on 22 July 2021. Study conceptualization, data curation and analysis, methodology, executions and supervision of experiments, and writing were performed by Urszula Warncke. Dr. Wisam Toma performed selected von Frey, cold acetone testing, assisted with study conceptualization, data curation and analysis, reviewed and edited the manuscript. Dr. Julie Meade assisted with study conceptualization, data curation and analysis, reviewed and edited the manuscript. Abigail Park and Danielle Thompson aided with data curation, performing behavioral assays, IENF immunohistochemistry, and manuscript editing. Dr. Martial Caillaud, Dr. John Bigbee, and Dr. Cameron Bryant assisted with formal analysis and writing (review and editing). Dr. M. Imad Damaj contributed in the conceptualization, formal analysis, funding acquisition, methodology, project administration, resources, supervision, and writing—review & editing. Breeding of NLRP3 and ASC mice was managed by Bryan McKiever, Jared Mann and Abigail Park. Mary Clare Kurtz, Madeline M. May, Alison N. Fowlkes, and Mackinsey J. Woods assisted in conducting behavioral

assays. This work was supported grants R01CA206028-01; R01 CA221260-01A1, and R01 CA219637 from The National Institutes of Health to MD. UW was supported, in part, by Virginia Commonwealth University's CTSA grant (UL1TR002649) from the National Institutes of Health's National Center for Advancing Translational Science and T32 DA007027 from NIDA. Microscopy was performed at the VCU Microscopy Facility, supported, in part, by funding from NIH-NCI Cancer Center Support Grant P30 CA016059. The remaining of chapter 3 was planned and conceptualized by Dr. M. Imad Damaj and Urszula Warncke. Data analysis, testing, and writing were done by Urszula Warncke.

ABSTRACT

INVESTIGATING THE ROLE OF NLRP3 INFLAMMASOME IN CHEMOTHERAPY-INDUCED PERIPHERAL NEUROPATHY

By Urszula Osinska Warncke, Ph.D.

A dissertation submitted in partial fulfillment of the requirements for the degree of Doctor of Philosophy at Virginia Commonwealth University.

Virginia Commonwealth University, 2022.

Director: M. Imad Damaj, Ph.D., Professor,
Department of Pharmacology and Toxicology

Paclitaxel and oxaliplatin are commonly used antineoplastic drugs that cause chemotherapy-induce peripheral neuropathy (CIPN) in up to 90% of patients. The sensory symptoms of CIPN include numbness, loss of proprioception, tingling, spontaneous burning, shooting or electric shock-like pain, mechanical and thermal allodynia, and cold hypersensitivity among others. Affected patients struggle with daily activities, have a low quality of life, and might stop cancer treatment. Unfortunately, there are no effective prophylactic or therapeutic treatments for these side effects. Many studies point to the involvement of inflammation as a major contributor of CIPN pathology. We investigated the effects of genetic (*NLRP3* KO and *ASC* KO) and pharmacological (JC124 compound) inhibitions of NLRP3 inflammasome activation in CIPN-associated sensory changes in mice treated with paclitaxel (Aim 1) and oxaliplatin (Aim 2). The findings of Aim 1 show involvement NLRP3 inflammasome activation and the potential of NLRP3 inflammasome inhibition as a pharmaceutical intervention in PIPN. We observed protective effects of NLRP3 inflammasome inhibition from induction of mechanical and cold hypertensives in NLRP3 KO, ASC KO and C57BL/6J treated with 8 mg/kg cumulative dose paclitaxel. Further subjecting of

NLRP3 KO mice to a second treatment of paclitaxel (16 mg/kg total) showed sex differences where male had a significantly deceased mechanical threshold. In contrast, both sexes of NLRP3 KO and JC124-co-treated C57BL/6J mice administered 16 mg/kg cumulative dose paclitaxel as one wave displayed a delayed onset of mechanical hypersensitivity. We also were able to observe elevated levels of IL-1β levels in spinal cords of mice treated with 32 mg/kg paclitaxel. In Aim 2, we investigated the role of NLRP3 inflammasome activation in oxaliplatin-induced peripheral neuropathy (OIPN). First, we characterized OIPN in two different strains of mice (C57BL/6J and Balb/cJ) treated with a low (3mg/kg cumulative) and high (30mg/kg cumulative) dose of oxaliplatin. We observed distinct dose-, sex-, strain-, and time-dependent differences. We utilized the low-dose schedule to assess the prophylactic approach to OIPN via inhibition of NLRP3 inflammasome activation measured by mechanical hypersensitivity. We were not able to observe any protection in NLRP3 KO mice, therefore further testing was halted. The results of these two aims suggest that, depending on the class of the chemotherapeutic agent, activation of NLRP3 inflammasome might play a distinct role in chemotherapy-induced peripheral neuropathy.

CHAPTER ONE

GENERAL INTRODUCTION

1.1. Chemotherapy-Induced Peripheral Neuropathy (CIPN)

The advancements in early diagnosis and improvement of antineoplastic drugs had led to an increase in cancer patients' survival rate in the last decade (Arnold et al., 2019). However, chemotherapeutics can induce many disabling and adverse effects, one of which is chemotherapy-induced peripheral neuropathy (CIPN) (Balayssac et al., 2011). There are several classes of chemotherapy agents available, including vinca alkaloids (vincristine, vinblastine), thalidomide, bortezomib, platinum compounds (cisplatin, carboplatin, oxaliplatin), and taxanes (paclitaxel, docetaxel). This dissertation work investigated the role of NLRP3 inflammasome in the initiation of CIPN employed two of the most commonly used antineoplastic drugs, paclitaxel and oxaliplatin.

1.1.1 Paclitaxel- and Oxaliplatin-Induced Peripheral Neuropathy: Disease Symptoms and Prevalence

Paclitaxel is an anticancer drug widely used as a first-line and adjuvant therapy for solid tumor malignancies of breasts, ovaries, prostate, stomach, head, and neck non-small-cell lung cancers (Roser Velasco & Bruna, 2015). Listed by the World Health Organization as one of the essential medications (World Health Organization, 2017). The main anticancer activity of paclitaxel derives from its binding to the N-terminal 31 amino acids of the beta-tubulin polymers leading to malformation of the mitotic spindle apparatus, chromosome segregation, and defective cell division (Rao et al., 1994). Stabilization of the microtubule polymerization interrupts axonal transport, which leads to cancer cell apoptosis (Wozniak et al., 2016). Other paclitaxel's tumor-suppressive mechanisms of action include increasing generation of nicotinamide adenine

dinucleotide phosphate via reactive oxygen species and increased levels of interleukin-10 via an immunomodulatory effect on type 2 helper T-cell (Th2) profile (Hadzic et al., 2010; Panis et al., 2012). In addition to involvement in cell division, microtubules act as scaffolding structures for molecular motor transport of nutrients and neurotransmitters and play an essential role in neuron outgrowth by directing the growth cone and filopodia (G. J. Bennett et al., 2011). Systemic administration of paclitaxel and rapid uptake of the drug by most tissues warrants its effects on a variety cells, such as peripheral nerves. However, only a very low level of paclitaxel was detected in spinal cord and other parts of the central nervous system after repeated administration, but a high concentration of paclitaxel was found in dorsal root ganglia (DRG), possibly due to the dense vascularization of the tissue by highly permeable capillaries (Cavaletti et al., 2000). The accumulation of paclitaxel in the peripheral nervous system imposes a greater risk for damage to these tissues. Notably, paclitaxel had been shown to cause changes in the axonal microtubules of sensory neurons resulting in disruption of intracellular calcium regulation, axonal transport, mitochondrial function, neuropeptide secretion, macrophage activation in dorsal root ganglia and peripheral nerves, and activation of microglial within the spinal cord (Amraoui et al., 2020; Bobylev et al., 2015; Ferrini et al., 2013; L. Li et al., 2019; Pease-Raissi et al., 2017; Peters et al., 2007).

Paclitaxel-induced peripheral neuropathy (PIPN) is a clinical manifestation of the drug's damage to the peripheral nerves. The first phase of PIPN can present itself within 4 days post-infusion as an acute muscle and joint pain syndrome: myalgia and arthralgia. Moreover, acute pain syndrome occurs in up to 70% of paclitaxel-treated patients and is predictive of developing debilitating chronic CIPN (Reeves et al., 2012; Saibil et al., 2010). The incident rate of CIPN among paclitaxel-treated patients continues to be as high as 87% (Banach et al., 2017). Sensory

symptoms of PIPN are primarily distributed in the feet and hands and present a characteristic "stocking and glove" neuropathy. These individuals experience numbness, loss of proprioception sense, tingling, spontaneous burning, shooting or electric school-like pain, mechanical and thermal allodynia that can persist for many years after cessation of the treatment (Park et al., 2013). Thus, the development of dose-dependent paclitaxel-induced comorbidities continues to severely affect patients' daily activities and quality of life (Argyriou et al., 2013).

Another frequently used antineoplastic agent is oxaliplatin. This third-generation platinum-based compound is used as a standard treatment for esophageal, liver, pancreatic, gastric, gastroesophageal, and colorectal cancers (Aschele et al., 2005; Dieras et al., 2002; Hall et al., 2019; Haller et al., 2011). Its tumor modulating properties arise from forming intra-strand and inter-strand cross-links with nuclear and mitochondrial DNA. The downstream effect of the alkylation results in cell apoptosis via halted DNA replication, RNA transcription, and altered mitochondrial functions (Canta et al., 2015; Ray et al., 2019; Riddell, 2018). Other notable changes include increased oxidative stress, activation of the immune system, and subsequent release of proinflammatory cytokines (Raymond et al., 1998; Tesniere et al., 2010). Like paclitaxel, the toxicity of oxaliplatin affects numerous types of cells and cell processes. Platinum compounds have been shown to accumulate in dorsal root ganglia and trigeminal ganglion neurons, causing selective loss of peripheral sensory axons and excitability of peripheral neurons (Kokotis et al., 2016; Zajaczkowską et al., 2019). Consequently, these changes manifest clinically as oxaliplatin-induced peripheral neuropathy (OIPN).

The incidence of OIPN varies between 65-98% of patients and is biphasic. The acute onset, frequently defined as transient, appears hours post-first infusion. It is predominantly characterized by cold hypersensitivity and resolves within a week (Gebremedhn et al., 2018). Other acute

symptoms may include cold-triggered paresthesia and dysesthesia, muscle fasciculation, and cramps. Repeated administration of the drug leads to chronic sensory neuropathy in 50-80% of patients, and is characterized by allodynia, numbness, sensory ataxia, and dysesthesia in the distal extremities and perioral regions (Kokotis et al., 2016; Park et al., 2011). Despite cessation of treatments, some patients report the development of new or progressive worsening of sensory symptoms, a phenomenon known as coasting (Staff et al., 2017). Neurological assessment of long-term outcomes shows that the severity of sensory impairments is significantly correlated with the cumulative dose of oxaliplatin. Moderate to severe neurotoxicity affects about 40% of patients more than two years after finishing their treatment (Park & Koltzenburg, 2012b).

1.1.2 Management of CIPN Symptoms in Patients

The possibility of developing CIPN increases with older age and in the presence of comorbidities such as diabetes, hypothyroidism, renal insufficiency, obesity, alcohol abuse, and preexisting neuropathy (Molassiotis et al., 2019). Moreover, the severity of chemotherapy-induced peripheral neuropathy is dependent on the class of antineoplastic agent, dosing schedule, and cumulative dose (Miaskowski et al., 2017). Patients receiving either paclitaxel or oxaliplatin are at an increased risk of suffering from debilitating side effects (Staff et al., 2017). Typical managements of symptoms focus on subduing neuropathic pain via pharmacological treatments such as antiepileptic agents, antidepressants, including selective serotonin and norepinephrine reuptake inhibitors (SNRIs), tricyclic antidepressants, a compounded topical gel containing baclofen amitriptyline HCL and ketamine, and opioids. Currently, no prophylactic measures are available for CIPN, while sensory symptoms treatments show low efficacy index. The American Society of Clinical Oncological (ASCO) Practice Guideline recommends duloxetine as the only drug for managing neuropathic pain (Hershman, Lacchetti, & Loprinzi, 2014). Duloxetine, a

serotonin-norepinephrine reuptake inhibitor, has proven mild efficacy in decreasing pain rating, and its adverse side effects lead to cessation of the treatment in 10-33% of CIPN patients (Hershman, Lacchetti, Dworkin, et al., 2014; Hirayama et al., 2015; Otake et al., 2015). Moreover, The ASCO reports reveal that the main medicines used for neurotoxic peripheral neuropathies are gabapentin and pregabalin, despite no clear evidence of their efficacy and the lack of ASCO recommendations (Gewandter et al., 2020; Selvy et al., 2021). Therefore, the search for alternative means of preventing and treating CIPN is ongoing.

1.2. Chemotherapy-Induced Peripheral Neuropathy (CIPN) in Animal Models

Although the precise cause of anticancer therapeutics-evoked peripheral neuropathy is yet to be elucidated, our current understanding of this disease's multifaceted nature comes from *in vitro* and *in vivo* studies. Animal models play a crucial role in predicting human response to therapeutics, studying disease pathogenesis, mechanisms, and potential treatments. Most pre-clinical CIPN studies employ rodents, such as rats and mice, in favor of their small size and easiness of handling, fast reproduction rates, and similarity to human pathology and physiology (Currie et al., 2019b; Radaelli et al., 2018). Many of these animal studies show neuropathological changes resembling those seen in human patients suffering from CIPN (Höke, 2012). Depending on the modulatory effects of antineoplastic drugs, clinical features associated with their neurotoxicity range from pure sensory to sensory-motor neuropathies (Argyriou et al., 2012). The outcome measures assess various symptoms associated with peripheral neuropathy, such as evoked and reflexive pain-like tests, sensory-motor coordination, sensory and motor nerve conduction, histological analyses; and affective-like behavioral changes (Bruna et al., 2020).

A systematic review of the literature indicates that the most commonly used strains of rats and mice were Sprague Dawley and C57BL/6, respectively. Heterogeneity of design factors such

as sex, species and sub-species, therapeutic intervention and dosing schedule, route of administration, and outcome measures account for the variability of results (Currie et al., 2019b). However, no substantial difference was observed between mice and rats in terms of clinical signs and histopathologic characteristics (Eldridge et al., 2020). In pre-clinical animal studies, systemic administration of anticancer drug predominates intraperitoneally (i.p.), and to a lesser degree, via an intravenous route, while in the clinic neurotoxic antineoplastic therapies are used intravenously (Bruna et al., 2020). The i.p. drug delivery is preferred because it is both safer for the animals and is a simpler method to learn for laboratory staff. Another difference between CIPN in patients and animal models is testing of the symptoms. Data from animal models usually represent the acute phase of the disease (Currie et al., 2019), whereas CIPN is commonly reported as a chronic condition in humans (Currie et al., 2019b; Hershman et al., 2011; Kidwell et al., 2012). Regarding dose equivalency, dose conversion factors show dosage relevance for both oxaliplatin and paclitaxel in animal studies. The highest recommended singe infusion of oxaliplatin and paclitaxel for patients is 110 mg/m^2 (2.97 mg/kg) and 157 mg/m^2 (4.73 mg/kg), respectively (Liston & Davis, 2017). The total human equivalent dose (THED) of antineoplastic agents varies between these rats and mice due to their differential species neurotoxic profiles. In terms of daily dosing, oxaliplatin dosing ranges 2-6 mg/kg/day, and total 2-16 mg/kg (0.32-2.6 mg/kg THED) in rats, while mice receive 0.04 -10.0 mg/kg/day or cumulative 3.0-30.0 mg/kg (0.24-2.4 mg/kg THED). Paclitaxel treatment varies 0.5-32 mg/kg/day, and the total dosage 8-80 mg/kg (1.3-12.9 mg/kg THED) in rats, while mice receive 2-18 mg/kg/day or cumulative 4-38.0 mg/kg (0.33-3.1 mg/kg THED) (Freireich et al., 1966; Polomano et al., 2001; U. S. Food and Drug Administration & Center for Drug Evaluation and Research, 2005).

1.2.1. Evaluation of CIPN Sensory, Electrophysiological, and Morphological Changes

Evaluation of chemotherapy-induced peripheral neuropathy in humans relies both on self-reported and objective measures (Yoshida et al., 2019). Notably, tools such as "CIPN20 quality-of-life measures", "Total Neuropathy Score clinical version", and "National Cancer Institute-Common Toxicity Criteria" are utilized by clinicians to determine the degree of sensory, autonomic and motor impairments (Cavaletti et al., 2013). Complete translatability of such tools into *in vivo* rodent models of neuropathy is hindered by anthropomorphic nature of reporting many of these symptoms. Therefore, preclinical CIPN studies rely mainly on evoked pain-like behaviors, such as mechanical, cold, and thermal hypersensitivities; where animals withdraw from nociceptive stimuli (Deuis et al., 2017).

Von Frey and the Randall-Selitto tests assess evoked nociceptive responses. The most common method for aversive behavior via a mechanical stimulation is using manual von Frey filament. Testing set up requires placement of animals in small elevated chambers with a mesh floor. Next, after rodent acclimated to the new environment, a monofilament is applied perpendicularly to the ventral side of the midplantar hind paw. Positive responses are counted when an animal briskly withdrawals, licks or shakes the affected paw when stimulated. There are three von Frey approaches to filament application and determination of mechanical sensitivity. The "up-down" von Frey method measures the mechanical force necessary to produce 50% withdrawal threshold. The initial filament corresponds to 50% of predicted withdrawal threshold. If a positive response is observed, the subsequent filament is lower, however, if no response is observed then the next filament would be higher. This approach continues until four sequential measurements are taken following the initial change in direction. The statistical formula used to calculate the LD_{50} can be found in *Dixon 1980* (Dixon, 1980). In the "ascending approach",

filaments are applied in sequence, with the sequence scaling from smallest force to largest force. If less than 2 responses are observed over 5 measurements, the next highest filament is applied. Depending on the predetermined acceptance criteria, if the observed response is between 20%-40% then the previous filament is designated as the threshold, and the testing is aborted (Minett et al., 2011; Scholz et al., 2005). The third von Frey method is the "percentages approach." Paws are probed with increasing force, and 5 to 10 measurements are taken per each filament. Upon completion of testing, results to be converted to a percent value. An automated version of the von Frey filaments is an electronic von Frey system, also known as Dynamic Plantar Aesthesiometer (DPA). The DPA automatically identifies and records latency time, and the force at the time of paw withdrawal. Unlike manual von Frey filament, the DPA utilizes a single rigid filament to elicit nocifensive response. Typically, 3-4 applications of a continual scale pressure suffice to determine mechanical threshold (Deuis et al., 2015). In the Randall-Selitto test, a clamp-like handheld tool with an internal cone-shaped probe is applied to an area on interest (paw, tail, etc.) while a rodent is restrained. An increasing mechanical pressure is administered until it results in pain-like responses via vocalization or withdrawal of the tested area (Randall & Selitto, 1957). While von Frey filament and Randal-Selitto offer measurement of mechanical threshold, the differences in applications and probe design might impact the type of receptor activation, low- and high-threshold mechanoreceptor in addition with nociceptor (Deuis et al., 2017).

Changes in temperature perception is common symptoms in CIPN patients, especially presence of cold allodynia in patients treated with oxaliplatin (N. Attal et al., 2009). Thus, investigating such alterations in animal models increases the translatability of pre-clinical studies. There are four approaches to evaluating cold-elicited noxious and innocuous behaviors in rodents. In the acetone evaporation procedure rodents are placed on elevated wire mesh and allowed

acclimation. A drop of acetone is applied to a plantar side of a paw by dabbing or spraying (Lindsey et al., 2000). Aversive responses can be recorded as the total reaction time, reaction latency recorded, or serenity of nocifensive behaviors (Brenner et al., 2012; Decosterd & Woolf, 2000). The innocuous evaporative temperature produced by acetone application fluctuates depending on ambient temperature and ranges between 15°C and 21°C (Colburn et al., 2007; Leith et al., 2010). Testing rodents' response to a noxious cold stimulus necessitates lower temperature. Introduced by Brenner et al., the cold plantar assay achieves cold simulation of plantar paw surface in 5°C to 12 °C range by placing a pellet of packed dry or wet ice against a glass platform. The time it takes for the paw to be withdrawn is recorded. Both the acetone evaporative test and the cold plantar assay allow for unilateral testing which enables comparison to contralateral side and reduces cold-stimulus associated animal distress. One of the fastest methods for evaluating behavioral reactions to both noxious and innocuous cold temperatures in rodents is the cold plate test. Nociceptive behaviors such as paw shaking or licking, guarding of an affected paw, and jumping are noted as either endpoints or the total response time in a given time interval (Deuis et al., 2013; Zimmermann et al., 2013). Cold plate assay protocols vary in terms of testing temperature which typically ranges from -5°C to 15°C, duration, and plate static or dynamic cooling program (Allchorne et al., 2005; Descoeur et al., 2011; Jasmin et al., 1998).

Thermal sensitivity alternations associated with anti-cancer therapeutics in rodents can be determined by numerous methods. Radiant heat assay, also known as Hargreaves test, utilizes infrared light as heat source which is delivered to a hind paw through a glass pane. The thermal emitter is linked to a timer that records response latency. The level of thermal emission and maximum exposure time can be adjusted to reflect typical response depending on the species and strain (Hargreaves et al., 1988). The hot plate test provides a broader assesses of heat-induced

nociceptive behavior by utilizes a Hot Plate Analgesia Meter. This method, first described by Eddy and Leimbach in 1953, simultaneous exposes all paws to a hot surface typically between 50°C and 56°C (Eddy & Leimbach, 1953). Aversive reactions include responses like licking and shaking of paws, and a flight response (jumping) from an open-ended animal enclosure (Langford & Mogil, 2008). Measuring nerve degeneration in rodents has been tested via changes to thermal sensitivity of the tail. In the tail-flick test, light beam is concentrated on the tip of a rodent's tail until animal presents pain-like response and withdraws its tail by a flick (D'amour & Smith, 1941).

An another functional sensory assay is the pinprick test. It allows for assessment of skin innervation though determining recovery of pain sensitivity in models of neuropathic pain. Like in von Frey test, awake animals are places on a mesh and allowed acclimation. A blunt needle is applied a few times to the skin of projection territory of the affected nerve. Graded positive responses are then summed up for each delimitated region (Cobianchi et al., 2014; X. Navarro et al., 1995). It is important to note that sensory algesimetry results are indicative of a reduced withdrawal threshold, and not directly of pain, which is a subjective sensation. Moreover, the major difference in assessing neuropathy outcomes between human and animal is loss and gain in sensory function.

While reflexive testing has become prevalent in research involving rodent CIPN models, other methods of assessment emerged. Electrophysiological tests are objective and clinically validated measures that quantify sensory and motor nerve activity in normal and diseased states. Thus, this test serves clinicians for diagnostic and therapeutic decision-making purposes via detection of severity and localization of the pathological changes to the axon or Schwann cells (Xavier Navarro & Udina, 2009). Application of this technique in peripheral neuropathy animal models enables correlation of discoveries in basic experimentations with clinical data. Hence,

rodent models of acquired and hereditary neuropathies are indispensable part of parsing out the mechanisms and development of therapeutic advances. The main sites for performing motor and sensory nerve conduction in rodents are the sciatic and caudal nerves, while stimulating saphenous, sural, and digital nerves provide solely sensory readings for the assessment of myelinated cutaneous afferent fibers. However, misdirected regenerated sensory nerve fibers connecting with motor nerve fibers might produce mix inflated compound nerve action potential (Brushart, 2011; Madison et al., 1996). Nerve conduction (NC) is recorded with electrophysiological systems composed of electrodes, an amplifier and stimulator connected to an oscilloscope or a computer (Gitter & Stolov, 1995; Liem et al., 1987). Such recordings can be obtained directly from an exposed or dissected nerve of interest by stimulation with short and incrementally increased intensity electrical pulses until a maximal response is recorded (Govbakh et al., 2019). A less invasive nerve conduction technique can be performed with subcutaneous insertion of needle electrodes in restrained anesthetized or awake animals (Osuchowski et al., 2009). Low-invasive electrophysiological assessments are preferred as they allow for longitudinal assessment of nerve changes (Xavier Navarro & Udina, 2009). As such, CIPN pre-clinical models revealed a significant decrease in sensory nerve action potential amplitude in mice treated with paclitaxel, bortezomib and cisplatin at mid and late time pointes, while the nerve conduction velocity (NCV) was augmented at middle time point in paclitaxel and cisplatin groups. Only cisplatin-treated mice showed continues reduction of NCV during late time point evaluation (Boehmerle et al., 2014).

Decreased nerve conduction velocity and amplitude can be attributed to morphological and structural alterations in myelin sheath and axonal compartments. Morphometric assessment of myelin sheath thickness, axonal nerve fiber count and perimeter, Wallerian degeneration and macrophage infiltration provide a more comprehensive insight into functional and morphological

changes in peripheral nerves pathological process of CIPN and the predominant cause of the neuropathy (Argyriou et al., 2012; Gómez et al., 1996). These changes can be observed by histopathological examination of tissues such as nerves of interest, typically sciatic nerve and its tributaries, or skin innervations; dorsal root ganglia, and spinal cord. Tissues can be preserved by cardiac perfusion, local immersion of tissues in fixatives, or embedding in freezing medium (Avraham et al., 2021; Kasukurthi et al., 2009; Sleigh et al., 2016). Microscopic examinations of sciatic nerve from mice showed reduction in the mean axon diameter post paclitaxel- and vincristine treatments and increase in bortezomib-treated animals. Moreover, cisplatin administration increased the mean g-ratio (the relationship between the inner axonal diameter to the total outer diameter) which is indicative of mild hypomyelination (Boehmerle et al., 2014). Other studies showed alterations in organelles of axons and Schwann cells such as loss of mitochondrial membrane, swelling and vacuolization of mitochondria suggesting mitochondrial dysfunction (Bruna et al., 2010; Sarah J.L. Flatters & Bennett, 2006; Imai et al., 2017; X. Wang et al., 2012).

The detrimental effect of chemotherapeutics on DRG shows drug class-specific outcomes. For instance, DRG derived from ixabepilone-treated mice showed morphologic alterations in perinuclear area and cytoplasm of satellite cells, such as cytoplasmic inclusions, vacuolization and swelling. While paclitaxel induced similar changes, proximal axons were also affected. In comparison, eribulin mesylate regimen caused mainly vacuolation of nerve cells (Wozniak et al., 2011). Additional measures of alteration caused by anticancer drugs include their effect on DRG neuron cell body, nuclear and nucleolar size and eccentricity, and changes to different functional populations of neurons (Barajon et al., 1996; Bruna et al., 2010; Joseph et al., 2008; Pover & Coggeshall, 1991). Lastly, immunohistochemical examination of skin innervation is a technique

used pre- and clinically (Lauria et al., 2010; X. Navarro et al., 1995). It utilizes staining of the pan-axonal marker protein gene product (PGP) 9.5 (also known as ubiquitin C-terminal hydrolase 1 or UCHL-1) to assess innervation of unmyelinated, small myelinated and the endings of large myelinated fibers of sensory and sympathetic neurons within the epidermis and dermis layers (Kennedy & Wendelschafer-Crabb, 1993). In rodent CIPN studies, PGP9.5 is used to quantifies the density of the unmyelinated intraepidermal nerve fibers (Eldridge et al., 2020; Warncke et al., 2021).

1.2.2. CIPN Behavioral Changes

Chemotherapy-induced peripheral neuropathy affects patients' somatosensory system, emotional and mental health. These negative health outcomes can often lead to disturbance of activities of daily living, depression, anxiety, sleep disorders, and memory and attention impairments (Mols et al., 2014). To mimic clinical manifestations of CIPN, researchers often use assays that approximate human emotional pain-associated responses in rodent models. Anxiety-like behaviors can be accessed via light/dark test, open field test and novelty suppressed feeding and open field test. A number of these assays was utilized throughout this dissertation work.

The light/dark box test exploits the innate conflict between the aversion to brightly lighted areas and spontaneous exploratory activity. The expected response of normal control animals is to explore the light compartment for longer period (Crawley & Goodwin, 1980). The novelty suppressed feeding test assesses a rodent's aversion to eating in a novel environment which can be a new cage placed under a bright light (Bodnoff et al., 1988). The open field test also integrates rodents' aversions to large, brightly lit, open and unfamiliar environments (Choleris et al., 2001; Seibenhener & Wooten, 2015).

For depressive-like behaviors in mice, researchers utilize a forced swim test. For instance, Toma et al (2017) assessed mice for immobility as a sign of anxiety in water during the last 4 minutes of a 6-minutes water immersion (Toma et al., 2017a). Immobility was counted when an upright floating positioned mouse made small movements to keep its head above water and did not cause water displacements. Anhedonia, a major symptom of clinical depression can be measured in mice via the wheel running and sucrose drinking tests (Cooper et al., 2018; Thompson & Grant, 1971). Lastly, the nesting procedure approximates activities of daily living (Negus et al., 2015; Niu et al., 2021). The last three assays are described in more detail in chapter 3.

1.2.3. Potential Mechanisms of Paclitaxel- and Oxaliplatin-Induced Peripheral Neuropathy

Morphometric studies of central and peripheral nervous systems show a verity of abnormalities induced by chemotherapies. Although oxaliplatin and paclitaxel belong to different classes of antineoplastic drugs, there are many common potential pathways attributing to development of CIPN phenotypes resulting from these treatments (Yamamoto & Egashira, 2021). Oxaliplatin's distinctive cold hypersensitivity is caused by its metabolite oxalate, while the anticancer properties are attributed to dichloro (1,2-diaminocyclohexane)platinum (II) (Pt (DACH)Cl_2). Oxaliplatin-induced peripheral neuropathy (OIPN) stems from neurodegeneration, oxidative stress, and altered expression level and/or function of ion channels (Sakurai et al., 2009). Paclitaxel, a microtubule targeting agent prevents proper formation of the mitotic spindle assembly which leads to arresting cancer cells at the G2-M phase of the cell cycle (Jordan et al., 1993; Yvon et al., 1999). The therapeutics agent disrupts axonal morphology, ion channels functions, and evokes inflammatory events. Together, the principal neurotoxic events shared between oxaliplatin and paclitaxel are (1) mitotoxicity, (2) functional impairments of ion channels, (3) triggered

immunological mechanisms via activation of satellite glial cells (Eldridge et al., 2020; Ferrier et al., 2013; Grisold et al., 2012; Park et al., 2013).

Paclitaxel has been shown to cause prominent abnormalities in axonal mitochondria, and release calcium by opening the mitochondrial permeability transition pore (mPTP) (Eldridge et al., 2020; Kidd et al., 2002). Increased levels of reactive oxidant such as peroxynitrite have been long implicated in PIPN pathogenesis. Increased peroxynitrite production is mediated by two mechanisms. The first involves activating nitric oxide synthase and NADPH oxidase to create the precursors of peroxynitrite, nitric oxide and superoxide. The second mechanism includes inactivating manganese superoxide dismutase, a catalytic enzyme which degrades peroxynitrite (Salvemini et al., 2012). The number of swollen and vacuolated mitochondria of A- and C-primary afferent sensory nerve fibers were considerably increased in paclitaxel-treated than control rats, 37.3 and 152%, respectively (W. H. Xiao et al., 2011). Moreover, paclitaxel indirectly causes sensitization of TRVP1 ion channels in DRG primary sensory neurons via increasing levels of 9,10-epoxy-12Z-octadecenoic acid and expression of the cytochrome-P450-epoxygenase CYP2J6. This further leads to sensitization of TRPV1 ion channels and elevated frequency of spontaneous excitatory postsynaptic currents in spinal cord manifested as mechanical and thermal hypersensitivity (Sisignano et al., 2016). Voltage gated T-type Ca^{2+}, Nav1.7, TRP vanilloid 4 and transient receptor potential ankyrin 1 channels have been also implicated in PIPN pathophysiology (Alessandri-Haber et al., 2004; Boehmerle et al., 2018; Y. Chen et al., 2011; Costa et al., 2018; Hara et al., 2013). Genetic and pharmacological inhibition of organic anion-transporting polypeptide 1B2 (OATP1B2) protects mice from developing sensory hypersensitivity, hence it is highly spectated that accumulation of paclitaxel in mouse DRG occurs (Leblanc et al., 2018). Uptake of paclitaxel in DRG sensory neurons induces dephosphorylation of axonal inositol 1,4,5-

trisphosphate receptor 1 (IP3R1) which in turn disrupts Ca^{2+} signaling and causing activation of calpain proteases (Pease-Raissi et al., 2017).

Neuroinflammation plays an important role in CIPN. In the peripheral nervous system, satellite glial cells (SGC) coupling was increased two-fold in DRG dissected from paclitaxel-treated rats (Warwick & Hanani, 2013). In addition, chronic pain state and decreasing pain threshold are associated with inflammatory cytokines such as tumor necrosis factor-α (TNF- α), interleukin-1β, IL-17 and/or other cytokines and glial transmitters released by paclitaxel-activated macrophages and SGC (Ledeboer et al., 2007; H. Luo et al., 2019; Peters et al., 2007). As noted earlier, morphological changers due to paclitaxel treatment were observed in Schwann cells of sciatic nerve. Imani et al proposed disruption in communication and dedifferentiation of Schwann cells into immature state as a potential mechanism of CIPN (Imai et al., 2017).

Elevation of pro-inflammatory cytokines and chemokines was observed in spinal dorsal horn presenting involvement of the central nervous system (CNS) in development and maintenance CIPN. Paclitaxel's limited ability to cross the blood-brain barriers suggests its indirect involvement in the spinal cord observed changes. Two mechanisms that provide an explanation of this phenomenon are activation of microglia and astrocytes within lamina III–IV of the lumbar spinal cord through degeneration of central terminals of injured primary afferent fibers or release of factors from injured neurons (Glantz et al., 1995; Watkins et al., 2001). Other mediators implicated in biomolecular signaling pathway of paclitaxel-induced peripheral neuropathy include lysophosphatidic acid (LPA) and sphingosine 1-phosphate (S1P) through LPA_1/LPA_3 and $S1PR_1$ receptors, respectively (Uchida et al., 2014). The proposed neuroinflammatory pathway of ceramide and S1P formation in the spinal dorsal horn of S1P receptor subtype 1 encompass activation of NFκB, ERK and p38, and pro-inflammatory and

neuroexcitatory cytokines such as TNF-α and IL-1β (Janes et al., 2014). Taken together, the complexity of PIPN induction and maintenance derives from a multitude of key neuroinflammatory and neuroexcitatory mechanisms.

Accumulation of Pt and oxaliplatin occurs via organic cation transporter 2 (OCT2) and organic cation/carnitine transporters OCTN1 and OCTN2 (Sprowl et al., 2013). Oxaliplatin-derived Pt in DRG results in functional deficit of mitochondria, induces oxidative stress, and activation of nuclear factor-erythroid-2-related factor 2 (Nrf2) signaling, which plays a crucial role in mitochondrial function (Wen Hua Xiao & Bennett, 2012; Yang et al., 2018). Moreover, sciatic nerve mitochondria respiratory chain complex I/II show reduced activity evident by decreased O_2 consumption and ATP production, increased lipid peroxidation, carbonylated proteins and DNA oxidation (Di Cesare Mannelli et al., 2012; Huaien Zheng et al., 2011). Hypomyelination observed in in the sciatic nerve of oxaliplatin treated animals is possibly linked to changes in the miR-15b, β-secretase 1, and cleaved neuregulin 1 pathways (Kawashiri et al., 2012). Oxalate, a labile oxalate ligand leaving group, chelates extracellular Ca^{2+} ions causing an increase in sodium conductance, neuronal depolarization and hyperexcitability (Deuis et al., 2013). Like paclitaxel, oxaliplatin treatment was shown to upregulate expression of transient receptor potential melastatin 8 (TRPM8) and transient receptor potential ankyrin 1 (TRPA1) via a nuclear factor of activated T-cell (NFAT)-dependent mechanism and inhibition of prolyl hydroxylase, respectively (Kawashiri et al., 2012; Nassini et al., 2011) TRPA1 is a polymodal cold and pain nociceptor. Hydroxylation of the N-terminal ankyrin repeat of TRPA1 and acidification of cytosolic milieu through ROS leads to increased sensitivity of the channel in dorsal root ganglia neurons (Miyake et al., 2016). Moreover, oxaliplatin reduces expression of TREK1 and TRAAK potassium channels and

increases the expression of hyperpolarization-activated channels (HCNs) leading to nociceptor over-excitability (Descoeur et al., 2011; Resta et al., 2018; Riva et al., 2018).

The main mechanism of oxaliplatin-induced peripheral neuropathy is Pt-induced ROS generation which caused cellular dysregulation (Hu et al., 2021). Notably, platination of nuclear and mitochondrial DNA, and production of ROS in DRG are attributed to mitochondrial respiratory chain complex I-III dysfunction, imbalance of endogenous ROS and cellular antioxidant system, and efflux of mitochondrial Ca^{2+} to cytosol (Agnes et al., 2021; Leo et al., 2020). Activation of inositol 1,4,5-trisphosphate receptors (IP3R) by ROS opens the permeability transition pore which leads to release of Ca^{2+}. Altered permeability of mitochondria causes further release more ROS (Csordás & Hajnóczky, 2009; Kiselyov & Muallem, 2016). Like paclitaxel, oxaliplatin has limited permeability across the blood-brain barrier (BBB). Nonetheless, central nervous system dysfunctions have been reported. In the spinal cord, oxaliplatin-induced expression and activation of *N*-methyl-d-aspartate receptor (NMDAR) leads to phosphorylation of Ca^{2+}/calmodulin dependent protein kinase II (CaMKII) (Mihara et al., 2011; Shirahama et al., 2012). CaMKII activation in the spinal cord might contribute to the development of oxaliplatin-induced CIPN persistent pain and inflammation (Dai et al., 2005; F. Luo et al., 2008; Yamamoto et al., 2017). Neuroinflammation has been implicated in many types of neuropathy, hence any disruption in the homeostasis between neuronal and glial cells might contribute to CIPN symptoms (Myers et al., 2006). Indeed, Janes K et al reported that rats-treated with oxaliplatin presented mechano-hypersensitivity which was associated with the hyperactivation of astrocytes, elevated pro-inflammatory TNF and IL-1β, and reduced anti-inflammatory/neuroprotective cytokines IL-10 and IL-4 in the dorsal horn of the spinal cord (Janes et al., 2015).

1.3. NLRP3 Inflammasome

1.3.1. Overview of NLRP3 Inflammasome: Structure and Function

The term inflammasome was coined nearly 20 years ago. It encompasses a family of inducible high molecular protein complexes involved in the proteolytic maturation of proinflammatory cytokines (Martinon et al., 2002). As a key component of the innate immune system, inflammasomes play an integral role in response to pathogens or noxious stimuli. Upon stimulation, heterogeneous groups of the protein complex assemble in the cytosol and serve as a platform to activate proinflammatory proteases: caspase-1, caspase-8, caspase-11 (in mice) and caspase-4/5 (in humans) (Heilig & Broz, 2018; Rathinam & Fitzgerald, 2016). Congregation of inflammasome complexes is contingent on cytosolic sensing of pathogen-associated molecular patterns (PAMP) and endogenous danger-associated molecular patterns (DAMP). Activation via DAMPs occurs in a sterile environment due to release of danger signals from damaged or dying cells (Latz et al., 2013). Some inflammasomes detect these patterns indirectly by changes in the cell's homeostatic environment, while others identify these patterns directly. The immune system's ability to initiate antimicrobial and inflammatory responses while preventing overt tissue damage depends on highly regulated assembly and signaling. Therefore, as it might be expected, there are several receptor proteins confirmed to assemble inflammasomes, including the nucleotide-binding oligomerization domain (NOD), leucine-rich repeat (LRR)-containing protein (NLR) family members (NLRP1, NLRP3, and NLRC4); the proteins absent in melanoma 2 (AIM2), and Pyrin (Broz & Dixit, 2016). Other less established pattern recognition receptors that promote caspase-1 activation include NLRP6, NLRP7, NLRP12, retinoic acid-inducible gene I (RIG-I), and interferon-inducible protein 16 (IFI16) (Broz & Monack, 2013; Vladimer et al., 2013).

The NLRP3 inflammasome is a macromolecular assembly of NLRP3, ASC, and Caspase-1 proteins. NLRP3 contains N-terminal pyrin domain (PYD), a central NACHT, and a C-terminal leucine-rich region (LRR). NACHT domain is composed of four subdomains NLP family apoptosis inhibitor protein (NAIP), class II major histocompatibility complex transactivator (CIITA), heterokaryon incompatibility protein from Podospora anserinea (HET-E) and telomerase protein component 1 (Koonin & Aravind, 2000). The NACHT domain possesses ATPase activity through which the NLPR3 protein self-associate (Duncan et al., 2007). The PYD domain is composed of six anti-parallel helices with a central hydrophobic core, and five connecting loops (Bae & Park, 2011). The hydrophobic interaction of NLRP3-PYD domain with ASC-PYD domain initiates inflammasome oligomerization (Oroz et al., 2016). The LLR domain partakes in recognition of stimuli and oligomerization of the NLRP3 inflammasome (Martinon, 2008). ASC is an adaptor protein composed of containing an N-terminal PYD and a C-terminal caspase activation and recruitment domain (CARD). NALP3 and Caspase-1 are associate by the CARD domains of each unit (Bae & Park, 2011; Shiohara et al., 2002). Caspase-1 is present in cytosol as procaspase-1 which contains pro-domain CARD and a catalytic domain made of p20 and p10 subunits. Formation of the inflammasome complex is required for proximity-induced autoproteolytic activation of procaspase-1 to yield active caspase-1 (Schroder & Tschopp, 2010). Experiments showed that the spatial distribution of each of the inflammasome components differs such that NLRP3 is associated with the endoplasmic reticulum, ASC is expressed in in the nucleus of epithelial and immune cells and redistributed to the cytoplasm upon stimulation; and pro-caspase-1 is typically found in the cytosol but traffics extensively to numerous intracellular organelles including mitochondria, nucleus, and extracellular space (Misawa et al., 2013; Luqiao Wang et al., 2016; R. Zhou et al., 2011). The proposed cellular site of NLRP3 and ASC interaction

is the mitochondria-associated endoplasmic reticulum membrane structure, however it might be cell specific.

Activation of the NLRP3 inflammasome is a tightly orchestrated system that occurs on a transcriptional, post-translational, and structural level (Bauernfeind et al., 2009; Juliana et al., 2012). It involves processes such as ubiquitination, deubiquitination, phosphorylation, dephosphorylation, sumoylation, and desumoylation (Seok et al., 2021). For instance, dephosphorylation and deubiquitination of NLRP3 LRR domain by PTPN22 and BRCC3, respectively, are required for the inflammasome assembly and activation (Py et al., 2013; Spalinger et al., 2016). Moreover, binding between NIMA-related kinase 7 (NEK7) and NLRP3 via interaction of NEK7 C-lobe interact with the LRR and NACHT domains positively regulates activation of the inflammasome (Niu et al., 2021). The pattern recognition receptor NLRP3 can be activated by numerous molecular stimuli such as lipopolysaccharide, bacteria-derived nucleic acids, pore-forming bacterial toxins, extracellular ATP, potassium efflux, ROS, lysosomal damage, and various metabolic crystals, lethal toxins, flagellin/rod proteins, muramyl dipeptide (MDP), M2 protein, virus-derived RNA or DNA, fungus-derived β-glucans, hypha mannan, zymosan, and protozoon-derived, self-derived glucose; β-amyloid, hyaluronan, cholesterol crystals, monosodium urate (MSU) crystals, calcium pyrophosphate dihydrate (CPPD) crystals, environment-derived alum, asbestos, silica, alloy particles, UV radiation, and skin irritants (Davis et al., 2011). The non-specificity of the receptor suggests an indirect activation of the inflammasome (Kelley et al., 2019). Depending on the DAMP or PAMP, one of the three NLRP3 inflammasome activation pathways can occur: canonical (classical), non-canonical, and alternative (Li Wang & Hauenstein, 2020).

The canonical pathway is a two-step process that requires priming and activation. During the priming event, pattern recognition receptors become activated by signaling molecules such as cytokines DAMPs or PAMPs. This leads to the transcriptional upregulation of NLRP3 and pro-IL-1β and via activation of nuclear factor-κB (Bauernfeind et al., 2009). For instance, binding of lipopolysaccharide to *Toll*-like receptor (TLR) 4 triggers stabilization of hypoxia-inducible factor 1α (HIF1α) and an increase in *IL1B* gene transcription in mouse macrophages. Moreover, caspase-8 and FADD (Fas-associated protein with death domain) are required for induction of NLRP3 of the priming step. The interaction between Caspase-8 with the IKK complex is an essential to NF-κB activation, induction of NF-κB transcription and translocation (Lemmers et al., 2007). Secondly, priming involves post-translational modifications of NLRP3. MyD88-IRAK4-IRAK1 signaling axis was required for early TLR and NLRP3 signal dependent inflammasome activation (Fernandes-Alnemri et al., 2013). In addition to dephosphorylation, the LRR domain undergoes ubiquitination by Pellino2 as a part of NLRP3 priming (Humphries et al., 2018).

In the second step of the canonical pathway, NLRP3 recruits ASC and procaspase-1, which results in caspase-1 activation and processing of cytoplasmic targets, including the pro-inflammatory cytokines IL-1β and IL-18. The activation signals include extracellular ATP, pore-forming toxins, viral RNA, and particulate matter, phosphatidylinositol-4-phosphate, ROS, and cathepsins (Kelley et al., 2019). Oligomerization of NLRP3 is mediated through NEK7 interaction with LRR and NACHT domains, and homotypic interactions between NACHT domains (He, Zeng, et al., 2016). Formed NLRP3 oligomers recruit ASC through PYD-PYD interactions which results in nucleation of helical ASC filaments known as an ASC speck (A. Lu et al., 2014; Schmidt et al., 2016). The organized ASC scaffold recruits pro-caspase-1 via CARD-CARD interactions allowing for heterodimerization, self-cleavage and activation of caspase-1 (Li Wang &

Hauenstein, 2020). Active caspase-1 converts pro-IL-1B and pro-IL-18 into their bioactive cytokine forms and cleaves gasdermin D (GsdmD) into two N- and C-terminal halves. The membrane pores created by GsdmDNterm are involved in cytokine secretion and facilitate cell-death by pyroptosis (Dinarello, 2009; Yang et al., 2018).

The non-canonical activation does not require the priming step. It was proposed that the non-canonical activation of NLRP3 inflammasome is triggered by cytosolic sensing of lipopolysaccharides (LPS) independently of TLR4 (Kayagaki et al., 2013). Murine caspase-11 (human orthologs caspase-4/5) receptor senses LPS via CARD domain causing oligomerization and activation of the caspases (Kayagaki et al., 2011). Oligomerized murine caspasep-11 or human caspase-4/5 cleaves GsdmD allowing for formation of GsdmD membrane pores which leads to potassium efflux and subsequently the autocrine activation of the NLRP3 inflammasome. This event leads to release of bioactive IL-1 β and IL-18, and pyroptosis (Kayagaki et al., 2015; Shi et al., 2014). The alternative pathway was observed in human and porcine monocytes, and murine bone marrow–derived and splenic dendritic cells (Gaidt et al., 2016; He, Hara, et al., 2016). It is suggested that LPS activates the priming step through TLR4-MyD88 pathway causing production of NLPR3 and pro-IL-1β. Additionally, LPS-stimulated TLR4 causes activation of NLRP3 inflammasome through RIP1-FADD-caspase-8 pathway without changes to K^+ and ATP concentrations. Although the TLR4 ligands-stimulated cells secreted nature pro-inflammatory cytokines it occurred without formation of ASC speck.

1.3.2. Role of NLRP3 Inflammasome in the Neuroinflammation, Pain and Neuropathy

IL-1β and IL-18, the products of NLRP3 inflammasome activation, play crucial roles in the CNS and may contribute to neuronal injury and cell death, such that several cell types in the brain

express their cognate receptors (Allan et al., 2005). Likewise, expression of the inflammasome components was observed in microglia, perivascular CNS macrophages, neurons, astrocytes, oligodendrocytes, and endothelial cells (Freeman et al., 2017; Gong et al., 2018; Kawana et al., 2013; McKenzie et al., 2018). IL-1β induces the proliferation, activation, and differentiation of immune cells and facilitates phagocytosis, degranulation, and oxidative burst activity, while IL-18 is an inducer of IFN-γ and is involved in the activation and differentiation of various T-cell populations (Ghayur et al., 1997; P. Li et al., 1995; A. Lu et al., 2016). Chronic inflammatory state induced by pro-longed inflammasomes activation leads to neuronal dysfunction and eventually neurodegeneration, a condition reported in traumatic brain injury and stroke, autoimmune-mediated injury multiple sclerosis (MS), Alzheimer's disease, amyotrophic lateral sclerosis, Parkinson's disease, and prion disease (Voet et al., 2019).

The role of inflammasomes activation in MS is evident in elevated expression of caspase-1, IL-18, and IL-1β; and increased ATP and uric acid (inflammasome activating DAMPs) in peripheral blood mononuclear cells and cerebrospinal fluid of patients affected by the disease (Inoue & Shinohara, 2013; Mamik & Power, 2017). Although microglia are involved in phagocytic removal of Aβ deposits, accumulation of this NLRP3 inflammasome inducer promotes production of IL-1 β and IL-18 (Sarlus & Heneka, 2017). The inflammatory environment attributed in part to microgliosis can also influence other CNS cells, cause synaptic dysfunction, and neuronal damage (Voet et al., 2019). Moreover, released IL-1β exerts its action on spinal neurons and astrocytes. Microglia are a major source of inflammasomes of the brain-resident immune cells. Scattered throughout the brain, microglia continuously survey the brain parenchyma for pathogens, debris. Moreover, they initiate immune responses, secrete inflammatory mediators, control of brain ion homeostasis (calcium) and growth factor supply (insulin-like growth factor-1) promoting nerve

cell functionality; regulating neural networks by synapse elimination or stabilization, thereby ensuring neuronal survival within such networks, vascularization, and myelination (Graeber, 2010; Q. Li & Barres, 2018; Nimmerjahn et al., 2005). When activated, microglial cells interact with neurons, astrocytes and endothelial cells, form an inflammatory network via soluble factors and cell-to-cell contact which can lead to prompting initial inflammatory responses, recruitment of other inflammatory cells, opening of the blood-brain barrier, and invasion of peripheral immune cells (Spittau, 2017; Streit, 2002). For instance, the mechanism of multiple sclerosis incorporates compromised BBB and infiltration of microglia, astrocytes and peripheral immune cells promoting chronic inflammatory response that lead to inflammation, demyelination, and neurodegeneration (Baecher-Allan et al., 2018).

The cross-talk of microglia, astrocytes, presynaptic (glutamatergic) terminal, and postsynaptic terminal forms the quad-synapse. Both immune cells respond to extracellular glutamate, while astrocytes release calcium-wave-driven ATP and activation of purinergic receptors (e.g. P2Y12 and P2Y6) of microglia (Macht, 2016). Glutamate is an important excitatory neurotransmitter involved in induction and the maintenance of central sensitization of the pain pathway. High concentrations of the neurotransmitter are toxic and disruption of the glutamate pathway is linked to chronic pain (Latremoliere & Woolf, 2009). Astrocytes are involved in maintaining proper concentration of glutamate by converting it to glutamine and shuttling it back to neurons (Chung et al., 2015).

Resulting from a tissue injury, acute pain sensitivity in the peripheral nervous systems could evolve to a persistent and irreversible pathological pain such as neuropathy. Interestingly, primary nociceptors are involved in acute and chronic pain conditions. Central sensitization refers to a pathological state of increased responsiveness of spinal cord pain-transmission neurons and an

activity in non-nociceptive primary sensory fibers. Whereas, peripheral sensitization results from lowering of nociceptor activation thresholds due to products of local tissue damage and inflammation such as prostaglandins, TNF-α, IL-1β, and nerve growth factor (Julius & Basbaum, 2001). Evidence suggests that IL-1β, one of the end products of NLRP3 inflammasome activation, modulates the faction of neuronal receptors and ion channels transient such as receptor potential and voltage-gated channels, N-methyl-D-aspartate and gamma-aminobutyric acid (GABA) receptors (Starobova, Mueller, et al., 2020).

The role of NLRP3 inflammasome in CIPN has gained more interest in the recent years due to research indicating a crucial involvement of IL-1β in sensitization of nociceptors and pain induction (Binshtok AM et al., 2008). Elevated levels of the pro-inflammatory cytokine were observed in pain-related conditions such as complex regional pain syndrome, neuropathic pain, MS, and fibromyalgia (Cordero et al., 2014; Helyes et al., 2019; Starobova, Nadar, et al., 2020; Vanitallie, 2010). In a multiple sclerosis mouse model, administration of MCC950 (an NLRP3 antagonist) successfully relieved mechanical allodynia in the hind limbs (Khan et al., 2018). Similarly, mice with spinal cord injury treated with an endogenous NLRP3 inflammasome inhibitor D-β-hydroxybutyrate presented significant alleviation of mechanical and thermal hypersensitivities and reduction of IL-1β and IL-18 protein expression levels in the spinal cord (Qian et al., 2017; Youm et al., 2015). Increased expressions of NLRP3, caspase-1, and IL-1β were also observed in a rat model of paclitaxel-induced neuropathy model. Administration of phenyl N-tert-butylnitrone attenuated mitochondrial damage and production of reactive oxygen species in sciatic nerve and lowered mechanical hypersensitivity (Jia et al., 2017). Spinal cords from oxaliplatin-treated rats had elevated expression of NLRP3 and caspase-1. Moreover, intrathecal injection of MCC950, a potent and specific inhibitor of the NLRP3, significantly alleviated

neuropathic pain-like symptoms in rats intraperitoneally treated with a cumulative 10 mg/kg oxaliplatin (Wahlman et al., 2018). Liu et al investigated the role of NLRP3 inflammasome in bortezomib-induced peripheral neuropathy. They observed increased expression of NLRP3 expression in DRG neurons and infiltrating macrophages after bortezomib treatment in mice. They also observed that intrathecal injection of NLRP3 siRNA prevented the mechanical hypersensitivity induced by bortezomib treatment (Liu et al., 2018).

The premise of this dissertation stems from a hypothesis that paclitaxel and oxaliplatin induce activation of the NLRP3 inflammasome by various processes causing release of IL-1β which results in chemotherapy-induced peripheral neuropathy. Thus, targeting NLRP3 inflammasome could be a potential treatment for CIPN. There are limited published studies investigating the role of NLRP3 inflammasome on changes in pain-like behavior in rodent models of oxaliplatin- and paclitaxel-induced peripheral neuropathy. This dissertation work investigated whether genetic and pharmacological intervention of disrupting NLRP3 inflammasome assembly would protect mice from developing neuropathic pain-like symptoms in mouse models of OIPN and CIPN.

1.4. Dissertation Aims

Aim 1: To investigate the role of NLRP3 inflammasome in paclitaxel-induced peripheral neuropathy. The impact of NLRP3 inflammasome protein function inhibition on the development of PIPN using ASC KO and NLRP3 functional KO mice. In addition, we used compound Jc-124 as a pharmacological approach of selective blocking of NLRP3 inflammasome activation in PIPN mouse model. We assessed activation of NLRP3 inflammasome in the lumbar 4-6 spinal cord, a region important in pain modulation, by measuring levels of IL-1β, and co-

localization of NLRP3 with ASC protein or NLRP3 with Caspase-1 in mice treated with three doses of paclitaxel. We hypothesized that paclitaxel will increase levels of IL-1β in a dose dependent manner and blocking NLRP3 inflammasome activation via genetic or pharmacological approach will protect mice from developing mechanical and cold hypersensitivity.

Aim 2: To investigate the role of NLRP3 inflammasome in oxaliplatin-induced peripheral neuropathy. First, we established OIPN mouse model by subjecting two C57BL/6J and Balb/cJ mice to two doses of oxaliplatin. We performed a battery of behavioral test, measured changes in nerve conductance and IENF density to determine differences caused by the anti-cancer drug in each strain. Secondly, we subjected ASC KO and NLRP3 functional KO mice to the lower dose of oxaliplatin to investigate if blocking NLRP3 inflammasome activation will protect the mice from oxaliplatin-induced peripheral neuropathy as measured by von Frey. We planned on performing additional experiments in C57BL/6J mice confirm that the lack of mechanical hypersensitivity was due disruption of NLRP3 inflammasome activation, however, data showed otherwise. We hypothesized that inhibition of NLRP3 inflammasome will protect mice from developing oxaliplatin-induced peripheral neuropathy.

Overarching hypothesis: NLRP3 inflammasome activation drives chemotherapy-induced peripheral neuropathy in non-specific anti-neoplastic drug manner.

Completion of these aims will help to establish the roles of the NLRP3 inflammasome in paclitaxel- and oxaliplatin-induced peripheral neuropathy thus revealing a potential target for therapeutic intervention.

CHAPTER TWO

THE ROLE OF NLRP3 INFLAMMASOME INHIBITION IN PACLITAXEL-INDUCED PERIPHERAL NEUROPATHY MOUSE MODEL

2.1. Introduction

Chemotherapy-induced peripheral neuropathy (CIPN) is one of the major dose-limiting side effects of several anticancer drugs, including paclitaxel (Banach et al., 2017). These symptoms include mechanical and cold allodynia, numbness, tingling, painful burning sensations and a decrease in the density of intraepidermal nerve fibers (Seretny et al., 2014). Although paclitaxel increases overall survival of breast, lung, and ovarian cancer patients, paclitaxel-associated CIPN can occur acutely and chronically, and persist after termination of chemotherapy severely affecting the life quality of the patients (Beijers et al., 2014; Saibil et al., 2010; Urits et al., 2018). Efficacious prophylactic or therapeutic treatments for CIPN are currently not available, therefore there is a great need to identify potential mechanisms and new treatment targets of CIPN.

Canonical NLRP3 inflammasome processes involve oligomerization of an innate immune pattern recognition receptor NLRP3 and its signaling adaptor ASC upon sensing danger-associated molecular patterns (DAMPS), that triggers recruitment of the cysteine protease caspase-1 to form a complex termed the inflammasome (F. Lu et al., 2020). Subsequently, autoproteolysis of caspase-1 results in cleavage and activation of the pro-inflammatory cytokines IL-1β and IL-18, and GSDM-D (Evavold et al., 2018; Mulvihill et al., 2018). The importance of NLRP3 inflammasome complexes as major mediators of inflammatory pathways in neuropathic pain has recently emerged. Cancer cells and antineoplastic drugs can trigger release of DAMPs from host or cancer cells (Donnelly et al., 2020). As such, NLRP3 and IL-1β expression level elevated in mouse

macrophages treated with paclitaxel and dorsal root ganglia of rats treated with paclitaxel (Deuis et al., 2014; Zeng et al., 2019).

Accordingly, we hypothesized that based on the evidence, NLRP3 inflammasome plays an important role in paclitaxel-induced peripheral neuropathic pain. The studies in this chapter investigated the role of NLRP3 inflammasome on the onset of mechanical and cold hypersensitivity in mice treated with paclitaxel. NLRP3 KO and ASC KO were subjected to intraperitoneal injections of two doses of paclitaxel. We evaluated whether JC124, a selective NLRP3 inflammasome inhibitor, would protect C57BL/6J male and female mice from various paclitaxel doses. Lastly, spinal cord dorsal horn areas of mice treated with various doses of paclitaxel were assessed for changes in IL-1β.

2.2. Materials and Methods

Animals

All experiments were approved by the Institutional Animal Care and Use Committee at Virginia Commonwealth University under the National Institutes of Health Guidelines for the Care and Use of Laboratory Animals. Adult C57BL/6J mice were supplied from the Jackson Laboratory (Bar Harbor, ME) and housed in an AAALAC-accredited facility in climate-controlled room on a 12 hours light/dark cycle (lights on 07:00hrs) with *ad libitum* access to food (Envigo, Teklad LM-485 mouse/rat sterilizable diet, cat # 7012, WI, USA) and water. C57BL/6J-*NLRP3*^{m1Btlr}/Mmucd (Mutant Mouse Research and Resource Center at Univ. of California, Davis) mice were backcrossed onto the C57BL/6J genetic background mice. The *NLRP3* knock-out is a functional loss-of-function protein induced by N-ethyl-N-nitrosourea. A resultant single point mutation of T to G transversion at position 3187 in exon 9 of 10 total exons of the Nlrp3 transcript causes a cysteine to tryptophan substitution at residue 987 of the NLRP3 protein (Hua Huang et al., 2019). *ASC* null mice have a neomycin-disrupted allele (Mariathasan et al., 2004). NLRP3$^{-/-}$ and *ASC*$^{-/-}$ mice were each intercrossed to generate mutant and control mice germline transmission and confirmed by PCR of tail genomic DNA. NLRP3^{m1Btlr} (*NLRP3*$^{-/-}$) and *ASC*$^{-/-}$ strains will be referenced throughout this dissertation as NLRP3 KO and ASC KO, respectively. Mice were ages 10–22 weeks at the beginning of each experiment.

Experimental Protocol

Experiments were carried out with the approval of Institutional Animal Care and Use Committee of Virginia Commonwealth University, in accordance with the National Institutes of Health Guidelines for the Care and Use of Laboratory Animals. Paclitaxel (NDC 70860-200-50)

was diluted in 1:1:18 volume ratio solution (vehicle) composed of ethanol, kolliphor (Sigma-Aldrich), and distilled water, respectively. Paclitaxel-treated mice were subjected to one of three regimens: low dose, medium dose, and high dose. Each regimen consisted of four intraperitoneal (i.p.) injections administered in a volume of 10 ml/kg body weight on days 0, 2, 4 and 6. The cumulative dose totaled 8 mg/kg, 16 mg/kg, and 32 mg/kg for low dose (Pac 2), medium dose (Pac 4), and high dose (Pac 8), respectively. NLRP3 and ASC mice were challenged with a second regimen of the low dose paclitaxel on days 37, 39, 41 and 43. The control group received the 1:1:18 solution at a volume of 10 ml/kg, i.p., of the same injection regimen (**Figure 1A**). We used JC124 (4-[2-(5-chloro-2-methoxy benzamide)ethyl]benzsulfamide), a compound synthesized and supplied by Dr. Shijun Zhang; as a mean of pharmacological of NLRP3 inflammasome. JC124 was dissolved in DMSO and then further diluted in PEG-400 and administered at the dose of 100 mg/kg according to published studies (Kuwar et al., 2019; Toldo et al., 2019). C57BL/6J mice received a daily intraperitoneal (i.p.) injection of the drug or vehicle for 10 consecutive days. JC124 or its vehicle was injected 30 min prior to paclitaxel. Control mice received an equal volume of the vehicle solution (10% DMSO in PEG-400). Body weight and overall well-being were monitored for any signs of drug toxicity. C57BL/6J mice designated for histological studies were sacrificed on day 7 by carbon dioxide overdose followed by decapitation.

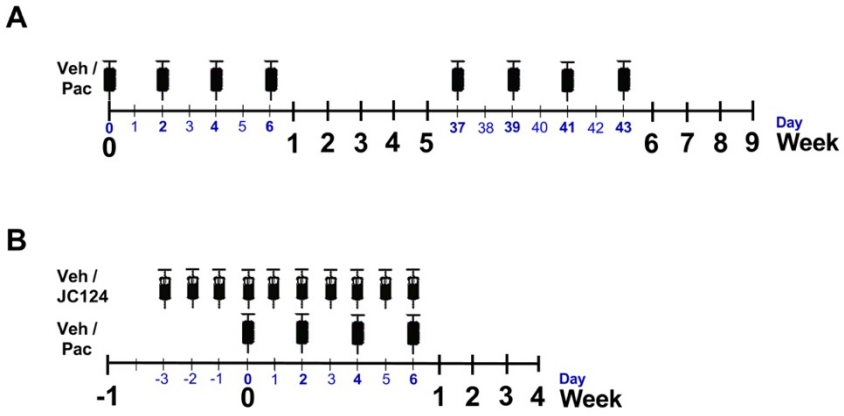

Figure 1. Paclitaxel dosing schedule. NLRP3 and ASC strain mice were administered different regimen of paclitaxel (A). Pharmacological inhibition of NLRP3 inflammasome with JC124 compound in mice co-treated with paclitaxel (B).

Mechanical Hypersensitivity

Mechanical hypersensitivity thresholds were measured with manual von Frey filaments according to the methods of Chaplan et al. (Chaplan et al., 1994). Male and female mice were tested at different times. Each mouse was placed in a Plexiglas chamber on an elevated mesh and allowed to acclimate for at least 30 min. Mechanical force (expressed in grams) was applied in increasing amounts to the ventral surface of the hind paw until a paw withdrawal response was demonstrated. The rate of in-house mice breeding was variable; therefore, two cohorts of each genotype were tested and data was pooled. Mice were tested at baseline (before paclitaxel treatment), one day post last paclitaxel injection, and then weekly. The number of animals tested is summarized in **Table 1**.

Mouse allocation		Number of animals per paclitaxel dose			
Strain	Sex	Vehicle	2 mg/kg	4 mg/kg	8 mg/kg
NLRP3 WT	Male	11	10	13	-
	Female	10	11	11	-
NLRP3 KO	Male	9	10	12	-
	Female	10	14	11	-
ASC WT	Male	10	10	5	-
	Female	3	4	3	-
ASC KO	Male	9	9	4	-
	Female	4	5	4	-
C57BL/6J	Male	Veh = 11 JC124 = 6	Veh = 6 JC124 = 6	Veh = 5 JC124 = 5	Veh = 5 JC124 = 5
	Female	Veh = 5 JC124 = 5	Veh = 5 JC124 = 5	-	-

Table 1. Summary of the number of mice in each treatment group assessed for mechanical hypersensitivity with von Frey test.

Cold Hypersensitivity (Acetone Test)

The acetone test was performed by habituating mice in Plexiglas chambers on mesh metal flooring for at least 30 min. After mice became calm, 20 μL of acetone (Fisher Bioscience) was sprayed onto the ventral surface of the hind paw from a 200 μL pipette (Eppendorf). Total time

lifting, licking, or clutching each paw was recorded over the course of 60 s. The number of tested animals is summarized in **Table 2**.

Mice allocation		Number of animals per paclitaxel dose		
Strain	Sex	Vehicle	2 mg/kg	4 mg/kg
NLRP3 WT	Male	4	4	-
	Female	6	7	-
NLRP3 KO	Male	6	6	-
	Female	6	7	-
ASC WT	Male	10	10	5
	Female	3	4	3
ASC KO	Male	9	9	4
	Female	4	5	4

Table 2. Summary of the number of mice in each treatment group assessed for cold hypersensitivity with acetone test.

Immunofluorescence

Spinal cord L4-L6 regions were removed, immersion fixed in 4% (v/v) formaldehyde in PBS (Sigma Aldrich) and kept at 4°C for at least 48 prior to processing. Spinal cords regions were embedded with paraffin and 10-micron thick sections were mounted on glass slides. Staining for NLRP3 inflammasome components was performed on Leica Bond RX and imaged with Vectra Polaris automated imaging system at 40X. Prior to primary antibody incubation, sections underwent EDTA-based antigen retrieval, washing with Bond Wash solution (Leica Biosystems Cat# AR9590), and 20-minute blocking with 5% normal goat serum. Antibodies were diluted in the blocking solution as follows: 1:100 goat anti-NLRP3 goat (ab4207, Abcam), 1:200 rabbit anti-ASC (AL177, Adipogen), 1:1000 donkey anti-goat AF594, and 1:2000 goat anti-rabbit AF750. Sections were incubated with a primary antibody for 60 minutes, washed with Bond Wash solution, incubated with a secondary antibody for 60 minutes, washed with distilled water, and

counterstained with DAPI. Images were previewed in Phenochart 1.1.0 (PerkinElmer Inc.) and the percentage of the positively stained cells was analyzed using inForm Tissue Analysis Software.

Immunoperoxidase

Spinal cord sections were dewaxed by incubation at 70°C for 3 minutes, dewaxed by three immersions in histoclear for 10 min each before rehydration with 100, 95, and 70% ethanol and dH_2O for 5 min each. Heat induced antigen retrieval in 95°C sodium citrate (0.01M, pH 6.0) was performed for 10 minutes. After sides cooled, sections were washed in PBS for 5 min three times and subjected to quenching in 3% H_2O_2 in methanol. Sections were incubated with a blocking solution (2.5% horse serum and 1% Triton-X in PBS) for 30 minutes to prevent any non-specific staining. Slides were incubated with the primary anti-IL-1β overnight at 4°C (1:200; AF-401-NA R & D Systems, USA) in a humidity chamber. After washing the slices 3x10 min with PBS, pre-diluted Sav-HRP (PK-7800, Vector Laboratories) conjugates were applied to the sections on the slides and incubated in a humidified chamber at room temperature for 30 mins. After washing the slides in PBS, freshly prepared 3, 3´-diaminobenzidine (DAB) solution (25 mg/100 ml of 0.0003% hydrogen peroxide in PBS) was added on slides for 5 min at room temperature, followed by washing in dH_2O and addition of hematoxylin. Slides were dehydrated and mounted with mounting medium. Images were taken in brightfield with an 10X objective (Nikon) and analyzed for the percentage of the positive staining using inForm Tissue Analysis Software. Each treatment group included tissues from mice of both sexes. Sections from the following number of mice were used: vehicle, males n = 4 and females n = 3; Pac 2, males n = 3 and females n = 3; Pac 4 and Pac 8, males n = 5 and females n = 3. The immunofluorescence (IF) and immunoperoxidase (IP) analyses

aimed to assess NLRP3 inflammasome activation and IL-1β production, respectively, induced by paclitaxel treatments in the spinal dorsal horns.

Statistical Analyses

The data were analyzed with GraphPad Prism software, version 8 (GraphPad Software, Inc., La Jolla, CA) and expressed as mean ± SEM. Repeated experimental designs were analyzed via three-way ANOVA with 'treatment' and 'genotype' or 'sex' as between-groups factors and 'time in weeks' as the within-group factor and followed by Tukey's post-hoc test. Two-way ANOVA was used to analyze Area Under the Curve (AUC) of cold hypersensitivity (genotype and treatment), JC124 effect on body weight and mechanical threshold changes (time x dose), and with Sidak's multiple comparisons test. Differences were considered significant when $p < 0.05$.

2.3. Results

Sex- and Dose-dependent Onset of Mechanical Hypersensitivity in NLRP3 KO mice

We began with a set of experiments to elucidate the role of NLRP3 inflammasome in the pathophysiology of PIPN by subjecting NLRP3 KO and their NLRP3 WT littermates to different schedules and doses of paclitaxel. A three-way ANOVA analyses showed a significant interaction between genotype x treatment x time [$F (8, 288) = 3.263$, $P = 0.0014$] and [$F (8, 336) = 2.454$, $P = 0.0136$] in male and female mice, respectively, treated with 2 mg/kg of paclitaxel. The low dose of paclitaxel administered to NLRP3 WT mice caused a significant decrease in mechanical threshold compared to NLRP KO mice (Figure 1B-C). Three weeks post last paclitaxel injection the threshold returned to baseline levels. The second wave of 2 mg/kg of paclitaxel triggered mechanical hypersensitivity which was observed in male NLRP3 WT and NLRP3 KO mice for

the remainder of testing. However, female NLRP3 KO showed a reduced mechanical threshold at week 7 only. NLRP3 WT female mice showed comparable results to NLRP3 WT male mice. We compared mice of the same genotypic background to determine possible sex differences. A three-way ANOVA analyses indicated significant differences in the NLRP3 KO strain ($F_{(8, 320)}$ = 4.318, $P < 0.0001$), driven by distinct changes observed at weeks 6, 7, and 9 ($P = 0.3656$, $P = 0.0477$, and $P = 0.0002$ respectively). No differences in the WT strain were noted ($F_{(8, 304)}$ = 0.7031, $P = 0.6888$, **Figure 2B-C**). The same cumulative dose of paclitaxel (16 mg/kg) was administered

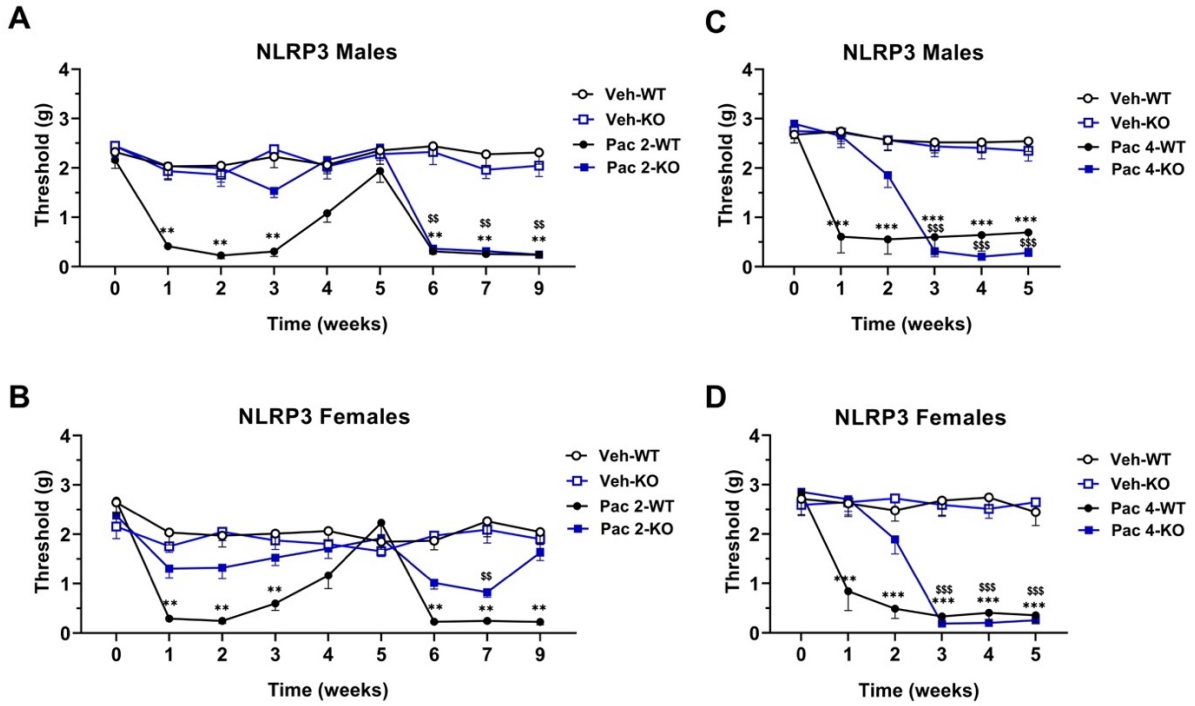

Figure 2. Induction of mechanical hypersensitivity by low and mid dose of paclitaxel in NLRP3 strain of mice. Baseline mechanical thresholds were assessed before the paclitaxel treatment (week 0) and then monitored after completion of each regimen (A). Male and female mice treated with 2 mg/kg paclitaxel received two waves of injections days 0-6 and 37-43 (B-C). The 4 mg/kg regimen was administered in male and female mice between days 0-6 and tested weekly (D-E). Values are expressed as mean ± SEM. Results were compared using three-way ANOVA (Treatment, Time as RM) for each strain and for each sex followed by Tukey's post hoc test. *p < 0.05, **p < 0.01, ***p < 0.001 indicates times at which NLRP3 WT paclitaxel-treated mice were statistically different from NLRP3 WT vehicle group. $^{\$}$p

< 0.05, $^{\$\$}$p < 0.01 and $^{\$\$\$}$p < 0.001 indicate times at which NLRP3 KO paclitaxel-treated mice were statistically different from NLRP3 KO vehicle group.

as four injections of 4 mg/kg. Data indicates a delayed onset of mechanical hypersensitivity in NLRP3 KO male and female mice at week 4 (males: $F_{(8, 288)} = 3.263$, $P = 0.0014$, females $F_{(8, 336)} = 2.454$, $P = 0.0136$). In comparison, mechanical hypersensitivity in NLRP3 WT mice was observed at week 1, one day after the last paclitaxel injection (**Figure 2D-E**).

Sex- and Dose-dependent Onset of Mechanical Hypersensitivity in ASC KO mice

The next experiment implemented the same dosing schedules of paclitaxel in ASC strain mice to further confirm if preventing NLRP3 inflammasome oligomerization and consequent activation of caspase-1 would ameliorate mechanical CIPN symptoms in mice. ASC WT male mice exhibited a similar pattern of CIPN development and recovery to NLRP3 WT male mice treated with the same low dose of paclitaxel. ASC KO female mice treated with one wave of 2 mg/kg of paclitaxel displayed full protection from development of mechanical hypersensitivity compared with the paclitaxel-treated ASC WT female mice ($F_{(8, 96)} = 4.708$, $P < 0.0001$, **Figure 3B)**. Comparable results were observed in ASC KO male mice, however, a decrease in mechanical below 1g was evident at week 2 ($F_{(8, 272)} = 2.107$, $P = 0.0354$, **Figure 3A)**. Compared with ASC KO female mice, ASC KO male mice treated with a second wave of 2 mg/kg of paclitaxel displayed significant mechanical hypersensitivity ($F_{(8, 184)} = 2.264$, $P = 0.0245$). ASC WT mice treated with the low dose of paclitaxel did not recover from established CIPN. The mid regimen of paclitaxel (4 mg/kg per injection) was sufficient to induce long lasting decrease in mechanical threshold in ASC WT male and female mice (**Figure 3C-D**). In contrast, deletion of ASC protein was sufficient to provide mild protection from CIPN.

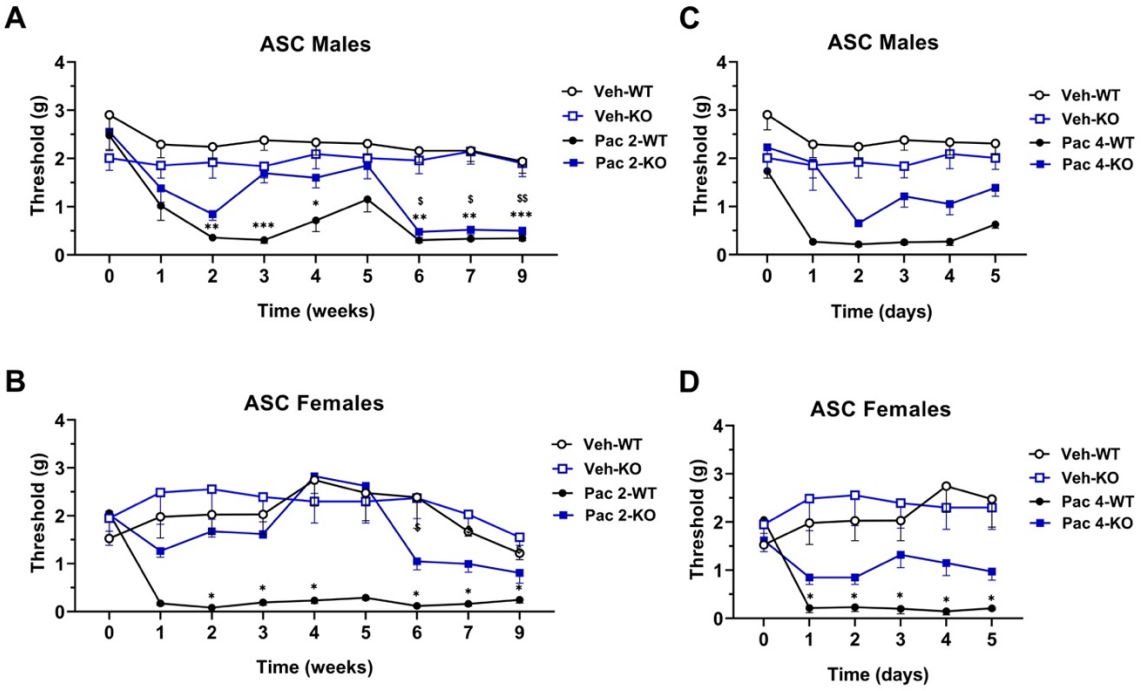

Figure 3. Induction of mechanical hypersensitivity by low and mid dose of paclitaxel in ASC strain mice. Mechanical thresholds were assessed at baseline (week 0) before the paclitaxel treatment and then monitored after completion of each regimen (A). Male and female mice treated with 2 mg/kg paclitaxel received two waves of injections on days 0-6 and 37-43 (B-C). The 4 mg/kg regimen was administered in male and female mice between days 0-6 and tested weekly (D-E). Values are expressed as mean ± SEM. Results were compared using three-way ANOVA (Treatment, Time as RM) for each strain and for each sex followed by Tukey's post hoc test. *$p < 0.05$, **$p < 0.01$, ***$p < 0.001$ indicates times at which ASC WT paclitaxel-treated mice were statistically different from ASC WT vehicle group. $^{\$}p < 0.05$ and $^{\$\$}p < 0.01$ indicate times at which ASC KO Pac-treated group vs from ASC KO control group.

Genetic Interference of NLRP3 Inflammasome Oligomerization Protects Mice From Developing Cold Hypersensitivity.

A characteristic paw withdrawal response to a cold stimulus in paclitaxel-treated mice was reported previously in our lab (Toma et al., 2017a). As such, we sought to investigate whether NLRP3 inflammasome dysregulation would protect mice from developing cold hyperalgesia. Hypersensitivity to acetone cooling sensation was significantly observed in NLRP3 WT mice after each 2 mg/kg paclitaxel wave of injections, while the response time of paclitaxel-treated NLRP3 KO males resembled their control group ($F_{(7, 112)} = 2.797$, $P = 0.0101$; **Figure 4A**). A three-way

ANOVA of results obtained from female mice did not find the 'genotype x treatment x time' interaction statistically significant. However, NLRP3 WT females demonstrated an observable change in magnitude of cold hypersensitivity compared to NLRP3 KO females (**Figure 4B**). Transformed cold sensitivity data into AUC revealed a significant interaction between treatment and genotype ($F_{(1, 172)} = 299.1$, $P < 0.0001$) and revealed that paclitaxel-treated NLRP3 WT mice indeed differed from NLRP3 WT control group ($P = 0.0101$, data not shown). Consistent with NLRP3 strain, ASC WT male and female treated with the low dose of paclitaxel had a greater magnitude of cold hypersensitivity (male $F_{(7, 238)} = 2.544$, $P = 0.0152$; female $F_{(7, 84)} = 4.612$, $P = 0.002$). ASC KO male and females showed comparable response time to their respective vehicle-treated groups (**Figure 4C-D**). Additionally, no aberrations were observed in ASC KO female mice treated with the mid-paclitaxel dose (**Figure 4E-F**). ASC WT female mice which were administered the 16 mg/kg cumulative paclitaxel regimen displayed a significant difference in the cold test response in comparison to the ASC WT control group. A three-way ANOVA analysis of ASC males treated with the mid dose paclitaxel was not significant, however, AUC of total response time revealed a significant interaction between treatment and genotype ($F_{(4, 40)} = 10.83$, $P < 0.0001$) and showed that paclitaxel-treated ASC WT group differed from ASC WT control group ($P < 0.00001$, data not shown). Within strain comparisons revealed a stronger response to cold stimulus in Pac 2 treated ASC WT females than ASC WT males ($F_{(7, 161)} = 2.651$, $P = 0.0128$; week 6 $P = 0.0007$, week 7 $P = 0.0154$).

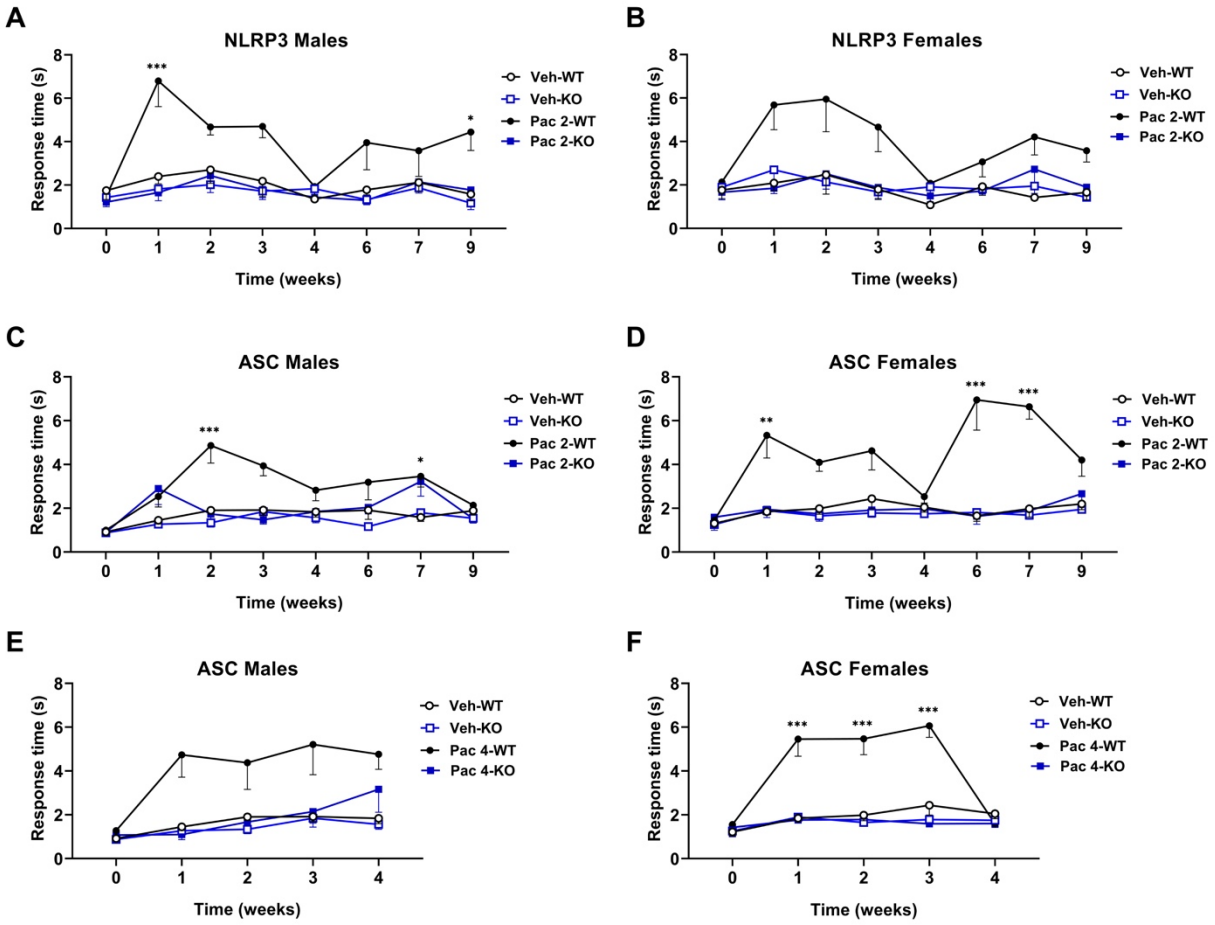

Figure 4. Induction of cold hypersensitivity with paclitaxel in WT mice. Two waves of 2 mg/kg paclitaxel injections were administered to NLRP3 (A-B) and ASC (C-D) mice on days 0-6 and 37-43. The 4 mg/kg regimen was administered to NLRP3 strain mice between days 0-6 and tested weekly (E-F). Values are expressed as mean ± SEM. Results were compared using three-way ANOVA (Treatment, Time as RM) for each strain and for each sex followed by Tukey's post hoc test. *p < 0.05, **p < 0.01, ***p < 0.001 indicate statistical different between Veh-NLRP3 WT and Pac-treated NLRP3 WT mice.

JC124 Prevents Mice from Low-Dose Paclitaxel-Induced Mechanical Hypersensitivity

We assessed general body conditions of mice receiving the JC124 compound and compared them to the vehicle-treated group. Figure 5 shows that co-administration of JC124 or its vehicle did not cause a statistically significant change in body weight in male and female C57BL/6J mice. The highest dose of paclitaxel (8 mg/kg) significantly altered body weight in males co-treated with the vehicle solution for JC124 on day 4 ($F_{(15, 115)} = 11.30$, $P < 0.0001$). Two-way ANOVA

analysis (dose x time) confirmed that administration of JC124 to vehicle-treated mice did not change the mechanical threshold of male nor female mice (males: $F_{(5, 75)} = 1.473$, $P = 0.2086$; females: $F_{(4, 32)} = 0.7917$, $P = 0.5393$). As anticipated, paclitaxel treatment caused a decrease in mechanical threshold of male and female mice (**Figure 6A and 6C**). JC124 treatment prevented development of mechanical hypersensitivity in male and female C57BL/6J mice treated with 2 mg/kg of paclitaxel (**Figure 6B and 6D**). The inflammasome inhibitor delayed onset of mechanical hypersensitivity caused by 4 mg/kg of paclitaxel, however, was not effective against the high dose of the chemotherapeutic in C57BL/6J male mice.

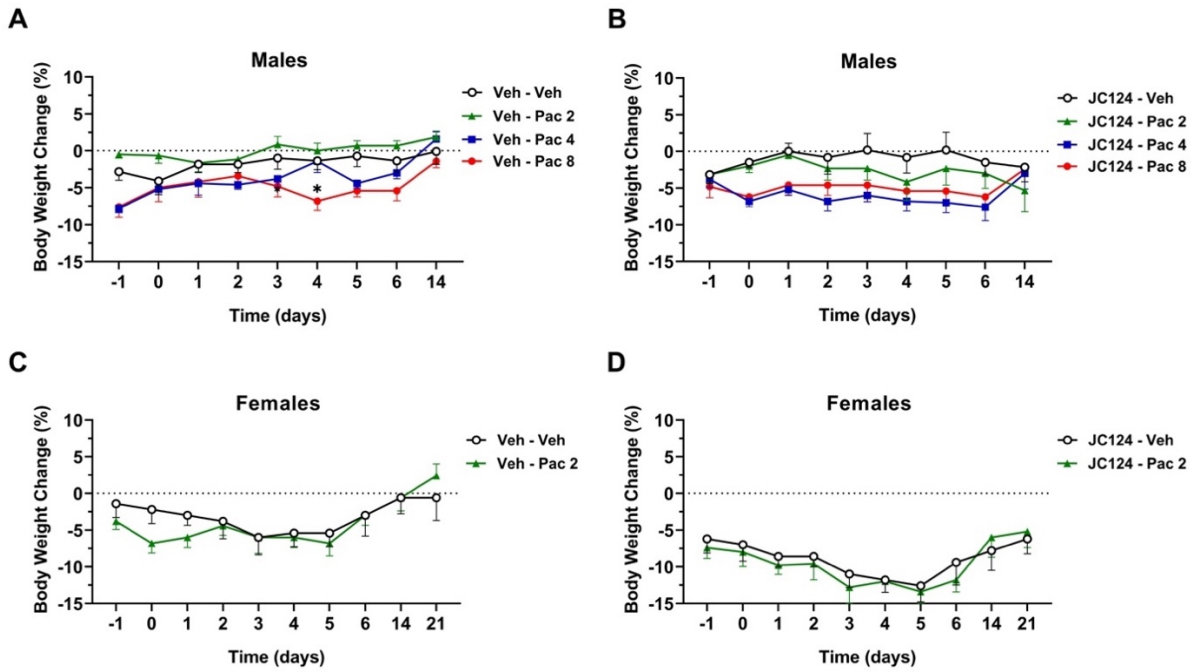

Figure 5. The effect of JC124 co-treated with paclitaxel on body weight. Percent body weight change changes from baseline in male C57BL/6J mice co-treated with paclitaxel (or its vehicle) and 10%DMSO in PEG-400 (A), C57BL/6J male mice co-treated with JC124 and paclitaxel (or its vehicle) (B), C57BL/6J female mice co-treated with vehicle for JC124 and paclitaxel (or its vehicle) (C), C57BL/6J female mice co-treated with JC124 and paclitaxel (or its vehicle) (D). Baseline measurements were taken before vehicle/JC124 treatment on day -3. Data expressed as mean ± SEM. Results were compared using two-way ANOVA and followed by Tukey's post hoc test. *$p < 0.05$ and compared to vehicle-treated mice.

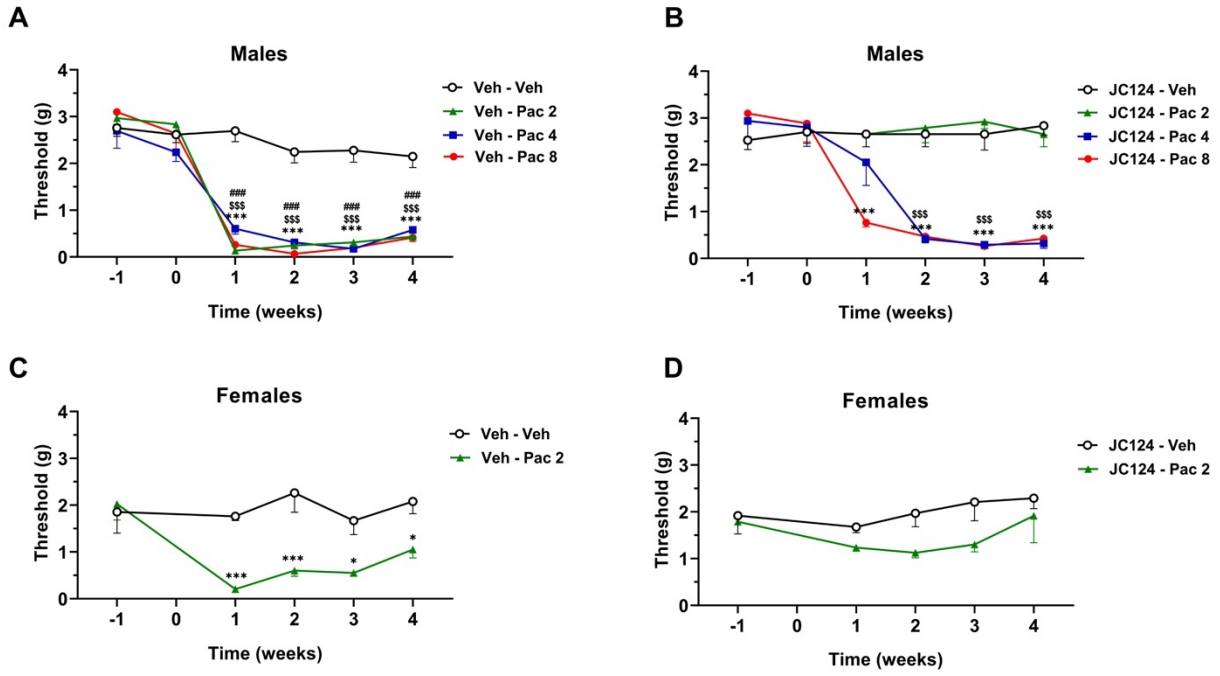

Figure 6. Prevention of CIPN in mice with NLRP3 inflammasome inhibitor. Mechanical hypersensitivity was assessed with von Frey assay in male C57BL/6J mice co-treated with paclitaxel (or its vehicle) and 10%DMSO in PEG-400 (A), C57BL/6J male mice co-treated with JC124 and paclitaxel (or its vehicle), C57BL/6J female mice co-treated with vehicle for JC124 and paclitaxel (or its vehicle) (C), C57BL/6J female mice co-treated with JC124 and paclitaxel (or its vehicle) (D). Values expressed as mean ± SEM.

IL-1β Levels Are Significantly Elevated in Spinal Cord Tissue of Mice Treated with High Dose Paclitaxel.

The percent of cells with positive IL-1β staining in the dorsal horn of spinal sections was compared between sexes in each group. Two-way ANOVA did not show difference between sexes; therefore, data was combined per treatment group. One-way ANOVA test revealed significant differences between the treatment groups ($F_{(3, 27)} = 3.546$, $P = 0.0276$, **Figure 7B**) while Tukey's test revealed a significant increase of IL-1β in the Pac 8 group compared to the control ($P = 0.0174$). These results suggested that the active IL-1β was increased in the dorsal horn in response to paclitaxel.

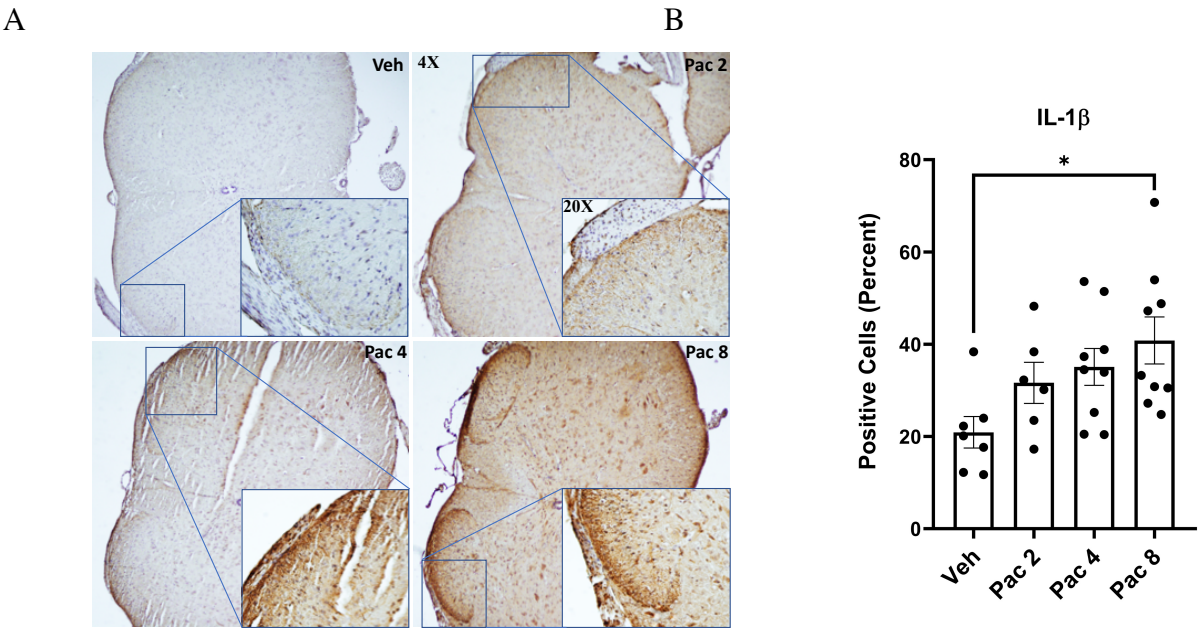

Figure 7. High dose of paclitaxel increased level of IL-1β in dorsal horns of spinal cords. A) Representative bright field images of L4-L6 spinal cord section from male C57BL/6J mice treated with paclitaxel. Images taken at 4X and 20X (small sections). B) Percentage of positive IL-1β-stained cells in male and female C57BL/6J mice. The overall effect of paclitaxel treatment was identified by one-way ANOVA analysis followed with post-hoc Tukey's multiple comparisons test, * $p < 0.05$.

NLRP3 Inflammasome Immunostaining Results

Immunohistochemistry was performed to confirm whether NLRP3 inflammasome activation was present in L4-6 spinal cord sections after paclitaxel treatment. Exemplary images of sections stained for ASC and NLRP3 proteins from vehicle- and paclitaxel-treated groups are shown in **Figure 8.** Sections stained for ASC protein showed green specs through tissue sections in all experimental groups. No specs were present on a slide of the control group that was subjected to the staining protocol with the omission of NLRP3 or ASC primary antibodies (images not shown). As ASC is a cytosolic protein, presence of fluorescence outside the cell might be indicative of the primary antibody non-specific binding. NLRP3 staining did not produce distinctive signal for the protein. High background autofluorescence was present in staining of both proteins. This

data is not conclusive as we were not able to detect a distinctive and typical signal for either protein possibly due to poor performance of the primary antibodies.

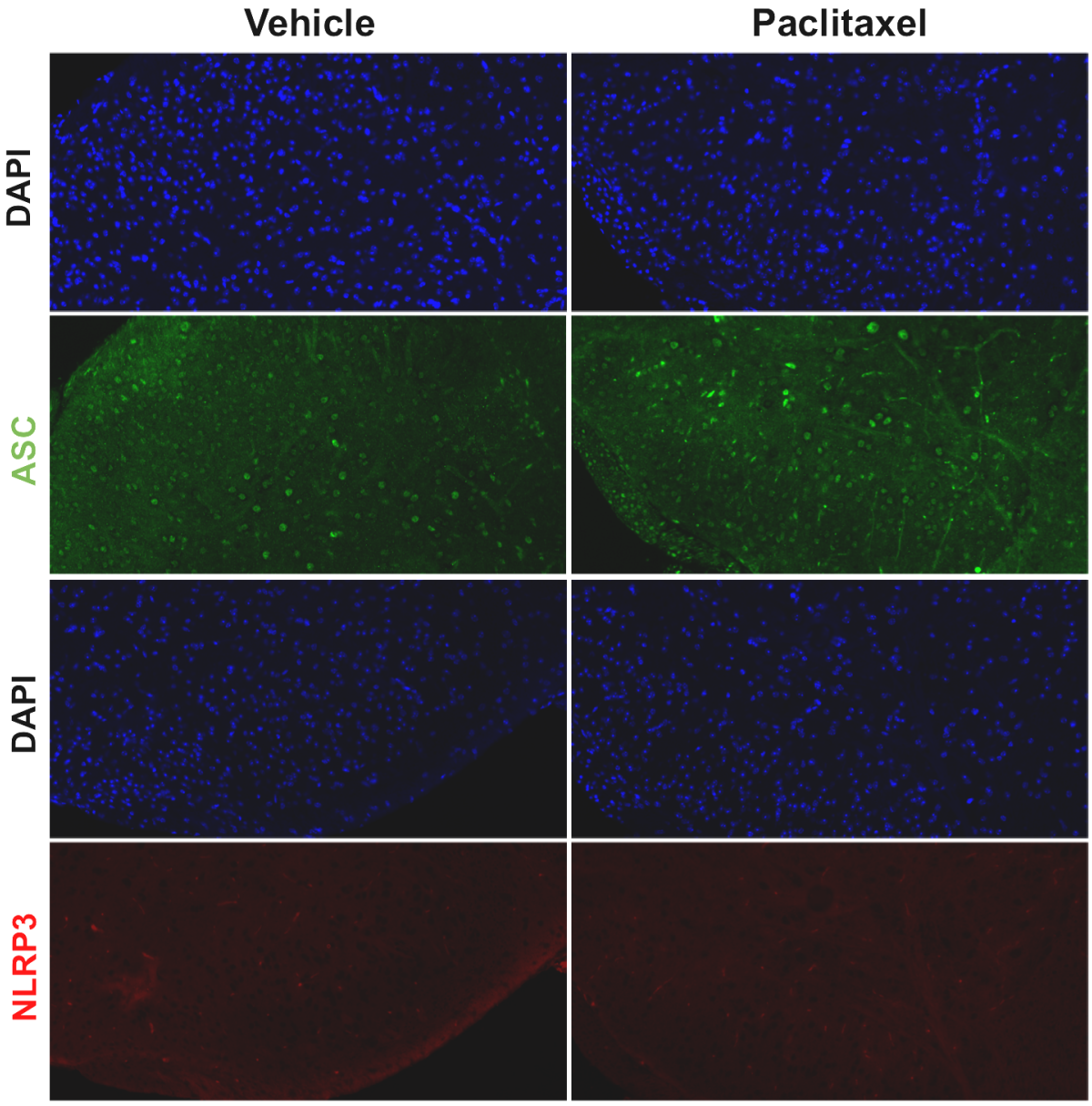

Figure 8. Immunohistochemistry images of L4-6 spinal cord sections. Tissue stained for NLRP3 (red), ASC (green), and DAPI (blue) in a vehicle and paclitaxel-treated male mice one day after the last injection of paclitaxel. Images taken at 20X magnification.

2.4. Discussion

Paclitaxel-induced peripheral neuropathy is a debilitating side effect that affects patients' quality of life. Presently, there are no effective prophylactic or therapeutic treatments available for CIPN. The precise pathology of paclitaxel-induced peripheral neuropathy is yet to be delineated, however, evidence suggests significant contribution of neuro-inflammation through triggering production of proinflammatory cytokines such as IL-1β which enhances neuropathic pain. Accordingly, researchers have been exploring different avenues of blocking production of IL-1β to ameliorate paclitaxel-induced nociception. We hypothesized that inhibition of NLRP3 inflammasome aggregation in mice treated with paclitaxel would prevent development of CIPN by diminishing levels of IL-1β.

Present work demonstrates that NLRP3 inflammasome plays an important role in the development of peripheral neuropathy induced by paclitaxel. Moreover, blocking NLRP3 inflammasome oligomerization via genetic knockout of the NLRP3 or ASC protein, and with a selective NLRP3 inflammasome inhibitor JC124 prevent the development of mechanical hypersensitivity and cold hypersensitivity in a paclitaxel-dose dependent manner. In addition, repeated administration of JC124 did not induce deleterious effects on the body weight. Finally, administration of paclitaxel correlated with dose-dependent increase of IL-1β in the dorsal horn of the spinal cord.

Release of cytokines after paclitaxel treatment has been documented in clinical as well as in pre-clinical models of PIPN (X. M. Wang et al., 2012). Canonical inflammasome activation requires a priming signal, such as ligands for Toll-like receptors, which leads to increased expression of NLRP3 and pro–IL-1β through NF-κB signaling (Kelley et al., 2019). Paclitaxel has been shown to directly prime macrophages promoting activation of caspase-1 through

inflammasome-activating signals (Son et al., 2019). Pre-treatment of bone marrow-derived macrophages and J774A.1 linage macrophages with paclitaxel enhanced ATP- or nigericin-induced NLRP3 inflammasome activation of downstream molecules in a paclitaxel-dose-dependent manner. This was evident by release of cleaved caspase-1 and mature IL-1β, greater formation of ASC speck and increased gasdermin D cleavage (Zeng et al., 2019). Rats treated with a cumulative 8 mg/kg paclitaxel of the same injection schedule showed elevated levels of IL-1B gene expression, mRNA and protein levels in spinal cords and DRGs (Jia et al., 2017; Kuyrukluyıldız et al., 2016). However, our results indicated a statistically significant increase of IL-1β-positive cells in the spinal cord dorsal horns of mice treated with a 32 mg/kg cumulative paclitaxel regimen. This discrepancy could stem from different methods of measuring the pro-inflammatory cytokine and between species differences. Furthermore, our method did not distinguish pro–IL-1β from and secreted mature IL-1β. We were unable to determine whether NLRP3 and ASC protein assemble in spinal dorsal horn in a paclitaxel-dose dependent manner due to poor performance of the primary antibodies. However, literature indicates a direct correlation between formation of ASC specks and paclitaxel treatment. In vitro experiments on primary murine macrophages treated with paclitaxel showed oligomerization of ASC and protein-protein interaction between NLRP3 and ASC in presence of a second signaling molecule such as ATP, nigericin, or efflux of K^+ (Son et al., 2019; Zeng et al., 2019). Moreover, Mia Jia et al 2017 reported an increased number of macrophages expressing NLRP3 protein by performing immunohistochemistry staining of L4-6 DRGs and sciatic nerve derived from rats treated with a cumulative 10 mg/kg paclitaxel.

Our data demonstrated that the activation of NLRP3 inflammasome was correlated with paclitaxel treatment-induced mechanical hypersensitivity. Overall, the literature indicates no sex

differences and a dose-dependent paclitaxel-induced mechanical hypersensitivity (Paton et al., 2022; Yan et al., 2015). Our group also previously observed mechanical hypersensitivity in the wild type mice using the same 8 mg/kg cumulative paclitaxel treatment regimen (Toma et al., 2017b). Using the same treatment schedule in a functional knock out of NLRP3 protein or global knockout of *ASC* gene had no effect on development of mechanical hypersensitivity mice. Moreover, JC124 treatment prevented paclitaxel-induced mechanical sensitivity in C57BL/6J male and female mice treated with the same dose of paclitaxel although the last JC124 injection was given 30 minutes prior to last paclitaxel infusion. Rats administered with the same paclitaxel paradigm demonstrated a short lasting but significant decrease in the pain threshold after a single administration of 100mg/kg anakinra, a competitive inhibitor of IL-1 receptors (Kuyrukluyıldız et al., 2016). Subjecting mice to another low-dose regimen of paclitaxel revealed sex differences in our knock out mice. Males of ASC KO and NLRP3 KO genotypes displayed a significant decrease in mechanical threshold that resembled their respective WT groups. However, female KO mice showed more resistance to developing nociceptive responses to mechanical stimuli. In comparison, development of mechanical hypersensitivity in KO males and females dosed with a cumulative 16 mg/kg as 4 injections of 4 mg/kg responded was comparable as seen in the wild-type mice. This highlights the importance of using appropriate chemotherapeutics regimen when investigating the pathology and its possible sex differences, particularly because paclitaxel is commonly used for the treatment of breast and ovarian cancers (D. Zhang et al., 2014). It has been noted in the clinic that neuropathic pain is more prevalent in women than in men (Fillingim et al., 2009). Taken together, NLRP3 inflammasome plays an important role in development of paclitaxel-induced mechanical hypersensitivity and has a distinct impact in female mice. Possible causes of sex differences that contributed to this observation will be discussed in the Chapter 4: Discussion.

Consistent with literature, wild-type mice treated with paclitaxel developed mechanical and cold hypersensitivity (Deng et al., 2015; Naji-Esfahani et al., 2016; Slivicki et al., 2016). The total response time to acetone of ASC KO and NLRP3 KO mice subjected to paclitaxel was comparable to their respective vehicle-treated group. While we did not assess cold hypersensitivity in the Pac 4 NLRP3 KO male and female groups, we predict the same response would be observed as in the Pac 4-treated ASC KO mice. Sex differences were observed for paclitaxel-induced cold hypersensitivity in ASC WT mice treated with two waves on the low-dose paclitaxel. In a mouse model of PIPN, Naji-Esfahani et al. injected 2 mg/kg paclitaxel for five consecutive days in NMRI mice, a significant sex difference was observed in cold sensitivity suggesting a critical role of genetic background and paclitaxel regimen differences (Naji-Esfahani et al., 2016). A potential explanation of the mechanism by which IL-1β mediates PIPN associated cold sensitivity came from Hee Lim Jun et al 2009 work. It was deduced that activation of NF-κB via the PC-PLC/PKC signaling leads to an increase in IL-1β that successively activates paracrine MCP-1/CCR2 signaling between DRG neurons (Youm et al., 2015). However, a 3 mg/kg total dose of IL-1ra i.p. administered to rats 31 days after the last dose of paclitaxel was not efficacious to reduce the duration of cold-stimulated responses (Al-Mazidi et al., 2018). This could be attributed to the differences in the experimental design where an established PIPN and associated changes on a molecular level.

CHAPTER THREE

THE ROLE OF NLRP3 INFLAMMASOME INHIBITION IN OXALIPLATIN-INDUCED PERIPHERAL NEUROPATHY MOUSE MODEL

3.1. Establishing a mouse model of OIPN

3.1.1. Introduction

Oxaliplatin is a platinum-based chemotherapeutic agent used against digestive tract tumors, esophageal, liver, pancreatic, and colorectal cancers (CRC) (Aschele et al., 2005; Dieras et al., 2002; Javle & Hsueh, 2010; Mascarenhas et al., 2013). Despite its high efficacy at fighting cancer, this drug is considered one of the most neurotoxic chemotherapeutics, where approximately 90% of patients develop acute neuropathy symptoms which appear hours after infusion (Argyriou et al., 2013). The feature characteristics of oxaliplatin-induced peripheral neuropathy (OIPN) are cold hypersensitivity, allodynia, pain, sensory ataxia, and dysesthesia in the distal extremities and perioral regions (Nakagawa & Kaneko, 2017). The negative impact of OIPN on continuation of treatment can be substantial leading to treatment delay, dose reduction, or cessation (Ruzzo et al., 2019). In a small clinical study, 40% of colorectal cancer patients treated with oxaliplatin aborted their treatment due to neurotoxicity (B. K. Bennett et al., 2012). Moreover, due to oxaliplatin cumulative toxicity, up to half of patients treated with this chemotherapeutic progress to chronic peripheral neuropathy, which can persist for years after discontinuation of the therapy (Beijers et al., 2014; Höke & Ray, 2014; Ta et al., 2009a; Tofthagen, 2010).

With the expanding medical use of oxaliplatin, an increasing number of patients are at risk of developing OIPN and other signs of neurotoxicity that burden their quality of life. Such signs include fatigue, distress, anxiety, and depression. Emotional distress reported in colorectal cancer patients treated with 6 cycles of oxaliplatin resulted from inability to cope with neuropathic symptoms and impairment of performing activities of daily living (Kanda et al., 2017).

Additionally, Bonhof and colleagues reported that CRC survivors with high chemotherapy-induced peripheral neuropathy scores experienced more anxiety, depressive symptoms, and fatigue than survivors with lesser neuropathic scores (Bonhof et al., 2019). Overall, the prevalence of depression and anxiety in cancer patients is 58% and 11.5%, respectively (Massie, 2004; Mehnert et al., 2014). Other affective disturbances associated with pain involve reduced appetite, anhedonia, disruptions to sleep cycles, and impaired social interactions (Massie, 2004).

To this day, there are no effective preventative measures or treatments against OIPN. The population of patients with neuropathies is rising and the search for new therapeutics that could significantly improve the quality of life and tolerance of cancer medications is continuing. In that regard, the use of animal models allows for studying variables influencing the progression of neuropathy and recovery, and evaluation of new preventive and therapeutic approaches for OIPN. However, studying OIPN in animal models has its own challenges. The majority of chemotherapy-induced peripheral neuropathy studies in rodents are heterogeneous in nature with respect to strain, sex, dosage, route of administration, duration of treatment, and outcome measures which hinder comparison between studies (Mehnert et al., 2014). Genetic diversity among different strains of rodents can influence responses to pain and neuropathy assays (Fiore & Austin, 2016). Additionally, the use of a single strain of inbred mice might not provide sufficient evidence for drug efficacy in clinical settings. As such, a recent study that looked at the susceptibility of different mouse strains (BALB-c, C57BL/6, DBA/2J, A/J, FVB and CD1 from Envigo) to OIPN-associated phenotypes found that morphometric, electrophysiological, and cold hypersensitivity measures are strain-dependent (Bruna et al., 2020).

Assessing complex OIPN pain phenotypes in rodents is challenging due to is multimodality in the sensory, behavioral, and cognitive aspects in human (Lacroix-Fralish & Mogi, 2009;

Marmiroli et al., 2017b). In that regard, relying upon stimulus-evoked assessment of pain sensitivity in animals might be insufficient for moving preclinical findings into clinical settings. In order to study intensity and relief of chemo-induced neuropathy, it is important to test additional endpoints which are relevant to human conditions and experiences. We recently reported that paclitaxel treatment in mice induced alterations in some affective-related behaviors which include nest building, burrowing, wheel running, anxiety- (light/dark box test), depression-, and anhedonia- (sucrose preference test) like behaviors (Nadine Attal et al., 2011).

The primary objective of this study was to provide a more comprehensive and systematic characterization of oxaliplatin-induced peripheral and painful neuropathy in mice. To accomplish this goal, both sexes of the two widely used strains of mice, C57BL/6J and BALB/cJ, were subjected to intraperitoneal injections of two doses of oxaliplatin (Finnerup et al., 2016). While most studies focus on measuring evoked sensory changes, we investigated the impact of the antineoplastic agent on several behavioral measures. Moreover, we evaluated two clinically relevant neuropathy markers, nerve conduction and intraepidermal nerve fiber density, in C57BL/6J and BALB/cJ male and female mice. This study aims to bridge the gaps in the literature between different experimental parameters in chemotherapy treatment, strain, sex, and dose, using a battery of assays in two inbred mouse strains frequently used in cancer research.

3.1.2. Methods

Animals

Experiments were performed on adult male and female C57BL/6J and BALB/cJ mice. All mice were supplied from The Jackson Laboratory (Bar Harbor, ME). Mice were 12 weeks old at the beginning of the experiments. C57BL/6J mice were group-housed, with the exception of a separate cohort of mice which was single-housed to perform nesting and sucrose preference studies.

BALB/cJ male mice were housed one or two per cage due to excessive fighting. Animals were housed in a climate-controlled room on a 12 hours light/dark cycle (lights on 07:00 hrs) with *ad libitum* access to chow (Envigo, Teklad LM-485 mouse/rat sterilizable diet, cat # 7012, WI, USA) and water. Cages contained compressed cotton nestlets and cardboard tunnels for enrichment items. All studies were approved by the Institutional Animal Care and Use Committee of Virginia Commonwealth University and followed the National Institutes of Health Guidelines for the Care and Use of Laboratory Animals.

Mice were handled for 1 week and habituated to the room prior to testing. Baseline nociception and affect-like behavior measurements were established. Experiments were performed during the light cycle by blinded female experimenters. To increase scientific rigor, behavioral and electrophysiological changes were measured in several cohorts of mice to reduce the stress associated with frequent testing and handling.

Drugs and induction of OIPN

Pharmaceutical grade oxaliplatin (5 mg/ml, Accord, NDC 16729-332-05) was prepared daily in a vehicle of sterile 5% dextrose solution (Hospira, Lake Forest, IL). Animals received intraperitoneal (i.p.) injections of vehicle, low-dose (0.3 mg/kg) or high-dose oxaliplatin (3 mg/kg) for 5 consecutive days, followed by 5 days of rest, followed by a second cycle of five daily injections, as per the method of Ta et al (Ta et al., 2009b). The total cumulative doses of oxaliplatin over the course of 10 injections was 3 mg/kg for the low-dose regimen and 30 mg/kg for the high-dose regimen. The low and high dosage of the drug were selected based on the literature evidence which indicate their effectiveness in inducing neuropathic pain without unspecific systemic toxicity. Moreover, the high dose used in this study is relevant to clinical dosing. Human equivalent dose conversion factors were applied to show dosage relevance for oxaliplatin. The highest

recommended dose of oxaliplatin patients is 110 mg/m^2 (2.97 mg/kg) (24). The total human equivalent dose (THED) of oxaliplatin daily dosing ranges in mice 0.04 -10.0 mg/kg/day, and the cumulative 3.0-30.0 mg/kg (0.24-2.4 mg/kg THED) (25-27). Our calculation shows that 30 mg/kg of oxaliplatin is equivalent to 1,110 mg/m^2 in humans. Both strains and sexes received vehicle, low-dose oxaliplatin, and high-dose oxaliplatin.

General Experimental Design

The first wave of five injections were considered week 0. The five-day rest period between the first and second wave of treatment was designated as the first week of testing (week 1). The 3rd week of testing began 24 hours following the 10th injection. Week 3 and subsequent testing intervals span for 7 days. If two tests were performed on the same day, the least stressful test occurred first to minimize the influence of one test on the successive test. No more than two tests were performed per day. A larger number of animals was assigned to the high-dose groups to account for potential severe adverse effects from the treatment. Therefore, the number of mice tested was variable across treatment groups and time points. The experimental timeline of behavioral tests, nerve conduction, and humane endpoints are summarized in Figure 1.

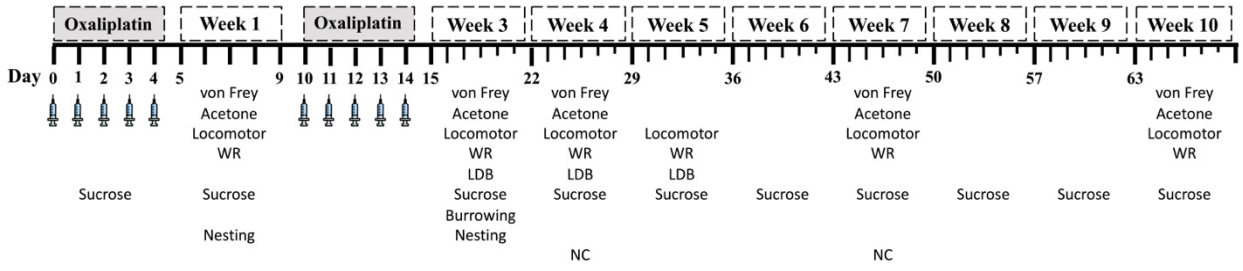

Figure 1. Experimental testing schedule. Weeks 1 and 2 spanned 5-day intervals. Starting at week 3, testing week span for 7 days. LDB: light/dark boxes; WR: wheel running; NC: caudal nerve conduction.

Assessments of Stimulus-Evoked Nociceptive Behaviors

Mechanical Hypersensitivity (von Frey Test)

Mechanical hypersensitivity thresholds were determined using manual von Frey filaments according to the methods of Chaplan et al., 1994. Shortly, each animal was placed in a Plexiglas chamber on an elevated mesh and acclimated for at least 30 min. Mechanical force was applied in increasing amounts to the ventral surface of the hind paw until the subject demonstrated a paw withdrawal response whereby the force is expressed in grams. The following number of mice were used in the von Frey test: C57BL/6J, males n = 17 and females n = 11; male BALB/cJ vehicle and low-dose n = 7, high dose n = 9; female BALB/cJ n = 10 females per group. All mice were tested at baseline, and weeks 1, 3, 4, 7 and 10 of the study.

Cold Hypersensitivity (Acetone Test)

Similar to the von Frey test, the acetone test was performed by habituating C57BL/6J mice in Plexiglas chambers on mesh metal flooring for at least 30 min. 20 μL of acetone (Fisher Bioscience) was projected onto the ventral surface of the hind paw from a 200 μL pipette (Eppendorf). Total time lifting, licking, or clutching each paw was recorded over the course of 60 s. C57BL/6J male mice (n = 8 per group) and female mice (n = 8 per group) were tested on weeks 1, 3, 4, 7, and 10. Cold hypersensitivity was not obtained in BALB/cJ mice due to hypermobility of the animals on the mesh which led to an inability of the tester to perform rigorous testing.

Assessments of Spontaneous Behaviors

Locomotor Activity (Locomotor)

Mice were individually placed into Omnitech (Columbus, OH) photocell activity cages (28 × 16.5 cm). Photocell beams interruptions, which assess walking and rearing, were recorded for 30 min. Data are expressed as the average number of beam breaks. Two groups (Group 1 and Group

2) of C57BL/6J animals were tested at different time points. Group 1 (n = 9 males/group, n = 6 females/group) was assayed at baseline, and week 1, 3, and 5, while Group 2 (n = 8 males/group, n=8 females/group) testing occurred at baseline and week 4, 7, and 10. BALB/cJ males (n = 7-9) and females (n = 10) locomotor activity were assessed at baseline and week 1, 3, and 5.

Voluntary Wheel Running (WR)

Mice were placed in free-standing running wheels (68 cm circumference) with the ability to spin in either direction. After a 5 min acclimation period to the wheels, the wheels were latched allowing for unidirectional spinning for a 2-hour session. Rotations were converted to distance traveled by multiplying the number of rotations by the wheel circumference. Data are expressed as the average distance traveled (m). The mice in this voluntary wheel running study were the same subjects as the locomotor activity cohorts, undergoing the same baseline and weekly testing schedule (on different days of the week than locomotor activity).

Light/dark box (LDB) Test

The light/dark box test was used to assess anxiety-like symptoms. This assay is based on a conflict between rodents' natural aversion to brightly-illuminated areas and their spontaneous exploratory activity (Crawley & Goodwin, 1980). In brief, the LDB apparatus consisted of a small, enclosed dim "dark" box (36 × 10 × 34 cm) with an opening (6 × 6 cm) leading to a larger, brightly illuminated "light" box (36 × 21 × 34 cm). The mice were acclimated to the testing room for 30 min prior to testing. Mice were placed in the light compartment and allowed to explore the apparatus for 5 minutes. The total time (s) spent in the light compartment was recorded via a video monitoring system and measured by ANY-MAZE software (Stoelting Co., Wood Dale, IL). To assess spontaneous exploratory behavior at different time points in C57BL/6J mice without

habituation to the LDB apparatus, Cohort 1 (n = 9 sex/group) was tested at baseline and week 3, while Cohort 2 (n = 8 sex/group) was tested at week 4 and 7. BALB/cJ males (n = 7-9) and females (n = 10) were tested at baseline and week 3 and 5.

Two-Bottle Choice Test (Sucrose Preference Test)

The sucrose preference test theoretically assesses anhedonia-like behavior (30). Mice were housed individually with *ad* libitum access to food. Mice were presented with two sipper tubes, one containing normal drinking water and the other containing 3% sucrose solution (w/v, Sucrose ≥ 99.5% (GC) Sigma, United States, cat# S7903). The total volume consumed from each tube was measured after 24 hrs. The position of both sipper tubes was switched for each drinking session to avoid place preference. Sucrose preference was calculated as a percentage of 3% sucrose volume consumed over the total fluid intake, multiplied by 100%. Preference is reported as the average per group. Measurements were collected daily during the first course of 5 injections, then after 10th injection, followed by weekly testing. Sucrose preference was measured in a separate cohort of vehicle-treated and high-dose oxaliplatin-treated C57BL/6J mice (n=10 group/sex). Due to a severe eye infection and tail injuries, one low-dose and one high-dose oxaliplatin BALB/cJ male mice were euthanized, resulting in sample sizes of n = 4-6. Female BALB/cJ mice sample size was 6/group.

Nesting

The nesting test assesses the impact of spontaneous nociception on activities of daily living. The assay was adapted as previously described by Oliver et al. with some modifications (Oliver et al., 2018). Briefly, the test was performed on individually-housed mice. All previous nesting material and enrichment items were removed from the home cage prior to conducting the nesting

assay. For each cage, two compressed cotton nestlets were cut in half, for a total of 4 rectangular pieces of equal size placed in each cage corner. The mice were allowed 120 min to nest in a quiet room. Nest quality was scored between 1 (no nestlet consolidation) and 5 (complete nestlet consolidation). The nesting assay was conducted in the same subjects as the sucrose preference test. The test was performed weekly for 5 consecutive weeks. Data are expressed as the average nesting score per group.

Burrowing Test

Like the nesting test, the burrowing test is another means of assessing voluntary spontaneous behaviors necessary for survival. The burrowing test was performed as previously described with some modification (Luedtke et al., 2014; Sherwin et al., 2004). Long gray PCV tubes (20 cm long x 7 cm in diameter) with an upright tilt of ~10º and sealed bottom ends were filled with approximately 180 grams of clean corncob bedding. Tubes were placed in rat cages (37 cm × 26 cm × 19 cm, L×W×H), with the tube opening facing towards the wall. Rat cages contained clean corncob bedding on the floor but lacked food and water. Mice were placed in the rate cages for 30 min sessions. Data are represented as the average amount of bedding displaced (g). Subjects from the sucrose preference test used in burrowing experiments at baseline and week 3 and 5.

Assessment of Peripheral Nerves

Immunohistochemistry and Quantification of Intra-Epidermal Nerve Fibers (IENFs)

Mouse hind paws were removed and placed in freshly prepared PLP fixative at 4°C for 24 hrs (McLean & Nakane, 1974). The glabrous skin on the ventral surface of the hind paws was excised and submerged in 30% (w/v) sucrose at 4°C overnight. The tissues were embedded in Optimal Cutting Temperature embedding medium for frozen tissues (ThermoFisher Scientific) and

sectioned at 25 μm on a cryostat. Sections were immersed in cold acetone (-20°C) for 20 minutes, washed with PBS, and incubated at room temperature for 45 min in blocking solution (5% normal goat serum and 0.3% Triton X-100 in PBS). Sections were incubated with a 1:200 dilution of the primary rabbit anti-mouse polyclonal PGP9.5 antibody (ProteinTech, cat# 14730-1-AP, IL, USA) overnight at 4°C in a humidified chamber. Following three PBS washes, sections received a second blocking step-and then incubated for 2 hours at room temperature with a 1:300 dilution of goat anti-rabbit IgG (H+L) secondary antibody conjugated with Alexa Fluor® 594 (Life Technologies, cat# A11037, OR, USA). Sections were mounted with Vectashield (Vector Laboratories, Burlingame, CA, USA) and examined using a Zeiss Axio Imager A1 – Fluorescence microscope (Carl Zeiss, AG, Germany). The IENFs of each paw section were counted under 63X magnification in a blinded fashion, and the density of fibers was calculated as fibers/mm. The mean of IENF density (n= 6/sex/group) was calculated from six mice.

Caudal Nerve Conduction (NC)

Nerve conduction velocity (NCV) and sensory nerve action potential amplitudes (SNAP) of the caudal nerve were recorded with PowerLab 4/35 electromyography system (AD Instruments, Inc, CO, USA). This test measures amplitude and latency of the evoked response, which are used to calculate nerve conduction velocity. The protocol was adapted from Marmiroli et al. (Marmiroli et al., 2017a). Anesthesia was induced in a chamber with 4% isoflurane carried in oxygen and maintained with 2.5% isoflurane by nose cone during the nerve conduction procedure. Needle recording electrodes (cathode and anode) were inserted 5 mm distal from the base of the tail, with the stimulating electrodes 5.0 cm apart from the recording points (distance measured from cathode to cathode). There was a ground electrode between the stimulation and recording electrodes. The nerve was stimulated with single square-wave pulses of 0.1 ms duration at 7 mA, with a repeat rate

of 1 Hz. The neurophysiological measures were conducted under standard conditions in a temperature-controlled room. NCV was calculated by dividing the distance between the recording and stimulating electrodes (0.05 m) by the latency between the stimulus artifact and the onset of the first peak of the elicited action potential latency of the sensory nerve action potential. NCV (m/s) and SNAP (μV) were measured one week after the 10th injection (week 4). C57BL/6J mice (n = 8 males/group, n = 8 females/group) and one cohort of BALB/cJ mice (n = 7-8 males/group, n = 10 females/group) were used for these measurements.

Statistical Analyses

The data analyses were carried out with GraphPad Prism software, version 8 (GraphPad Software, Inc., La Jolla, CA) and the data are expressed as mean ± SEM. Statistical analyses were performed as unpaired *t* tests to compare behaviors of vehicle- and oxaliplatin-treated mice at a single time point, one-way (treatment) or two-way (time x treatment) analysis of variance (ANOVA) with repeated measures or mix effect analysis. When appropriate, Dunnett's or Tukey's post-hoc comparison tests were performed. Nesting test scores were analyzed by employing Mann-Whitney test with correction for multiple comparison using the Hold-Sidak method. A three-way ANOVA with repeated measures was performed to investigate a) differences between sexes of each mouse strain, and b) strain differences of same sex between both strain. Time and treatment were common factors for each comparison. $p< 0.05$ was considered statistically significant.

3.1.3. Results

Oxaliplatin Has Strain- and Sex-Dependent Effects on body Weight

Oxaliplatin induced strain- and sex-dependent effects on weight change. Oxaliplatin had transient effects of body weight in C57BL/6J mice (**Figure 2**). Vehicle and low-dose treated male C57BL/6J mice steadily gained weight over time. The high-dose oxaliplatin regimen caused a

robust weight loss and slowed weight gain, as compared to vehicle controls ($F_{(12, 234)} = 3.615$, $P < 0.0001$, **Figure 2A**). Tukey's multiple comparisons test identified significant weight loss on week 1, 2, and 3, with gradual weight gain starting at week 4. The high dose oxaliplatin-treated male C57BL/6J mice returned to baseline weights by week 7 and continued to have stunted weight gain through 10 weeks ($P < 0.0001$) compared to vehicle-treated animals. Likewise, female C57BL/6J mice treated with the high dose of oxaliplatin lost 6 % their body weight during the injection periods, which was a statistically significant change ($F_{(12, 234)} = 2.743$, $P = 0.0017$), however, they returned to their baseline measures one week after the last injection and caught up with vehicle controls by week 7. The low-dose treated females showed nearly identical profile of body weight gain as the vehicle group (**Figure 2B**). High-dose oxaliplatin treatment induced a more profound body weight reduction in male C57BL/6J than female C57BL/6J or male BALB/cJ mice ($F_{(1, 52)} = 6.360$, $P = 0.0148$; $F_{(1, 41)} = 21.39$, $P < 0.0001$; respectively; **Supplementary Table 1A-B**).

Overall, comparable to C57BL/6J mice, vehicle-treated BALB/cJ mice steadily gained weight over the course of the study. Similarly, low dose oxaliplatin did not affect body weight in male nor female BALB/cJ mice. The high-dose oxaliplatin treatment significantly reduced body weight in male BALB/cJ mice after the second wave of injections (week 3), as compared to vehicle controls ($F_{(10, 105)} = 2.525$, $P = 0.02$, **Figure 2C**). This effect on body weight was transient as the BALB/cJ male mice rapidly regained weight and had body weights indistinguishable from vehicle controls by week 5. While the high-dose oxaliplatin regimen did not cause weight loss in female BALB/cJ mice, it stunted their weight gain, as compared to vehicle controls ($F_{(12, 162)} = 3.438$, $P = 0.0002$). Tukey's multiple comparisons test identified significant effects of high-dose oxaliplatin on preventing weight gain in female BALB/cJ mice at week 3 and week 4, though these oxaliplatin-treated mice caught up to vehicle controls by week 5 (**Figure 2D**).

Assessments of Stimulus-Evoked Nociceptive Behaviors

Oxaliplatin Induces Long-term and Dose-dependent Mechanical Hypersensitivity

We tested the effects of two doses of oxaliplatin on the time-course of stimulus-evoked nociception-related behaviors. No significant difference in mechanical threshold was observed between groups at baseline. Both doses of oxaliplatin caused a comparable long-term mechanical hypersensitivity in both sexes of both strains of mice (**Supplementary Table 1A-B**). Five injections of 3.0 mg/kg oxaliplatin reduced mechanical thresholds in all subjects, regardless of sex or strain. Further, all subjects treated with 10 injections of oxaliplatin (low-dose and high-dose) mechanical hypersensitivity for up to 10 weeks. Male C57BL/6J mice treated with low and high dose of oxaliplatin developed significant mechanical hypersensitivity $F_{(10,240)} = 10.52$, $P < 0.0001$;

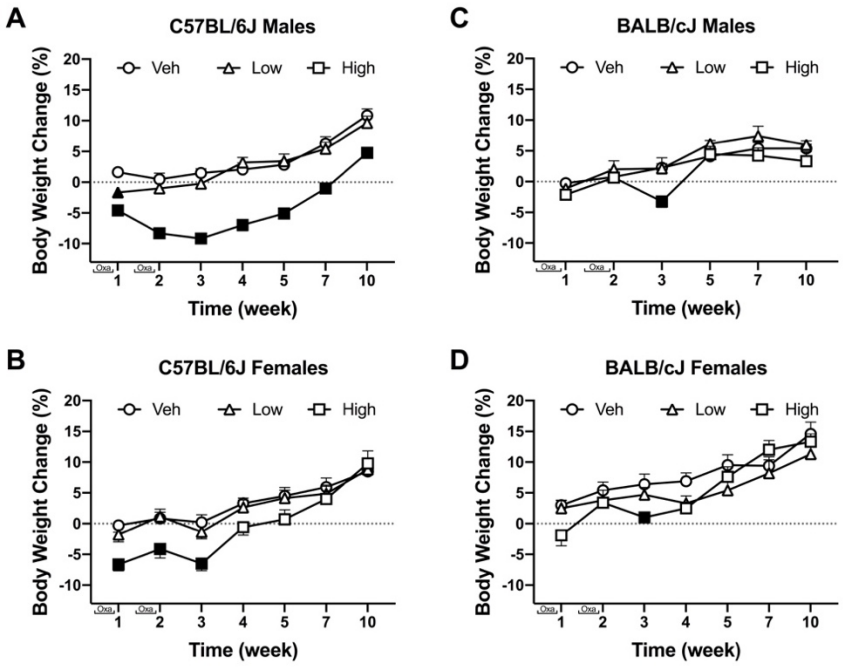

Figure 2. The effect of oxaliplatin on body weight changes from baseline over the course of a 10-week observation period. C57BL/6J males (n = 14/group) (A) C57BL/6J females (n = 14/group) (B) BALB/cJ males (n = 7-9/group) (C) BALB/cJ females (n = 10/group) (D). Filled points indicate times at which body weight was statistically different from vehicle. Values are expressed as mean ± SEM. Results were compared using two-way ANOVA (Treatment, Time as RM) for each strain and for each sex followed by Tukey's post hoc test, $p < 0.05$.

Figure 3A), however, the low-dose treated males showed significant difference from the high-dose group at week 11 ($P = 0.0105$). Female C57BL/6J mice developed mechanical hypersensitivity following high-dose oxaliplatin treatment ($F_{(10, 155)} = 5.896$, $P < 0.0001$; **Fig. 3B**). Interestingly, administration of the low dose regimen did not decrease the mechanical threshold at week 1-time point. No difference was found between the low- and high-dose treatments at weeks 3 through 10. BALB/cJ males treated with the low- or high-dose oxaliplatin were significantly different from the control vehicle group after the first 5 injections and remained hypersensitive until the end of experiment ($F_{(10, 105)} = 5.797$, $P < 0.0001$; **Figure 3C**). Likewise, the mechanical threshold of BALB/cJ females subjected to both the low- and high doses of oxaliplatin reached significantly reduced mechanical threshold at week 1 and remained low until the end of the experiment ($F_{(10, 125)} = 8.335$, $P < 0.0001$; **Figure 3D**).

Oxaliplatin Induces Cold Hypersensitivity in C57BL/6J Mice

Cold hypersensitivity is a hallmark of oxaliplatin-induced neuropathy, and it that can be measured in rodents via acetone test. A dose-dependent effect on the time course of cold hypersensitivity was observed in male C57BL/6J mice (n = 8 per group; $F_{(10, 105)} = 3.852$, $P = 0.0002$). The low-dose of oxaliplatin treatment significantly increased the duration of acetone-elicited behaviors as compared to vehicle control at week 3 only ($P < 0.0001$; **Figure 3E**). The high-dose group showed an increased in responses to acetone at weeks 1,3, and 4 ($P = 0.024$, $P = 0.0005$, and $P < 0.0001$, respectively). Corresponding results were found in female C57BL/6J mice (**Figure 3F**). The low dose significantly increased response time in female C57BL/6J mice after the first and second week of injections (n = 8 per group; $F_{(10, 105)} = 4.011$, $P = 0.0001$; $P < 0.0001$, $P = 0.0012$), while the high dose of oxaliplatin prolonged the duration of acetone-elicited behaviors

until week 4 ($P = 0.041$). Excess locomotion activity of male and female BALB/cJ on the elevated mesh hindered performing the acetone test, hence no data is available.

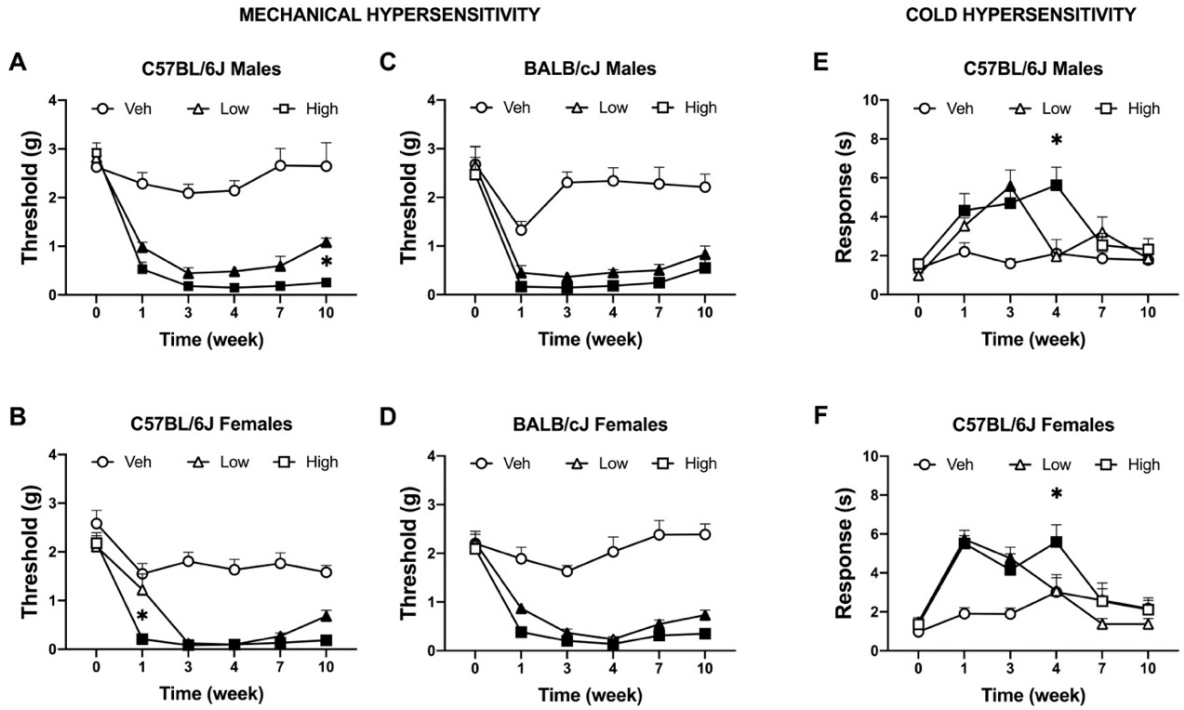

Figure 3. Induction of mechanical and cold hypersensitivity by low and high dose of oxaliplatin. Development of mechanical hypersensitive was monitored after each regimen of oxaliplatin (5 injections of 0.3 or 3 mg/kg) with the von Frey test in C57BL/6J males (n = 17/group) (A), C57BL/6J females (n = 11/group) (B), BALB/cJ males (n = 7-9/group) (C), BALB/cJ females (n = 10/group) (D). Similarly, cold hypersensitivity was tested on the same week in in C57BL/6J males (n = 8/group) (E), C57BL/6J females (n = 8/group) (F). Values are expressed as mean ± SEM. Results were compared using two-way ANOVA (Treatment, Time as RM) for each strain and for each sex followed by Tukey's post hoc test, $p < 0.05$. Filled points indicate times at which mechanical hypersensitivity was statistically different from vehicle. * $p < 0.05$ high vs low dose**.**

Oxaliplatin Has Strain-, Sex-, and Assay-dependent Effects on Spontaneous Behaviors

Oxaliplatin Reduces Locomotor Activity in C75BL/6J Male Mice

The high dose of oxaliplatin significantly reduced locomotor activity in male C57BL/6J mice ($F_{(12, 134)} = 1.915$, $P = 0.0377$). Decreases in locomotor activity were observed after completion the first and second regimens as compared to vehicle controls. This reduction was still observed one week post last injection of the drug (**Figure 4A**). Although, there was a significant

effect of time {F_{time} (6, 114) = 13.67, $P < 0.0001$}, and dose {F_{dose} (2, 45) = 4.75, $P = 0.0134$}, with no significant interaction between time and dose {$F_{interaction}$ (12, 114) = 1.506, $P = 0.1218$} in female C57BL/6J mice, as revealed by two-way ANOVA analysis. In addition, the Tukey post hoc analysis indicated a decrease in the number of beam breaks in female C57BL/6J mice as compared to vehicle controls at week 4 ($P = 0.0053$, **Figure 4B**). In contrast, no alterations in the locomotor activity were observed in BALB/cJ males and females after administration of the two doses of oxaliplatin till week 5 of testing. Strain comparison indicated a significant difference between female C57BL/6J and female BALB/cJ mice treated the high dose of oxaliplatin ($F_{(1, 104)} = 7.881$, $P = 0.006$, **Supplementary Table 1B**).

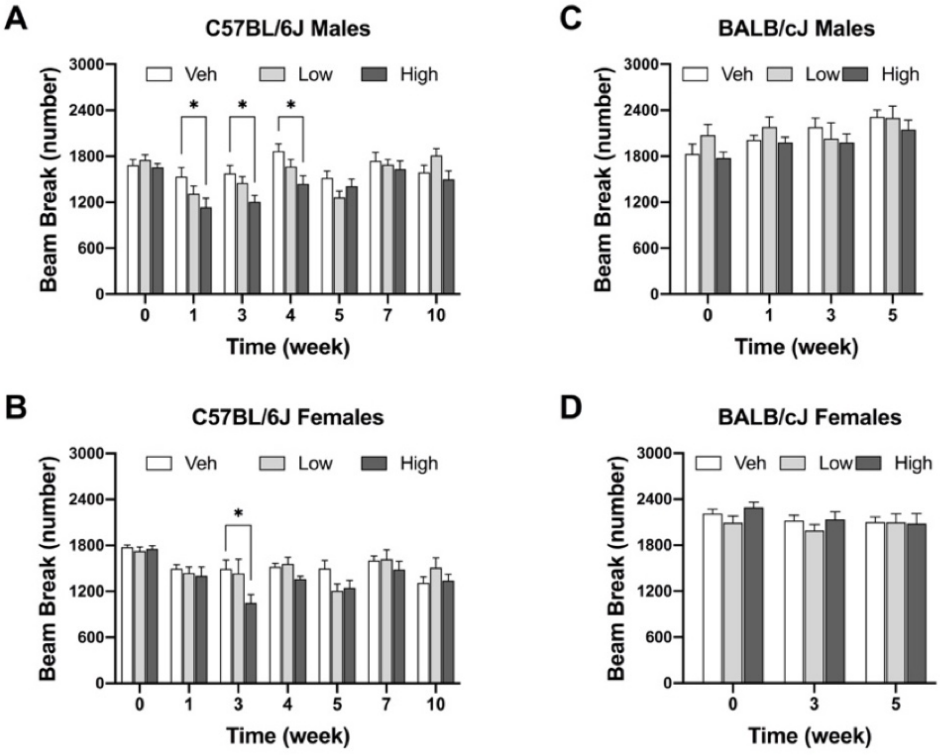

Figure 4. High dose of oxaliplatin reduce spontaneous locomotor activity in C57BL/6J mice. One regimen of the high dose of oxaliplatin was sufficient to reduce locomotor activity in C57BL/6J males (n = 8-10/group) (A) which continued one week after the treatment. C57BL/6J females (n = 6-8/group). (B) showed lower activity after two regimens. No alteration in motor coordination was obsessed in BALB/cJ males (n = 7-9/group) (C) nor females (n = 10/group) (D). Overall effects of oxaliplatin treatment were identified by two-way or mixed-analysis model ANOVA (Treatment, Time as RM) for each strain and for each sex with post-hoc Tukey's multiple comparisons test, * $p < 0.05$.

Oxaliplatin Does Not Affect Voluntary Wheel Running

Oxaliplatin treatment did not significantly change voluntary wheel running at any of the investigated time points. Male C57BL/6J mice treated with high-dose oxaliplatin were trending towards a decreased in wheel running, however, with no significant interaction between time and dose {$F_{interaction}$ (12, 138) = 1.382, P = 0.1813} as revealed by two-way ANOVA analysis. Irrespectively of treatment, strain, or sex, animals ran more over time with repeated exposure to the running wheels (**Figure 5**).

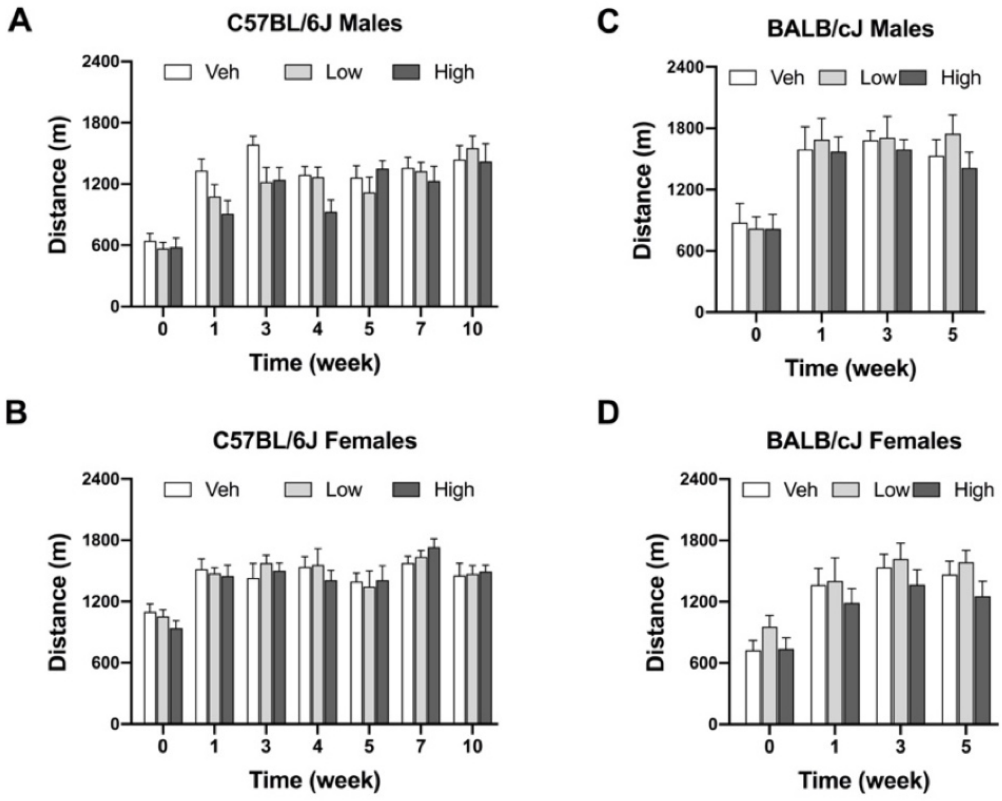

Figure 5. Oxaliplatin has no effect on voluntary wheel running in mice. C57BL/6J males (n = 8-10/group) (A), C57BL/6J females (n = 6-8/group) (B), BALB/cJ males (n = 7-9/group) (C), BALB/cJ females (n = 10/group) (D). Values are expressed as mean ± SEM. Results were analyzed using two-way or mixed-analysis model ANOVA (Treatment, Time as RM) for each strain and for each sex followed by Tukey's post hoc test, $p < 0.05$.

Oxaliplatin Reduces Exploration of Light/dark Boxes in Female C57BL/6J Mice

The high-dose oxaliplatin treatment significantly decreased the time spent in the light compartment of the LDB apparatus only in female C57BL/6J mice at the 4-week time point, as compared to the vehicle controls ($F_{(6, 51)} = 2.641$, $P = 0.021$; veh vs high dose, $P = 0.0021$). This effect was transient and by week 7 these animals matched their control group. No effects of oxaliplatin on LDB performance were observed in female BALB/cJ mice (**Figure 6D**). For BALB/cJ males, there was a trend towards elevated time spent in the light compartment (**Figure 6C**) with significant effect of dose {$F_{dose}(2, 21) = 6.479$, $P = 0.0064$} and no significant interaction

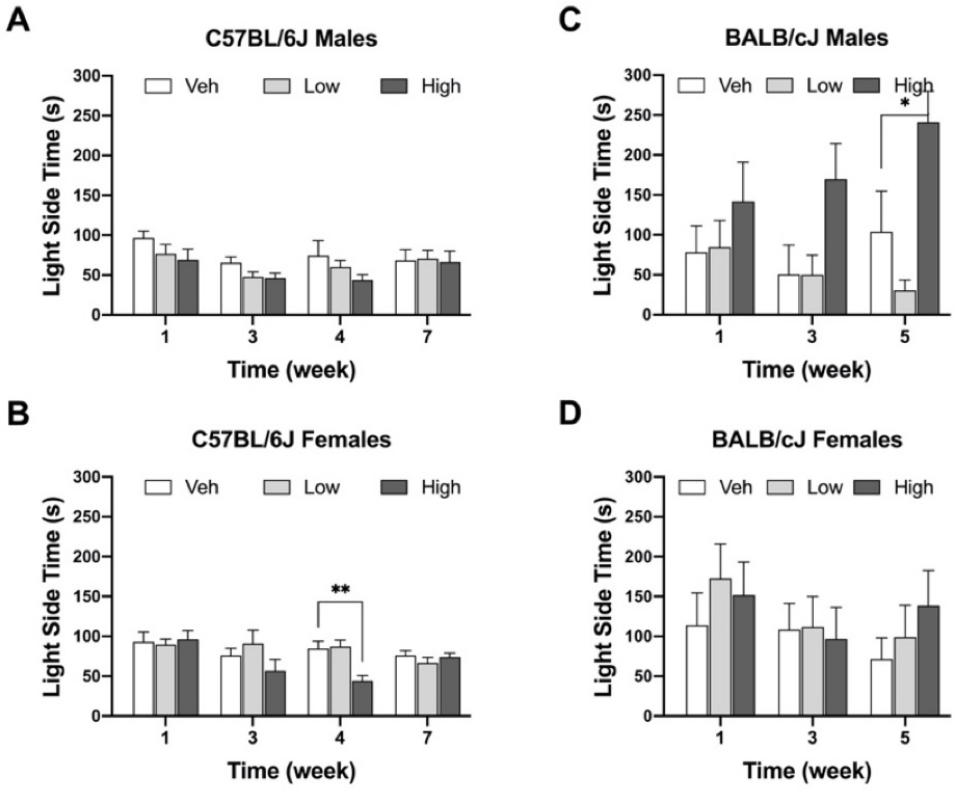

Figure 6. Decrease in time spend in the light area after oxaliplatin exposure. Anxiety-like behavior was assessed in C57BL/6J males (Cohort 1, BL and week 3, n = 9/group; Cohort 2, week 4 and week 7, n = 8/group) (A), C57BL/6J females (Cohort 1, BL and week 3, n = 9/group; Cohort 2, week 4 and week 7, n = 8/group) (B), BALB/cJ males (n = 7-9/group) (C), BALB/cJ females (n = 10/group) (D). Values are expressed as mean ± SEM. Overall effects of oxaliplatin treatment were identified by two-way mixed-analysis model ANOVA (Treatment, Time as RM) for each strain and for each sex ANOVA with post-hoc Tukey's multiple comparisons test, ** $p < 0.001$.

between time and dose {$F_{interaction}$ (4, 42) = 1.591, P = 0.1944} as revealed by two-way ANOVA analysis. Tukey's multiple comparison test indicated a significant increase in the time spent in the light chamber in male BALB/cJ mice as compared to vehicle controls at week 5 (P = 0.025)**.** Testing of BALB/cJ mice was discontinued after week 5 due to equipment malfunction.

Oxaliplatin Induces Aversion to 3% Sucrose Solution in the Two-Bottle Choice Test

The first 5 injections of high dose oxaliplatin caused a significant drop of sucrose preference in both C57BL/6J and BALB/cJ mice compared to their control groups. C57BL/6J males showed a significant deficit in sucrose preference below on day 5 and 15 ($F_{(10, 105)}$ = 4.591, P < 0.0001; P = 0.0001 and P = 0.0037, respectively). No statistically significant difference was observed in the C57BL/6J males beyond that time point, and the preference recovered to the vehicle group. The mean preference for sucrose in the female C57BL/6J group treated with a high-dose of oxaliplatin was also reduced to 40% after the 5th injection and persisted for two more weeks ($F_{(10, 110)}$ = 43.703, P = 0.0003, **Figure 7B**). Notably, the reduction in sucrose preference by oxaliplatin was more pronounced and lasted much longer in male BALB/cJ than male C57BL/6J mice ($F_{(1, 27)}$ = 25.00, P < 0.0001, **Supplementary Table 1B**). Male BALB/cJ mice showed significantly diminished sucrose preference compared to control mice on day 1, 5, 15, 24, 32, 43, 57 and 64 ($F_{(16, 96)}$ = 1.795, P = 0.0426) at the high dose of oxaliplatin (**Figure 7C**). Similarly, BALB/cJ females showed significantly diminished sucrose preference compared to control mice on day 1, 5, 24, 32 and 43 ($F_{(18, 135)}$ = 2.116, P = 0.0082) upon receiving the high dose regimen of oxaliplatin (**Figure 7B**). The low-dose of oxaliplatin did not cause significance decrease in sucrose preference in both BALB/cJ male and female mice (**Figure 7**). High-dose oxaliplatin treated male C57BL/6J mice decreased their fluid intake until 35 days post first administration of the drug while the low-dose treated male C57BL6J mice consumed less fluid on day 1, 24, and 35 ($F_{(10, 105)}$ = 3.033, P =

0.00021; **Fig 7E**). Although, female C57BL/6J mice subjected to the low dose oxaliplatin consumed comparable fluids to the control group, the high dose-treated females reduced drinking on days 1, 5, 15 and 25 ($F_{(10, 110)} = 3.238$, $P = 0.0011$; **Fig 7F**). Fluid consumption behavior was not altered by either does of oxaliplatin in BALB/cJ mice (**Fig 7G-H).**

Oxaliplatin Does Not Change Nesting Behavior

The effect of oxaliplatin on innate behavior was measured in the nest-building tests. The test was administered in the vehicle and high-dose treated C57BL/cJ mice. Neither males nor females C57BL/6J treated with oxaliplatin performed differently than their control groups after completion of each treatment regimen. Similarly, BALB/cJ mice treated with low or high dosage of oxaliplatin were unaffected in their nesting behavior (**Figure 8A-D**).

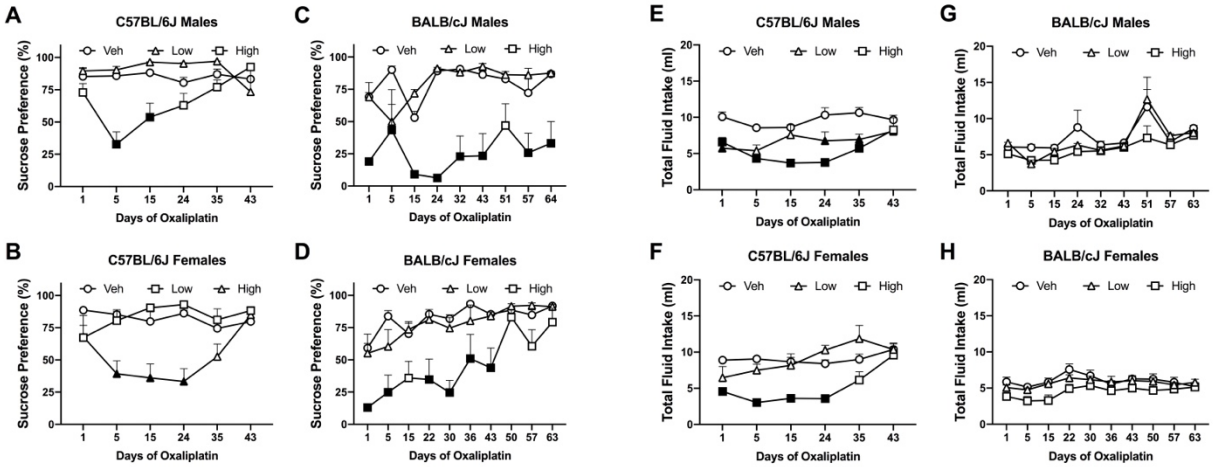

Figure 7. **Differential pattern of 3% sucrose solution preference among oxaliplatin-treated animals**. Preference was tested in a two-bottle choice test in C57BL/6J males (n = 4-10/group) (A), C57BL/6J females (n = 4-10/group) (B), BALB/cJ males (n = 4-6/group) (C), and BALB/cJ females (n = 10/group) (D). The total fluid intake is summarized in C57BL/6J males (n = 4-10/group) (E), C57BL/6J females (n = 4-10/group) F), BALB/cJ males (n = 4-6/group) (G), and BALB/cJ females (n = 10/group) (H). Values are expressed as mean ± SEM. Results were compared using two-way ANOVA (Treatment, Time as RM) for each strain and for each sex followed by Tukey's post hoc test, $p < 0.05$. Filled points indicate times at mechanical hypersensitivity was statistically different from vehicle.

Oxaliplatin Does Not Change Burrowing Behavior

Oxaliplatin did not alter burrowing activity in C57BL/6J mice when observed after completion of the first and second treatment regimens ($F_{(1, 18)} = 0.00171$, $P = 0.9674$, males; $F_{(1, 18)} = 0.7891$, $P = 0.0.3861$, females; **Figure 8E-F**). Comparably, oxaliplatin treatment had no effect on bedding displacement in either sex of BALB/cJ mice at week 3 ($F_{(2, 11)} = 0.4666$, $P = 0.6390$, males; $F_{(2, 27)} = 0.9337$, $P = 0.4054$, females; **Figure 8G-H**)

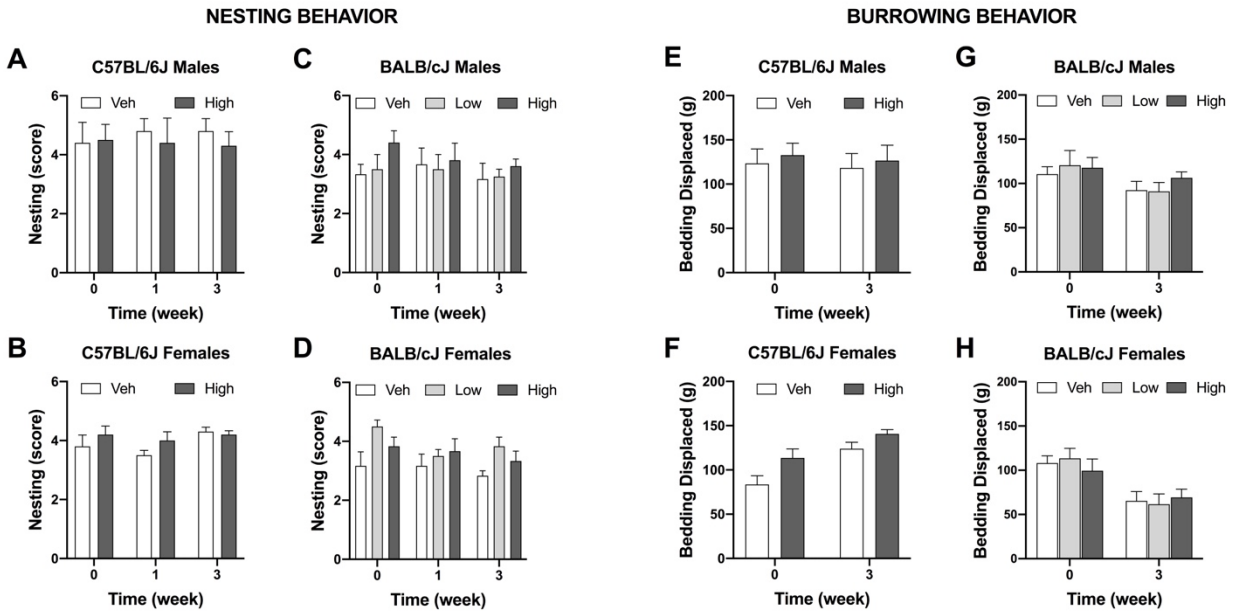

Figure 8. Oxaliplatin has no effect on burrowing and nesting behavior in mice. Nest consolidation after 2 hours in C57BL/6J males (n = 10/group) (A), C57BL/6J females (n = 10/group) (B), BALB/cJ males (n = 4-6/group) (C), and BALB/cJ females (n = 6/group) (D). Burrowing assessment is depicted for C57BL/6J males (n = 10/group) (E), C57BL/6J females (n = 10/group) (F), BALB/cJ males (n = 4-6/group) (G), BALB/cJ females (n = 6/group) (H).

Oxaliplatin Has Sex- and Strain-dependent Effects on Caudal Nerve Conductance

Caudal NCV and SNAP of male and female C57BL/6 and BALB/cJ were measured to determine the functional effect of oxaliplatin on peripheral sensory nerves at baseline (pretreatment and 4 and 7 weeks post-treatment). First, we determined sex and strain differences in nerve

conduction amplitude and velocity at baseline. The SNAP and NCV of male and female C57BL/6J mice was statistically different, while male BALB/cJ mice had a lower SNAP and higher NCV than female BALB/cJ mice ($F_{(3, 96)} = 13.25$, $P < 0.0001$; $P = 0.0233$, $P < 0.0001$). Moreover, strain differences in the nerve conduction amplitude differed between both sexes (**Supplementary Figure 1B**). Male and female C57BL/6J mice had a significantly higher amplitudes than male and female BALB/cJ mice, respectively (**Supplementary Figure 1A**: $P < 0.0001$ male C57BL/6J vs BALB/cJ; **Supplementary Figure 1B**: $P = 0.0233$ female C57BL/6J vs female BALB/cJ), and the baseline NCV of male C57BL/6J was lower than male BALB/cJ mice ($P < 0.0001$) One-way ANOVA revealed a significant impact of high-dose oxaliplatin on SNAP in BALB/cJ females compared to vehicle group at week 4 ($F_{(4, 54)} = 2.888$, $P = 0.001$, **Figure 9D**). No significant changes were observed in nerve conduction velocities post oxaliplatin treatment (**Figure 9E-H**).

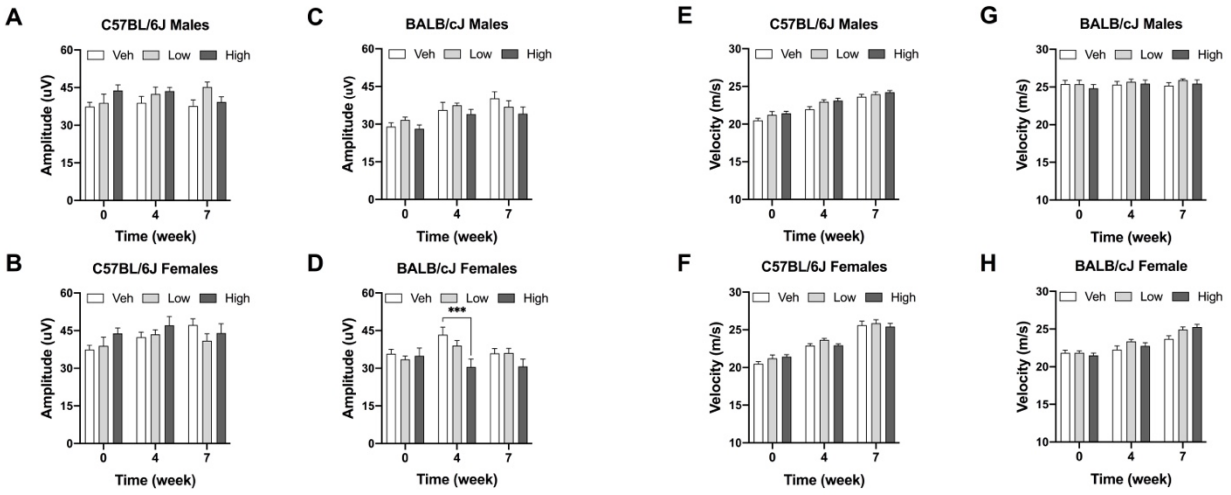

Figure 9. Electrophysiological analysis of the caudal sensory nerves. Electrophysiological analysis of the caudal sensory nerves. One-week post completion of oxaliplatin or vehicle treatment, sensory nerve conduction amplitude A,B,C,D) and velocity (E,F,G,H) were measured in C57BL/6J males and females (n = 8/group) and BALB/cJ males and females (n = 7–10/group). Values are expressed as mean ± SEM. Overall effect of oxaliplatin treatment per sex of each strain was identified using two-way ANOVA and post-hoc Tuckey's test (***p < 0.001).

Oxaliplatin Treatment Reduces Intraepidermal Nerve Fiber Density in the Ventral Surface of the Hind Paw

The density of IENFs was evaluation in hind paw samples after completion of behavioral testing at week 11. Both doses of oxaliplatin significantly reduced IENF density in male C57BL/6J mice, as compared to vehicle control (One-way ANOVA: $F_{(2, 16)} = 7.311$, $P = 0.0035$, low vs veh $P = 0.0035$, high vs veh $P = 0.0298$). Comparably, C57BL/6J females presented a similar pattern of the nerve fiber loss (One-way ANOVA: $F_{(2, 15)} = 9.437$, $P = 0.0022$, low vs vehicle $P = 0.0015$, high vs vehicle $P = 0.0132$; **Figure 10A**). A dose-related decrease of IENF density was observed in female BABL/cJ mice where only the high-dose treated mice demonstrated reductions in the density of IENFs when compared to vehicle-treated group (One-way ANOVA: $F_{(2, 15)} = 14.3$, $P = 0.0003$; **Figure 10B**). However, BALB/cJ males treated with the anti-tumor drug had similar density of IENF to the control group. Representative foot pad sections from stained for PGP9.5 protein show the variation in IENFs density following oxaliplatin treatment (**Figure 10C**).

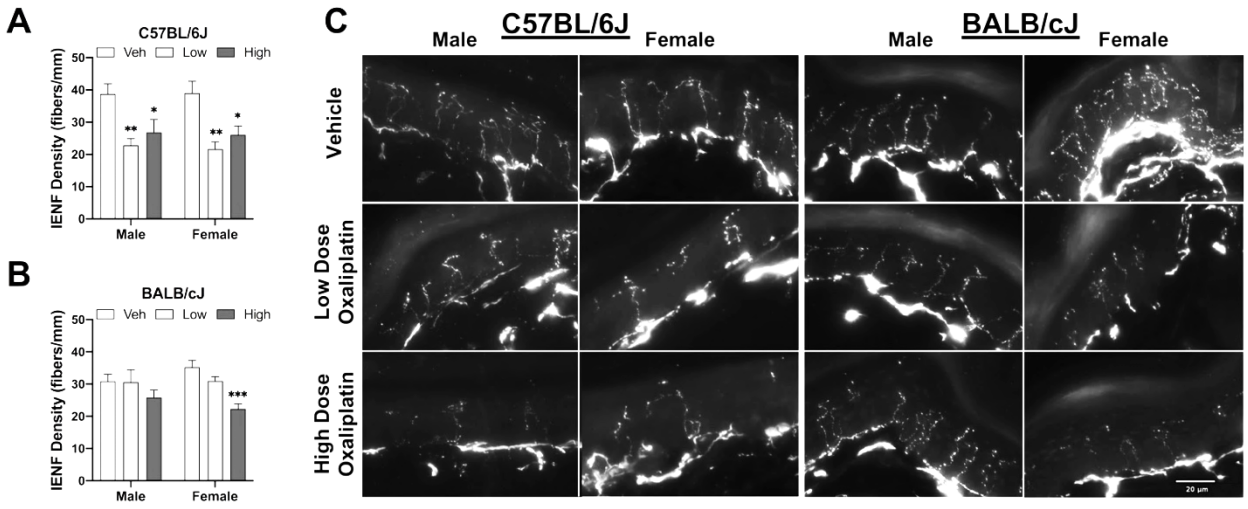

Figure 10. Reduction of intraepidermal nerve fiber density in the hind paw at week 11. Figure (**A**) shows C57BL/6J males and females (n = 6/group), while changes to IENF density in BALB/cJ males and females (n = 6/group) are shown in (**B**). Representative fluorescence microscopic images of IENF taken at 40X (**C**). Values are expressed as mean ± SEM. Overall effects of oxaliplatin treatment per sex of each strain were identified using one-way ANOVA Treatment) for each strain and for each sex, and *post-hoc* Dunnet's test (* $p < 0.05$; ** $p < 0.001$; *** $p < 0.0001$).

3.1.4. Discussion

Oxaliplatin is a platinum-based chemotherapeutic agent widely used for colorectal cancer therapy and other gastrointestinal tumors, but its use is associated with various adverse effects, including OIPN (Beijers et al., 2014; Saltz et al., 2008). Clinically, OIPN appears in two distinct forms: an acute and transient neuropathy that develops in almost 90% of patients within hours of infusion that can last up to 7 days, and in 40-80% of patients develop a chronic dose-limiting cumulative sensory neuropathy (Argyriou et al., 2013). OIPN is also associated with functional impairment and affective disorders (depression and anxiety) induced by the drug, reducing the quality of life for many cancer patients (Avan et al., 2018; Currie et al., 2019b; Oh & Cho, 2020). Pre-clinical models play a pivotal role in understanding the pathophysiology of OIPN and in testing potential therapies. Unfortunately, this translational effort has not been very successful, and no effective preventive treatment exists. In addition, pharmacological management of OIPN related pain remains very challenging. Possible reasons for this could include limitations and inconsistencies in the experimental design of animal studies, such as the use of single dosing regimen, different testing times post treatment, the lack of testing in both sexes, and the genetic background of animals. In addition, the use of outcome measures and behavioral endpoints other than sensory gain, that are translatable to the human pain-related experiences is not common (Currie et al., 2019a).

In consideration of the aforementioned factors, this study examined alterations in the nociceptive, behavioral, and morphological aspects of OIPN in both sexes of C57BL/6J and BALB/cJ mice. The impact of oxaliplatin on affective-like behaviors was measured at multiple time points via battery of testing, which included light/dark boxes, sucrose preference, wheel running, nesting, and burrowing. Overall, our results demonstrate that C57BL/6J mice seem more

sensitive to oxaliplatin-induced behavioral changes compared to BALB/cJ mice, with the exception of change in preference for sucrose solution. In addition, oxaliplatin had sex-, dose-, and strain-dependent effects on caudal nerve conduction and IENF degeneration. Furthermore, none of the low-dose regimen treated mice showed changes in affective-like behaviors.

Sensory nociceptive changes in rodents are routinely assessed via cold and mechanical hypersensitivity. Administration of 5 injections of the low oxaliplatin dose triggered mechanical hypersensitivity at week 1 in male and female BALB/cJ mice. In contrast, male C57BL/6J but not female C57BL/6J mice developed mechanical hypersensitivity at week 1. Regardless of sex or strain, all mice exhibited mechanical hypersensitivity after completion of the high-dose regimen of oxaliplatin. Treatment with the low and high doses of oxaliplatin produced significant mechanical hypersensitivity that persisted throughout the observation period of 10 weeks. In the same OIPN model, Ta and colleagues reported mechanical hypersensitivity lasted until week 6 of the experimental timeline in male C57BL/6J mice treated with the high dose of oxaliplatin (Ta et al., 2009b). However, in Ta's et al. measurements were carried out with electronic filaments, while we used manual filaments. In regard to cold and mechanical hypersensitivity, the literature on oxaliplatin-induced peripheral neuropathy shows heterogeneity in terms of experimental set up, dose, and route of administration (Pozzi et al., 2020; Renn et al., 2011).

Cold-sensitive sensory symptoms is a main clinical feature of OIPN (Kang et al., 2020). In line with clinical and animal data, our results show time- and dose-dependent cold hypersensitivity in both sexes of C57BL/6J mice. Male C57BL/6J mice showed an increase in response to acetone after the first week of high-dose oxaliplatin treatment that persisted for at least one week after cessation of the treatment regimen. Similarly, Meade et al. demonstrated that oxaliplatin causes cold hypersensitivity in male and female C57BL/6J mice (Meade et al., 2021). Administration of

cumulative 3mg/kg of oxaliplatin spread over 15 days resulted in cold hypersensitivity that lasted for 1 week after last injection. Interesting, a single bolus of 3 mg/kg i.p. induced cold hypersensitivity in the acetone test that persisted for 3 weeks in male C57BL/6 mice (Andoh et al., 2019). One research group demonstrated that BALB/c mice treated with intravenous oxaliplatin may have greater cold hypersensitivity than C57BL/6 mice in the cold plate test (Marmiroli et al., 2017a). However, we were not able to assess cold hypersensitivity with the acetone test in female and male BALB/cJ mice due to excessive hyperactivity on the mesh testing apparatus.

Degeneration of intraepidermal nerve fibers has been implicated in neuropathic pain in preclinical and clinical studies (Meyer et al., 2011; Park & Koltzenburg, 2012a; Topp et al., 2000). IENFs are free nerve endings originate from unmyelinated and thinly myelinated nociceptors within the dermis. They play and important role in transmission of peripheral pain (Boyette-Davis & Dougherty, 2011). Various classes of chemotherapeutics have been shown to cause structural changes and degradation of unmyelinated nerve fibers, suggesting a common etiology of CIPN (G. J. Bennett et al., 2011; H. Zheng et al., 2012). With respect to IENF changes, we observed that C57BL/6J mice showed differential degeneration of IENF compared to BALB/cJ mice as both the low and high oxaliplatin doses caused a significant reduction of IENF density in C57BL/6J mice 8 weeks after cessation of treatment. BALB/cJ mice showed sex-dependent decrease of the fibers' density: only the female BALB/cJ mice treated with the high dose of oxaliplatin had a significant degeneration of nerve fibers. In contrast to our findings, the work of Marmiroli et al. shows that BALB/c mice are more susceptible to the effects of intravenous treatment with 28 mg/kg oxaliplatin on IENF than C57BL/6, one-week post treatment completion (Marmiroli et al., 2017b). The discrepancy between these results could be explained by difference in timing of tissue collection, route of administration, and C57BL/6 substrain differences that could affect these

results (Taylor, 1972). Indeed, we and others recently reported that C57BL/6J and C57BL/6N substrains differ in their responses in acute and tonic pain models (Bryant et al., 2019; Ulker et al., 2020; Wotton et al., 2020).

Preclinical research on chemotherapy-induced peripheral neuropathy points to involvement of pro-inflammatory cytokines in modulation of peripheral nerve damage. Upon treatment with chemotherapy, tumor necrosis factor alpha (TNFα), IL-1 β and IL-6, and interferons alpha and gamma are all elevated (Basu & Sodhi, 1992; Gan et al., 1992; Ni et al., 2020; O'Brien et al., 1994). These cytokines contribute greatly to both pain and damage to neuron and supporting cells. Taken together, this suggest that neuropathies affect not just the peripheral nerves, but also the homeostasis of the skin. The innate immune response in C57BL/6 and BALB/c has been shown to differ. Upon with macrophage-activating lipopeptide-2 or lipopolysaccharide, macrophages derived from female C57BL/6 mice produced higher levels of TNF-alpha and interleukin than macrophages female BALB/c mice macrophages (Watanabe et al., 2004). Additionally, proinflammatory cytokine production is sexually dimorphic and variable depending on the genetic background of mice (Everhardt Queen et al., 2016). Underlying differences in immunological responses between the two strains might explain this phenomenon. Further, it is possible that sub-strain genetic variations might play an important role in the degree of degradation of IENF due to oxaliplatin treatment. Presence of mechanical hypersensitivity, despite loss of IENF, might be mediated by hyperactive and/or sensitized nociceptive fibers sensitized resulting from the release of chemical mediators of inflammation (Baral et al., 2019).

Oxaliplatin highly impacts peripheral sensory neurons (Carozzi et al., 2015). To measure alterations in peripheral nerve function and potential degradation of the myelinated fibers, the amplitude and velocity of the sensory caudal nerve conductions were measured. Our results

indicate that the SNAP was significantly affected by the high dose of oxaliplatin in female BALB/cJ mice only. Similarly, 28 mg/kg intravenous oxaliplatin reduced the action potential amplitude in tails of female BALB/c mice (Renn et al., 2011). Platinum compounds, such as oxaliplatin, irreversibly bind to DNA thus inducing damage and apoptosis of primary sensory neurons (R. Velasco & Bruna, 2010). While sensory nerve conduction examines large-fiber neuropathy, skin innervation is a parameter of small-fiber sensory neuropath (Sumner et al., 2003). CIPN patients diagnosed with loss of IENF can have normal nerve conduction results (Devigili et al., 2008; Løseth et al., 2008). Correspondingly, in our study, C57BL/6J mice showed reduced mechanical hypersensitivity and IENF density but no changes in the caudal sensory nerve amplitude. The results of a quantitative analysis by Marmiroli and colleagues reports significant reduction of DRG neuronal structures upon oxaliplatin treatment (Marmiroli et al., 2017b). However, DRG from oxaliplatin-treated C57BL6 mice did not different from their naïve controls. This further confirms that oxaliplatin impairment of neurophysiological morphology and functions is distinctive among different strains of mice.

Body weight can be an indication of rodent welfare. Male C57BL/6J mice treated with high-dose regimen of oxaliplatin lost more weight and took longer to return to baseline body weights than female C57BL/6J or male BALB/cJ mice (**Supplementary Table 1A-B**). The high dose of oxaliplatin caused a significant decrease in BALB/cJ females one week post last administration of the antineoplastic agent. Reduction of body weights or slower body gain due to platinum-based chemotherapeutics, such as oxaliplatin, was noted by others in male rats and C57BL/6J mice and BALB/c mice (Feather et al., 2018; Jamieson et al., 2005; Le Bricon et al., 1995). It has been shown that male C57BL/6J mice treated with the same treatment regimen of oxaliplatin experienced skeletal myopathy (Sorensen et al., 2017). Both male and female C57BL/6J mice decreased their

spontaneous locomotor activity. A similar finding was observed in male C57BL/6J mice with reduced locomotor activity (Ta et al., 2009a). The changes in body weight and locomotor disturbances indicate that BALB/cJ mice are less sensitive to oxaliplatin-induced toxicity.

Pain is a complex phenomenon that has both sensory and emotional components (Raja et al., 2020). Additionally, reflexive reactions to nociceptive stimuli do not necessarily indicate the experience of spontaneous pain in humans (Finnerup et al., 2016). According to epidemiological studies, the prevalence of depression may be as high as 85% in patients suffering from chronic pain (Bair et al., 2003; Williams et al., 2003), and around 30% for patients suffering from neuropathic pain (Gustorff et al., 2008). Individuals diagnosed with depression report increased frequency and severity of acute pain. Furthermore, the magnitude and duration of acute pain has indicated higher level of anxiety and depression in people (Michaelides & Zis, 2019). Pre-clinical models of nerve injury induced by mechanical, chemotherapeutic, or inflammatory insults saw changes in affective behavior suggestive of a depression-like state(Jesse et al., 2010; Okun et al., 2016; Toma et al., 2017a). Correspondingly, it has been reported that male C57BL/6J mice treated single i.p. dose of 6 mg/kg oxaliplatin showed an increased immobility time in forced swim test, suggesting that oxaliplatin can induce depressive-like behavior in rodents (Micov et al., 2020).

In our study, the low dose of oxaliplatin did not affect the behavioral assays measured at the tested time points in mice in both mouse strains. The high-dose of oxaliplatin had some impact on female C57BL/6J. We show that female C57BL/6J treated with high-dose of oxaliplatin spent significantly more time in the dark side, indicating an increase in anxiety-like behavior. This is first study to report testing anxiety-like behavior via light/dark box in mice treated with oxaliplatin. Anxiety-like behavior was measured and observed in a paclitaxel-induced peripheral neuropathy model. Repeated administration of the chemotherapeutic drug in C57BL/6J males caused a long-

lasting mechanical hypersensitivity and anxiety-like phenotype, as observed 9 weeks post treatment (Toma et al., 2017a). Two studies examining the impact of oxaliplatin on neurotoxicity in male Swiss mice and male Sprague-Dawley rats demonstrated reduction of time spent in the open arms and the percent of open arm entries in an elevated plus-maze assay, indicative of anxiety-like state (Reis et al., 2020; X. Zhou et al., 2020). Moreover, male C56BL/6J mice treated with oxaliplatin took a longer time to reach the center in a novelty suppressed feeding test; however, no difference in elevated plus maze were observed (Hache et al., 2015; Kerckhove et al., 2019). In a spared nerve injury model, female mice were identified as more susceptible to anxiety-like behavior (Sieberg et al., 2018). Conversely, oxaliplatin did not alter wheel running, nesting nor burrowing behaviors. These assays have been shown to reflect motivation and innate behaviors that are used to assess general well-being of rodents. While BALB/c and C57BL/6 mice are the most commonly used strain in anxiety and biomedical studies (Johnson, 2012), the literature is inconsistent on which stain is more anxious (Ennaceur & Chazot, 2016). Male BALB/cJ mice exhibited elevated time spent in the light compartment. This could have been attributed to freezing behavior, a sign of anxiety-like behavior. The general activity of these animals was not affected, as indicated by locomotor activity test results, however between-strain analysis identified significant difference between female C57BL/6J and BALB/cJ mice treated with high dose of oxaliplatin (**Supplementary Table 1B**). Overall, detection of behavioral depression of mice treated with oxaliplatin might be dependent on the assay. Characteristic phenotypical differences exist across mouse strain and they should be considered when selecting strain and sex of the rodents.

A large and long-term deficit was observed after oxaliplatin administration in the sucrose preference test. Rodents show a natural preference for the sweet taste (Valenstein et al., 1967), and a deficit in sucrose preference has been shown to be sensitive to different animal models of

depression (Harkin et al., 2002; Willner et al., 1992). We observed a decreased preference for a 3% sucrose solution in both C57BL/6J and BALB/cJ mice treated with the high-dose oxaliplatin regimen. Oxaliplatin treatment produced a longer-lasting reduction of sucrose preference in BALB/cJ males than C57BL/6J males, even though both had significant mechanical hypersensitivity for the duration of the study (**Supplementary Table 1B**). The decrease in sucrose seen in C57BL/6J males and female mice at the higher dose regimen of oxaliplatin may be the consequence of a general decrease in drinking behavior. It should be noted that a significant decrease in body weight was noted in these oxaliplatin-treated mice. Future studies assessing quinine and saccharine preference will be useful to understand if oxaliplatin's effects on sucrose preference in C57BL/6J mice are not due to sensory loss. Total fluid intake was not altered in BALB/cJ mice undergoing the high-dose oxaliplatin regimen. It is possible that the sucrose preference deficit seen reflects taste alteration by oxaliplatin in mice. In the clinic, about 12% of patients receiving oxaliplatin report alteration in taste (90). However, in a pre-clinical paclitaxel-induced CIPN model, Toma et al., 2017 reported a transient reduction sucrose preference in C57BL/6J males accompanied by time-dependent changes in other affect-like behaviors. The aversion to sucrose preference was proposed to be mediated by kappa opioid receptor (KOR) signaling dysregulation, as the selective KOR antagonist norbinaltorphimine was able to reversible sucrose preference deficit (Meade et al., 2020). Another explanation for changes in sucrose preference is gustatory alteration induced by oxaliplatin. However, in our recent study, C57BL/6J and BALB/cJ mice subjected to the same high-dose oxaliplatin schedule consumed similarly number of sucrose pellets as the vehicle control group (Meade et al., 2021).

In this study, we looked at the differences in the development of oxaliplatin-induced neuropathy in male and female mice. The specific alterations in affect-like behaviors, IENF

density, and nerve conduction amplitude show different profiles of C57BL/6J and BALB/cJ mice. However, these changes are not uniform across strains indicating strain differences as well. A three-way ANOVA with repeated measures was performed to investigate the interaction between sex, treatment, and time (**Supplementary Table 1A**). A significant difference in percent body weight of female and male was observed in C57BL/6J mice treated with the high dose of oxaliplatin and their control vehicle. We were not able to determine whether the cause of the body weight loss in C57BL/6J mice was caused by a decrease in fluid intake or reduction of lean and fat tissue mass as suggested (80). Regarding sex differences between male and female BALB/cJ mice, two behavioral assays showed trending statistical tendencies. BALB/cJ males tended to spent more time in the light compartment than the female BALB/cJ mice ($F_{(1, 95)} = 2.774$, $P = 0.0991$; **Supplementary Table 1A**). The second trending difference between male and female BALB/cJ mice treated with the high dose of oxaliplatin was alteration in in IENF density ($F_{(1, 20)} = 3.549$, $P = 0.0742$). While BALB/cJ females exhibited a significant reduction of IENF, male BALB/cJ mice had comparable IEND to their control group. One possible explanation of these sex differences is the role of hormonal mechanisms of OIPN. These differences can also be due to genetic and neuroimmune mechanisms of OIPN processing in male and female mice such as the release of pronociceptive substances substance P and calcitonin gene-related peptide, as well as exposure to pro-inflammatory cytokines released by infiltrating and resident immune cells (Carozzi et al., 2015).

This study has some limitations. While the primary aim of this study was to compare our results to literature on rodent studies using the same route of administration, oxaliplatin delivery method via intraperitoneal injections poses some translational limitations. The absorption, distribution, metabolism, or excretion of chemotherapeutic agents have been shown to influence the development of CIPN in human patients (Cliff et al., 2017; Lee et al., 2013). Moreover, a

pharmacokinetics study in rats showed significant differences in the AUC for peritoneal fluid and plasma drug concentrations after 90 minutes post treatment with 5 mg/kg of oxaliplatin (Pestieau et al., 2001). A future study assessing pharmacokinetics of oxaliplatin via intraperitoneal and intravenous routes of administration in C57BL/6J and BALB/cJ would be beneficial and could explain some of the observed differences. Additionally, it is plausible that the early time point behavioral alterations are associated with loss of IENF, hence, it would be useful to assess IENF density at week 3 or 5.

CONCLUSIONS

We demonstrated that affective-like behaviors in male and female C57BL/6J and BALB/cJ mice were differentially and dose-dependently affected by oxaliplatin. We demonstrate that the low and high treatments of oxaliplatin induced a long-lasting mechanical hypersensitivity which did not largely correlate with deficit in affect-like behaviors. The remaining portion of this chapter is dedicated to investigating whether the effect of NLRP3 inflammasome assembly inhibition seen in Chapter 2 would extend to the above mentioned oxaliplatin-induced peripheral neuropathy mouse model.

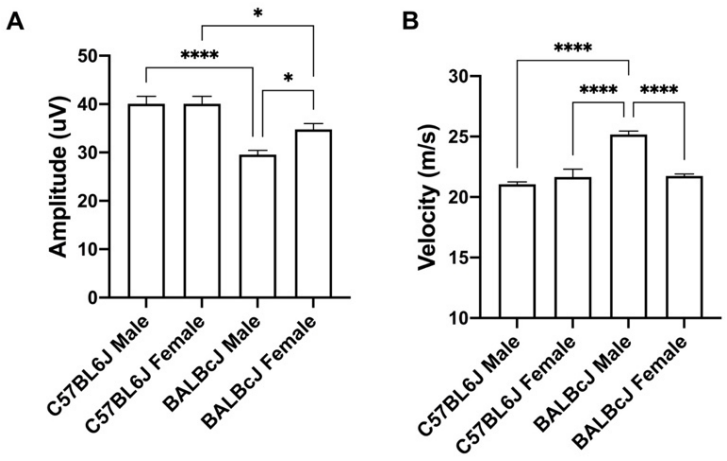

Supplementary Figure 1. Baseline Electrophysiological analysis of the caudal sensory nerves. Sensory nerve conduction amplitude(A) and velocity (B) were measured in C57BL/6J males and females (n = 8/group), and BALB/cJ males and females (n = 7-10/group) respectively. Values are expressed as mean ± SEM. Overall effects of oxaliplatin treatment per sex of each strain were identified using one-way ANOVA (Treatment) for each strain and for each sex, and *post-hoc* Tuckey's test (* $p < 0.05$, *** $p < 0.0001$).

A

Measurement	Males vs. Females	Treatment	Sex x Treatment
Percent Body Weight Change	C57BL/6J	Veh vs Low Dose	F (1, 52) = 0.03851; P=0.8452
		Veh vs High Dose	F (1,52)= 6.360; P=**0.0148**
	BALB/cJ	Veh vs Low Dose	F (1, 31) = 1.400; P=0.2458
		Veh vs High Dose	F (1, 33) = 0.04765; P=0.8286
Mechanical Hypersensitivity	C57BL/6J	Veh vs Low Dose	F (1, 53) = 1.122; P=0.2943
		Veh vs High Dose	F (1, 55) = 2.472; P=0.1216
	BALB/cJ	Veh vs Low Dose	F (1, 31) = 0.02937; P=0.8650
		Veh vs High Dose	F (1, 31) = 0.03572; P=0.8513
Cold Hypersensitivity	C57BL/6J	Veh vs Low Dose	F (1, 28) = 0.2260; P=0.6382
		Veh vs High Dose	F (1, 28) = 0.2858; P=0.5972
Locomotor Activity	C57BL/6J	Veh vs Low Dose	F (1, 224) = 0.5713; P=0.4505
		Veh vs High Dose	F (1, 226) = 1.116; P=0.2919
Light/Dark Box	C57BL/6J	Veh vs Low Dose	F (1, 116) = 0.2847; P=0.5947
		Veh vs High Dose	F (1, 116) = 0.5115; P=0.4759
	BALB/cJ	Veh vs Low Dose	F (1, 29) = 0.7639; P=0.3893
		Veh vs High Dose	F (1, 95) = 2.774; P=0.0991
Sucrose Preference	C57BL/6J	Veh vs Low Dose	F (1, 25) = 0.4840; P=0.4930
		Veh vs High Dose	F (1, 36) = 1.721; P=0.1979
	BALB/cJ	Veh vs Low Dose	F (1, 18) = 0.2419; P=0.6288
		Veh vs High Dose	F (1, 19) = 2.439; P=0.1349
Total Fluid Intake	C57BL/6J	Veh vs Low Dose	F (1, 25) = 10.56; P=**0.0033**
		Veh vs High Dose	F (1, 36) = 0.1929; P=0.6631
	BALB/cJ	Veh vs Low Dose	F (1, 19) = 0.03389; 0.8559
		Veh vs High Dose	F (1, 19) = 0.005325; 0.9426
Nerve Conduction Amplitude	BALB/cJ	Veh vs Low Dose	F (1, 30) = 0.6407; P=0.4298
		Veh vs High Dose	F (1, 31) = 0.7612; P=0.3897
IENF Density	C57BL/6J	Veh vs Low Dose	F (1, 21) = 0.06181; P=0.8061
		Veh vs High Dose	F (1, 20) = 0.02172; P=0.8843
	BALB/cJ	Veh vs Low Dose	F (1, 20) = 0.5786; P=0.4557
		Veh vs High Dose	F (1, 20) = 3.549; P=0.0742

B

Measurement	C57BL/6J vs. BALB/cJ	Treatment	Strain x Treatment
Percent Body Weight Change	Males	Veh vs Low Dose	F (1, 39) = 1.929; P=0.1728
		Veh vs High Dose	F (1, 41) = 21.39; P<**0.0001**
	Females	Veh vs Low Dose	F (1, 44) = 0.5143; P=0.4771
		Veh vs High Dose	F (1, 44) = 0.3482; P=0.5582
Mechanical Hypersensitivity	Males	Veh vs Low Dose	F (1, 46) = 0.008642; P=0.9263
		Veh vs High Dose	F (1, 49) = 0.2708; P=0.6051
	Females	Veh vs Low Dose	F (1, 38) = 0.5723; P=0.4540
		Veh vs High Dose	F (1, 37) = 0.4533; P=0.5050
Locomotor Activity	Males	Veh vs Low Dose	F (1, 128) = 3.475; P=0.0646
		Veh vs High Dose	F (1, 138) = 1.592; P=0.2092
	Females	Veh vs Low Dose	F (1, 104) = 0.2369; P=0.6275
		Veh vs High Dose	F (1, 104) = 7.881; P=**0.0060**
Light/Dark Box	Males	Veh vs Low Dose	F (1, 23) = 0.1954; P=0.6626
		Veh vs High Dose	F (1, 25) = 3.199; P=0.0858
	Females	Veh vs Low Dose	F (1, 51) = 0.2634; P=0.6100
		Veh vs High Dose	F (1, 27) = 0.09829; P=0.7563
Sucrose Preference	Males	Veh vs Low Dose	F (1, 20) = 2.029; P=0.1697
		Veh vs High Dose	F (1, 27) = 25.00; P<**0.0001**
	Females	Veh vs Low Dose	F (1, 23) = 0.8560; P=0.3645
		Veh vs High Dose	F (1, 28) = 2.759; P=0.1079
Total Fluid Intake	Males	Veh vs Low Dose	F (1, 22) = 6.307; P=**0.0199**
		Veh vs High Dose	F (1, 161) = 21.87; P<**0.0001**
	Females	Veh vs Low Dose	F (1, 23) = 0.4342; P=0.5165
		Veh vs High Dose	F (1, 28) = 6.314; P=**0.0180**
Nerve Conduction Amplitude	Females	Veh vs Low Dose	F (1, 32) = 0.1114; P=0.7408
		Veh vs High Dose	F (1, 32) = 5.241; P=**0.0288**
IENF Density	Males	Veh vs Low Dose	F (1, 21) = 7.535; P=**0.0121**
		Veh vs High Dose	F (1, 20) = 1.342; P=0.2603
	Females	Veh vs Low Dose	F (1, 20) = 6.995; P=**0.0155**
		Veh vs High Dose	F (1, 20) = 0.0004404; P=0.9835

Supplementary Table 1. A three-way ANOVA with repeated measures was performed to investigate the interaction between a) sex x treatment x time; and b) strain x treatment x time.

3.2. Role of NLRP3 Inflammasome in OIPN

3.2.1. Introduction

Cancer patients and survivors often suffer from adverse side effects of chemotherapy. Not only does chemotherapy-induced peripheral neuropathy reduce the quality of life, it may also impact cancer treatment (Oh & Cho, 2020; Pachman et al., 2016). Oxaliplatin is a third-generation platinum derivative used for the treatment of colorectal cancers (Deuis et al., 2017). The majority of patients treated with oxaliplatin report at least one symptom of acute neurotoxicity, such as cold hypersensitivity. About two-thirds of patients experience oxaliplatin-induced peripheral neuropathy (OIPN) long after completing their cancer treatment due to changes in sensory perception like mechanical hypersensitivity, allodynia, numbness and paresthesia, depression-like behavior, anxiety-like behavior, and preferential damage of peripheral sensory fibers and dorsal root ganglia - including pain (Hache et al., 2015; Marmiroli et al., 2017b). Currently, there are no effective prophylaxis or treatment options for OIPN (Hershman, Lacchetti, & Loprinzi, 2014).

Sensory changes and chronic pain state in neuropathy caused by antineoplastic encompasses pathologies of the peripheral and central nervous systems (Vichaya et al., 2015). The specific mechanism of CIPN caused by oxaliplatin is yet to be elucidated, however, a wide array of proposed molecular processes incorporate neuro-inflammatory components (Fumagalli et al., 2021). One of these CIPN pathologies points to a change in sensory capacity via altered neuronal excitability caused by cytokines, which is further supported by the presence receptors for cytokines on neurons in peripheral sensory afferents and spinal cord dorsal horn (Ohtori et al., 2004). Proinflammatory cytokines such as TNFα, IL-1 β and IL-6 can stimulate the production of a range of neuroexcitatory elements (Hucho & Levine, 2007). In a rat model of OIPN, elevated levels of

IL-1β and TNF-α in the spinal cords correlated with decreased mechanical hypersensitivity 3 weeks post treatment cessation (Janes et al., 2015).

Inflammasomes are cytoplasmic multiprotein complexes that assemble in response to cellular distress and promote maturation and secretion of IL-1β and IL-18 (Schroder & Tschopp, 2010). Upregulation of NLRP3 (nucleotide oligomerization domain-like receptor pyrin domain–containing 3) inflammasome response has been shown in numerous neurodegenerative diseases and sensory syndromes of different inflammatory pathologies, and it has been reviewed in section 1.3.2 of this dissertation. Recent research has made it increasingly evident that the NLRP3 inflammasome may also play a crucial role in neuropathic pain attributed to anticancer drugs of different classes (R. Chen et al., 2021). Oxaliplatin might be indirectly involved in activation of the NLRP3 inflammasome signaling pathway through a convergent mechanism, a cellular event such as decreased K^+ concentration, generation of reactive oxygen species, and extracellular ATP (Mariathasan et al., 2004; Pétrilli et al., 2007; Sutterwala et al., 2014).

In line with our results with paclitaxel in Chapter 2, we sought to investigate the contribution of the NLRP3 inflammasome in development of CIPN in mice treated with a different class of antineoplastic drug. We hypothesize that inhibition of NLRP3 inflammasome assembly would protect mice from developing mechanical hypersensitivity by oxaliplatin as seen with paclitaxel.

3.2.2. Methods

Animals

The Institutional Animal Care and Use Committee at Virginia Commonwealth University approved all experiments, under the National Institutes of Health Guidelines for the Care and Use of Laboratory Animals. NLRP3 KO mice were bred in-house on C57BL/6J background mice supplied from The Jackson Laboratory (Bar Harbor, ME). *NLRP3* gene KO indicates the protein functional loss-of function due to a point mutation as described in chapter 2. Adult mice were between 10-22 weeks old at the beginning of the experiments. Animals were housed in a climate-controlled room on a 12 hours light/dark cycle (lights on 07:00hrs) with free access to water and chow (Envigo, Teklad LM-485 mouse/rat sterilizable diet, cat # 7012, WI, USA).

Treatment

Oxaliplatin-induced peripheral neuropathy in mice was conducted according to methods previously published in our laboratory (Warncke et al., 2021). In brief, pharmaceutical grade oxaliplatin (5 mg/ml, Accord, NDC 16729-332-05) was dissolved in a vehicle (Veh) of sterile 5% dextrose solution (Hospira, Lake Forest, IL) fresh prior to each injection. The dose of 0.3 mg/kg oxaliplatin or its vehicle was administered intraperitoneally daily on days 0-4, and then again 10-14 for a total cumulative dose of 3 mg/kg. Animals were divided into the following groups: vehicle-treated NLRP3 WT (4 male and 4 female mice), vehicle-treated NLRP3 KO (4 male and 5 female mice), oxaliplatin-treated NLRP3 WT (4 male and 4 female mice), and oxaliplatin-treated NLRP3 KO (5 male and 5 female mice).

Mechanical sensitivity

Mechanical sensitivity thresholds were determined using von Frey filaments as described by Chaplan et al. (1994). All mice were tested at baseline, and weeks 1 (day 5), 2 (day 15), 4 (day 22), 5 (day 29) and 8 (day 51) of the study. The mechanical threshold is expressed as log10 (10 £ force in [mg]).

Cold sensitivity

Cold sensitivity was assessed with the acetone test the following day after von Frey assay. After a habituation period in Plexiglas chambers on mesh metal flooring, the ventral surface of each paw was sprayed with 20 μL of acetone (Fisher Bioscience) as described in the early section of this chapter.

Statistical analysis

The statistical analyses were carried out in GraphPad Prism software, version 9 (GraphPad Software, Inc., La Jolla, CA) and the data are expressed as mean ± SEM. Two-way (time x treatment) analysis of variance (ANOVA) with Sidak comparison tests was executed to verify treatment effect in each strain and sex. A three-way ANOVA with multiple comparison correction was performed to investigate a) differences between sexes of each mouse strain, b) strain differences of same sex between both strain, and c) strain differences of sex-combined mice. Time and treatment were common factors for each comparison. Additionally, two-way ANOVAs (treatment × genotype) were performed of the area under curve (AUC) for cold sensitivity test. paw withdrawal thresholds. Tukey's tests were used to delineate main effects. Statistical differences were reported when $p < 0.05$.

3.2.3. Results

NLRP3 protein loss-of-function Does Not Protect Mice from Developing Mechanical Hypersensitivity

The effects of a low dose of oxaliplatin regimen (3 mg/kg cumulative) on the time-course of stimulus-evoked nociception-related behaviors in NLRP3 knockout male and female mice was examined. No significant difference in mechanical threshold was observed between groups at baseline. First, we looked at the treatment effect in NLRP3 WT male mice to confirm that the low dose of oxaliplatin produced predicted onset of mechanical hypersensitivity. Indeed, a two-way ANOVA revealed a statistically significant interaction between treatment and time ($F_{(5, 30)} = 3.05$, $P = 0.0242$) confirming that the low dose of oxaliplatin is sufficient to induce long term mechanical hypersensitivity (**Figure 11A**). Similar results were observed in NLRP3 KO male mice (treatment x time; $F_{(5, 35)} = 8.736$, $P < 0.0001$). Female mice were evaluated accordingly. Data shows comparable results of oxaliplatin causing statistically significant change in mechanical hypersensitivity over time in NLRP3 WT ($F_{(5, 35)} = 8.263$, $P < 0.0001$) and KO ($F_{(5, 40)} = 4.835$, $P = 0.0015$) female mice (**Figure 11B**). The results indicate no difference between both genotypes.

Lastly, we evaluated male and female mice of the same strain to determine possible sex-driven differences. A three-way ANOVA did not reveal significant interaction of treatment x time x sex, therefore, data from male and female mice of the same strain and treatment were combined increasing the number of animals. The protective role of NLRP3 inflammasome activation inhibition on development of mechanical hypersensitivity was assessed by performing a three-way ANOVA test (treatment x genotype x time) in the male ($F_{(5, 65)} = 0.7299$, $P = 0.6036$) and female ($F_{(5, 75)} = 1.048$, $P = 0.3960$) mice. The results indicate no difference between both genotypes treated as visualized in **Figure 11C**. Two-way ANOVA of within strain analyses showed that

oxaliplatin treatment significantly reduced mechanical threshold of male (WT: $F_{(5, 30)} = 3.050$, $P = 0.0242$, KO: $F_{(5, 35)} = 8.736$, $P < 0.0001$) and female (WT: $F_{(5, 35)} = 8.263$, $P < 0.00001$, KO: $F_{(5, 40)} = 4.835$, $P = 0.0015$) mice as measured from week 1 and it persisted through testing. Overall, oxaliplatin caused a comparable long-term mechanical hypersensitivity in both sexes of both strains of mice.

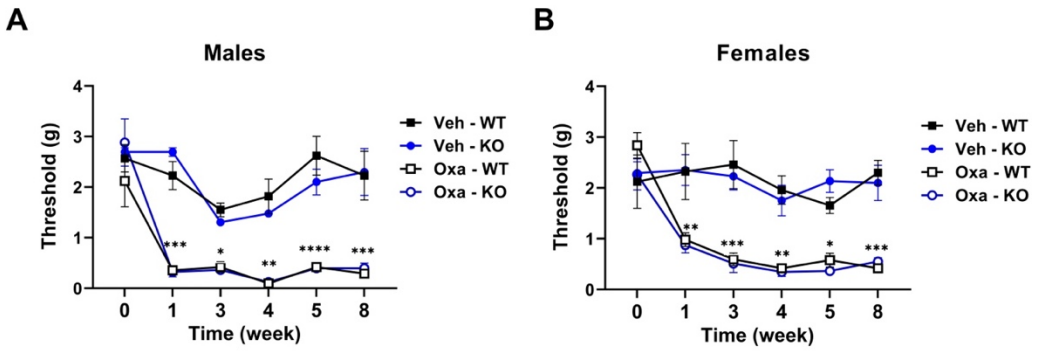

Figure 11. *NLRP3* knockout does not protect mice from developing oxaliplatin-induced mechanical hypersensitivity. Development of mechanical hypersensitive was monitored after each regimen of oxaliplatin (5 injections of 0.3 mg/kg) until week 8 with the von Frey test in NLRP3 KO male (n = 4-5/group), NLRP3 WT male (n = 4/group) (A), NLRP3 KO female (n = 5/group), and NLRP3 WT female (n = 4-5/group) (B). Treatment groups were assigned as follows: vehicle treated NLRP3 WT (Veh-WT), vehicle treated NLRP3 KO (Veh-KO), oxaliplatin treated NLRP3 WT (Oxa-WT), and oxaliplatin treated NLRP3 KO (Oxa-KO).Values are expressed as mean ± SEM. Results were compared using two-way ANOVA (Treatment, Time as RM) for each strain and for each sex followed by Tukey's post hoc test (A-B), and three-way ANOVA followed by Sidak's post hoc test (C). $P < 0.05$ was considered significant. Asterisks indicate times at which mechanical hypersensitivity was statistically different from vehicle. * $p < 0.05$, ** $p < 0.01$, ***$p < 0.005$, **** $p < 0.0001$.

Low-dose Oxaliplatin and Development of Cold Hypersensitivity in Mice

No significant difference in response time to acetone cooling sensation was observed between groups at baseline. Males and females were assessed separately. Oxaliplatin treatment was insufficient to notably increase the duration of acetone-elicited behaviors as compared to vehicle control in both male and female mice when examined with a three-way ANOVA analysis of the male ($F_{(5, 65)} = 0.4502$, $P = 0.8116$) and female ($F_{(5, 75)} = 2.231$, $P = 0.0598$) mice (**Figure 12A-B**).

Data was analyzed with AUC due to a small sample size and large within treatment group variability and revealed greater mechanical hypersensitivity in oxaliplatin-treated male and female NLRP3 WT mice compared to NLRP3 KO mice (**Figure 12C-D**).

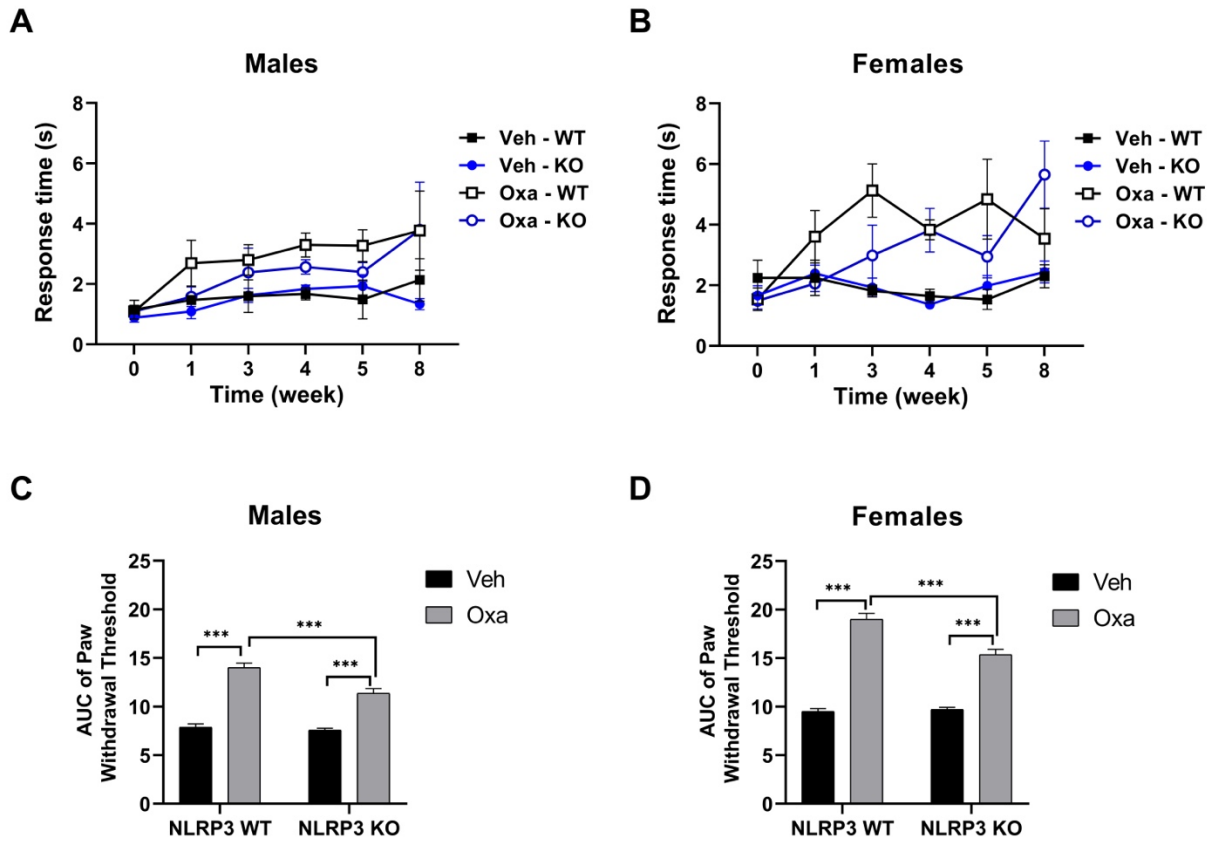

Figure 12. Induction of cold hypersensitivity in oxaliplatin-treated mice. Development of cold hypersensitivity was monitored after each regimen of oxaliplatin (5 injections of 0.3 mg/kg) until week 8 with the cold acetone test in NLRP3 KO male (n = 4-5/group), NLRP3 WT male (n = 4/group) (A), NLRP3 KO female (n = 5/group), and NLRP3 WT female (n = 4-5/group) (B). AUC analysis of paw withdrawal threshold of data between weeks 0-8 depict a greater mechanical hypersensitivity in NLRP3 WT male (C) and female (D) mice treated with paclitaxel. Values are expressed as mean ± SEM. Results were compared using two-way ANOVA (Treatment, x Genotype as RM) for each for each sex followed by Tukey's post hoc test (C-D). $P < 0.05$ was considered significant, ***$p < 0.0001$.

3.2.4. Discussion

Chemotherapy-induced peripheral neuropathy is a complex disease that involves many mechanisms including neuro-inflammatory factors (Fumagalli et al., 2021). *In vivo* and *in vitro* oxaliplatin studies show elevated expression level of IL-1β, one of the most prominent inflammatory mediators in DRG, spinal cords, macrophages and sciatic nerves (Miguel et al., 2019). We sought to investigate whether inhibition of NLPR3 inflammasome, a complex involved in production of active IL-1β and IL-18, protects mice from developing CIPN. The present study demonstrates the effect of *NLRP3* protein loss-of-function on the development of mechanical hypersensitivity after oxaliplatin administration in mice. Our results indicate comparable changes induced by oxaliplatin treatment on mechanical hypersensitivity in both NLRP3 KO and NLRP3 WT mice. Moreover, application of a cold stimulus in oxaliplatin-treated mice evoked a greater response total response time in WT mice.

The low-dose oxaliplatin regimen oxaliplatin was selected based on literature and our laboratory results showing that the cumulative dose of 3.0 mg/kg is effective in inducing neuropathic mechanical hypersensitivity without systemic toxicity as described in the first part of chapter 3 (Warncke et al., 2021). We planned to investigate the effectiveness of NLRP3 inflammasome assembly disruption ASC KO mice, and utilize higher doses of the chemotherapeutic and in NLRP3 KO and ASC KO mice. However, to our surprise, NLPR3 KO mice treated with the lowest experimental dose of oxaliplatin developed mechanical hypersensitivity similarly to the NLRP3 WT mice, hence, further testing was terminated. Research involving NRP3 inflammasome in OIPN is limited, yet, some of the results show positive association between blocking NLRP3 inflammasome oligomerization and development of mechanical hypersensitivity. The discrepancy between results and the literature might stem from

differences in the experimental set up, strains and species of animals tested. The NLRP3 KO (C57BL/6J-*Nlrp3*^{m1Btlr}/Mmucd) mice used in our experiment express a functional knockout of the NLRP3 protein due to T to G transversion found at position 3187 of the *Nlrp3* transcript. This single nucleotide polymorphism results in a cysteine to tryptophan substitution at residue 987 (C987W) of the leucine-rich repeat domain of the NLRP3 protein. The LLR domain is involved in interaction between NLRP3 and NEK7 (Hua Huang et al., 2019). In the inactive form, the LRR domain is bound to the NOD domain of the NLRP3 (Ye & Ting, 2008). Mutations in the LLR domain have been shown to be critical in NEK7 recruitment and phosphorylation of NLRP3 (Niu et al., 2021). However, Iva Hafner-Bratkovič et al. showed that truncated NLRP3 (1–965 aa) on the C-terminal LRR failed to respond to nigericin (Hafner-Bratkovič et al., 2018). Described as a "probably benign" mutation, C987W substitution was sufficient to reduce levels of IL-1β in peritoneal macrophages isolated from C57BL/6J-*Nlrp3*^{m1Btlr}/Mmucd homozygous mice when treated with LPS and nigericin (Sharif et al., 2019). Based on these results we presumed that the functional knock out of *Nlrp3* gene yields consistent changes in all cells that express the protein. However, we did not assess the concentration of IL-1β in tissues from oxaliplatin-treated NLRP3 WT nor NLRP3 KO mice. In this study, mice were subjected to 10 injections of a 0.3mg/kg oxaliplatin spanning 15 days. The cumulative dose of oxaliplatin utilized in our study was lower than the doses used in mouse and rat oxaliplatin models in the compared above-mentioned studies. A possible explanation for the observed decrease in mechanical hypersensitivity could be explained by oxaliplatin-induced changes in peripheral nerves which leads to hyperexcitability. As noted in section 3.1, the intraepidermal nerve fiber density in C57BL/6J mice treated with the same oxaliplatin regimen was significantly decreased weeks after the treatment. The difference in oxaliplatin-dosing regimen might impact the site and magnitude of damage.

Inflammation plays an important role in chemotherapeutic tumor suppression; however, prolonged inflammation can lead to tumor survival through neovascularization and contribute to development of CIPN (Greten & Grivennikov, 2019). Elevated levels of pro-inflammatory cytokines, such as TNFα, IL-1 β and IL-6, interferon alpha (IFN-α) interferon gamma (IFN-γ) in DRG have been associated with modulation of peripheral nerve damage and development of mechanical hypersensitivity in preclinical models of CIPN (Ni et al., 2020). Notably, a cumulative 6 mg/kg dose of oxaliplatin increased GFAP, IL-1β, TNFα, and Iba-1 mRNA levels in L3-L5 DRG and L4-L5 segments spinal cord in rats, indicating glial activation in peripheral and central nervous system (Miguel et al., 2019). IL-1β has been attributed to the progression of pain and inflammation from acute to chronic. Binshtok et al showed that IL-1β can induce pain by activating and increasing excitability of nociceptors, while others indicated its role in peripheral or central sensitization (Binshtok AM et al., 2008; Helyes et al., 2019).

Conversion of precursor IL-1β into mature form is tightly regulated at several levels due to its pleiotropic role in immunity and inflammation (Stehlik, 2009). One important mechanism underlying such regulation is mediated via NLRP3 inflammasome. Growing evidence suggests that activation of NLRP3 inflammasome and subsequent conversion of IL-1β by caspase-1, is an important pathological pathway mediating chemotherapy-induced peripheral neuropathy (Jia et al., 2017). Several studies have examined NLRP3 expression and involvement in oxaliplatin-induced peripheral neuropathy with conflicting reports. Pharmacological blockage of NLRP3 inflammasome assembly with MCC950, a selective NLRP3 inhibitor, significantly attenuated oxaliplatin-induced mechanical hypersensitivity in rats (Wahlman et al., 2018). Additionally, Wahlman et al. also reported increased level of expression of NLRP3 and maturation of caspase-1 and correlated neuropathic pain-like responses in rats to increased adenosine kinase in the dorsal

horn of the spinal cord and the dysregulation of adenosine A3AR signaling. Inhibition of ADK with MRS5698 or activating A3AR with a selective A3AR agonist resulted in NLRP3 activation, IL-1β production, and development of mechanical hypersensitivity. In a study examining the effect of blocking Connexin43 (Cx43) hemichannels with Peptide5 to diminish ATP accumulation in the extracellular space and subsequent formation of NLRP3 inflammasome, 20mg/kg of oxaliplatin significantly increased Cx43 protein in murine spinal cords 7 days after the last injection. However, NLRP3 expression was not affected by oxaliplatin and a concurrent treatment with Peptide5 did not improve mechanical hypersensitivity in C57BL/6J mice (Tonkin et al., 2018). In a study that looked at blocking the priming and activation steps of the NLRP3 inflammasome, mice with homozygous depletion of TLR4 or caspase-1/11 and treated with a total of 40 mg/kg oxaliplatin showed resistance to mechanical hypersensitivity as well as diminished and no upregulation of IL-1β in spinal cords, respectively (Agnes et al., 2021). As IL-1β can directly act on nociceptors and increase their excitability, treatment with an IL-1 receptor antagonist (IL-1Ra) could diminish symptoms of OIPN (Binshtok AM et al., 2008). Our results indicate that dysregulation of NLRP3 protein was insufficient to prevent development of mechanical hypersensitivity in mice treated with a low dose of oxaliplatin. Data from one group shows the lack of efficacy of anakinra, a clinically available IL-1Ra, on decreasing mechanical allodynia in rats intraplantarly injected with oxaliplatin (Starobova et al., 2021). DRG from rats treated with oxaliplatin presented significantly elevated level of NF-κB (Ni et al., 2020). An *in vitro* study showed that oxaliplatin treatment did not stimulate IL-1β release from LPS-primed murine bone marrow-derived dendritic cells (Antonopoulos et al., 2013). Therefore, the association of oxaliplatin and NLRP3 inflammasome OIPN is not direct.

CHAPTER FOUR

GENERAL DISCUSSION

4.1. Study Overview and Major Findings

Oxaliplatin and paclitaxel treatments can lead to axon degeneration, altered neuronal excitability, oxidative stress, apoptotic signaling, calcium dysregulation, and involvement of proinflammatory signaling, such as IL-1β in the peripheral and central nervous system. These changes can present themselves in 10-100% of patients as paresthesia, numbness, burning pain, and allodynia. Together, these symptoms are known as a sensory-predominant syndrome called chemotherapy-induced peripheral neuropathy (Ramnarine et al., 2016). CIPN sensory symptoms can be accompanied by distress, anxiety, depression, sleep disturbance, and cognitive deficits, and last years after cessation of chemotherapy, decreasing the quality of life (Colloca et al., 2017; Poupon et al., 2015; H. Zhang et al., 2013). Debilitating CIPN symptoms caused by a cumulative dose neurotoxicity may impact the oncological prognosis through dose reduction or complete discontinuation of the chemotherapy. Unfortunately, no prophylactic or efficacious therapeutic treatments are available for this toxicity (Majithia et al., 2016). Our work addresses a huge unmet medical need while filling a major gap in our understanding of the role of NLRP3 inflammasome in chronic neuropathic pain associated with CIPN.

The overall objective of the present project was to investigate the role of NLRP3 inflammasome in paclitaxel and oxaliplatin mouse models of CIPN and evaluate this mechanism as a potential treatment strategy. Emerging evidence suggests neuroinflammation is an important element in the development of CIPN. In Aim 1 of this dissertation, we demonstrated that mechanical and cold hypersensitivity developed in a paclitaxel-dose dependent manner in wild type mice, as anticipated. Inhibition of NLRP3 inflammasome oligomerization via genetic approach

through a global ASC protein knockout or a functional knockout of NLRP3 protein was protective against the low dose of paclitaxel (cumulative 8 mg/kg) treatment. Additional cycles of the low dose treatment revealed a sex-dependent pattern of protection against mechanical hypersensitivity in female ASC KO and NLRP3 KO mice. Delayed onset of mechanical hypersensitivity was recorded in both sexes of the knockout strains when a higher dose (one wave of 16 mg/kg cumulative) of paclitaxel was administered, as compared to wild type mice. Pharmacological inhibition of NLRP3 inflammasome with JC124 also showed similar protection of paclitaxel-dose CIPN dependent in C57BL/6J mice. However, when tested in male mice, prophylacticly treated JC124 was not sufficient against the high paclitaxel regimen (32 mg/kg) treatment. Immunoperoxidase showed increased IL-1β staining in the L4-L6 spinal cord region of C57BL6J males, supporting the claim that paclitaxel can induce proinflammatory signaling. In Aim 2, we characterized oxaliplatin-induced peripheral neuropathy model in two commonly used strains of mice. We observed strain-, sex-, and oxaliplatin dose-dependent changes in the IENF density, sensory and behavioral and aspects of OIPN. The low dose regimen of oxaliplatin (3 mg/kg cumulative) was sufficient to induce persistent mechanical hypersensitivity and reduce IENF density without altering affective-like behaviors in C57BL/6J mice, rendering it a suitable paradigm for investigating the role of NLRP3 inflammasome in oxaliplatin-induced CIPN. Contrary to our expectations, NLRP3 KO male and female mice treated with a low oxaliplatin dose developed mechanical hypersensitivity that closely resembled the NLRP3 WT mice profile. Overall, our data suggest that NLRP3 inflammasome may play role in CIPN in a chemotherapy drug class specific manner.

4.2. Establishing a Mouse Model of Oxaliplatin-Induced Peripheral Neuropathy

Animal models allow researchers to investigate and identify CIPN pathophysiological mechanisms in a body system which can lead to the development of therapies. In Chapter 3 of this dissertation, we characterize a OIPN mouse model in C57BL/6J and Balb/cJ mice of both sexes. Administration of oxaliplatin to mice at cumulative doses of 3 and 30 mg/kg i.p. induced mechanical and cold hypersensitivity, measured by von Frey and acetone tests, respectively. Alterations in the nociceptive, behavioral, and morphological features of OIPN were measured at multiple time points via battery of testing when appropriate. Comparison of the two mouse strains demonstrated that C57BL/6J mice show more oxaliplatin-induced behavioral changes than BALB/cJ mice, except for change in preference for sucrose solution. Moreover, oxaliplatin affected caudal nerve conduction and IENF degeneration in a sex-, dose-, and strain-dependent manner. The low-dose regimen of oxaliplatin induced mechanical and cold hypersensitivity, and decreased IENF in C57BL/6J male and female mice, without showing disturbance in affective-like behaviors. It was imperative to characterize any changes in behavior, sensory responses and peripheral nerves morphology of C57BL/6J mice as this strain was used as genetic background for backcrossing ASC KO and NLRP3 KO mice. Previous work in our lab paclitaxel identified differences in the development of neuropathy and affective behaviors in C57BL/6J mice treated with various doses of paclitaxel (Toma et al 2017). Information obtained from characterizing OIPN and PIPN in our lab allowed for selecting appropriate paclitaxel and oxaliplatin treatment regimen for investigating the role of NLRP3 inflammasome in CIPN.

4.3. Differential Role of NLRP3 Inflammasome Inhibition in CIPN Induced by Paclitaxel and Oxaliplatin

While paclitaxel and oxaliplatin induce common CIPN sensory symptoms, they differ in anti-tumor mechanisms. Paclitaxel can be used alone or as an adjuvant therapy for different types of solid tumors such as lung, breast, ovarian, head, and neck cancers (Jauhari et al., 2008). The anticancer effects of paclitaxel are mediated by polymerization of tubulin which leads to distortion of the microtubules and prevents their depolymerization. Resulting cell cycle arrest division leads to apoptosis and cell death (Mekhail & Markman, 2002). Oxaliplatin is commonly used in combination with fluorouracil and leucovorin, referred to as FOLFOX regimen (Hong et al., 2019; Simpson et al., 2003). Oxaliplatin forms intrastrand DNA adducts that disrupts DNA replication and transcription (Arango et al., 2004). The shared neurotoxic events between oxaliplatin and paclitaxel are mitotoxicity, functional impairments of ion channels, and triggered immunological mechanisms via activation of satellite glial cells (Eldridge et al., 2020; Ferrier et al., 2013; Grisold et al., 2012; Park et al., 2013). Paclitaxel and oxaliplatin treatments have been implicated in elevated levels of IL-1β through the NLRP3 inflammasome pathway. Oxaliplatin's capacity to stimulate NLRP3 inflammasome oligomerization is possibly indirect and in response to elicited cell death damage associated molecular patterns, such as ATP released from the dying cell (Stojanovska et al., 2019). Tumor cells treated with oxaliplatin are capable of activating the NLRP3 inflammasome in dendritic cells evident in secretion of IL-1β (Ghiringhelli et al., 2009). However, an *in vitro* study showed that addition of oxaliplatin to LPS-primed murine bone marrow-derived dendritic cells did not induce IL-1β release (Antonopoulos et al., 2013). This suggests that oxaliplatin alone is insufficient to trigger maturation of IL-1β via the NLRP3 inflammasome pathway, such that it does not act as a signaling molecule. In contrast, Son s. et al showed that pre-treatment of bone marrow-derived macrophages with paclitaxel induced robust activation of caspase-1 when challenged with ATP or nigericin(Son et al., 2019).

The persistence of mechanical and cold hypersensitivity after oxaliplatin treatment in NLRP3 KO mice can be explained by neuronal damage that precedes establishment of the inflammatory processes. Transcriptomic analysis of dorsal root ganglia extracted from C57BL/6J mice 72 hours post a single high dose of oxaliplatin (40 mg/kg) revealed a shift in differentially expressed genes (DEG) that highly regulate genes which are associated with DNA and RNA processing, and biological processes of neuronal damage. In contrast, treatment with vincristine, a microtubule interfering compound, regulated majority of DEGs that overlap with immune system-associated processes and no neuronal processes or DNA and RNA processing (Starobova et al., 2021).

4.4. Sex-Dependent Differences in CIPN Prevention via NLRP3 Inflammasome Inhibition

In this study we demonstrated that sex plays an important role in onset of mechanical hypersensitivity observed post paclitaxel treatment. Female ASC KO and NLRP3 KO mice showed resistance to developing mechanical hypersensitivity when challenged with two waves of low-dose paclitaxel treatment. This observation was paclitaxel-dose dependent, suggesting that higher doses of the chemotherapeutic might mask subtle but important sensory alterations when investigating potential mechanism and targets of PIPN. Epidemiological studies indicate a higher rate of chronic pain in females, and hormones such as estradiol, progesterone, and testosterone significantly impact immune response (E. J. BartleyR. B. Fillingim). (75). Estrogen, progesterone, and testosterone receptors are expressed on T cells, B cells, macrophages, dendritic cells, neutrophils, natural killer cells, and neuronal cells (neuronal cells ref) (76). Sex hormones affect the immune system in various ways during injury or disease states, thus, it is possible that the immune response to chemotherapy-induced injury differs between males and females.

Paclitaxel primes NLRP3 inflammasome via TLR4 receptor. Interestingly, Sorge et al. revealed that male mice require microglia and TLR4, while female mice require T cells to mediate

chronic neuropathic pain induced by spared nerve injury (Sorge et al., 2011, 2015). In the periphery, estrogen suppresses release of histamine by mast cells which results in fewer neutrophils recruitment to a site of injury in females, and reduces the number of macrophages (Atkins et al., 1993; Pease-Raissi et al., 2017). High levels of estrogen and testosterone promote M2 (anti-inflammatory) and M (proinflammatory) phenotype of macrophages, respectively, driving a higher expression of TLR4 and NLRP3 in males. However, it has been shown that more tissue-resident immune cells and prolonged cytokine levels in females than males (Cheng et al., 2019; Jaillon et al., 2019; Martinez & Gordon, 2014). In a post-operative pain model, a global deletion of NLRP3 reduced levels of IL-1β and mechanical sensitization in male mice only. Deletion of NLRP3 from sensory neurons had a lower impact on incision-induced mechanical hypersensitivity in males than females, indicating sensory neuron-restricted NLRP3 pain responses (Cowie et al., 2019).

4.5. Limitations and Future Directions

Studies conducted in this dissertation project revealed that inhibition of NLRP3 inflammasome had sex-, chemotherapy dose-, and chemotherapy drug-dependent effect on development of CIPN. The exact cause of these effects are unknown, however future studies could explain such observations. Because were not able to assess NLRP3 inflammasome activation in the DRG and spinal cord after paclitaxel treatment, it would be imperative to optimize the staining protocol and possibly acquire different primary ASC and NLRP3 antibodies that show more specificity. Further, to investigate which cell types participate in NLRP3 inflammasome dependent CIPN, spinal cord and DRG sections could be double immuno-stained stained for NLRP3 and ASC protein with markers for neurons (NeuN), astrocytes (GFAP), and microglia (Iba1). This information might help elucidate observed sex- and chemo-specific differences as activation of glial cells (astrocytes and microglia) in the CNS, DRG-surrounding Schwann and satellite glial

cell, infiltration of macrophages and T-cells in the PNS, have been shown in a rat model of PIPN (Zhang et al., 2016). Rats treated with paclitaxel showed microglial activation occurs in the dorsal horn of the spinal cord and activation of NLRP3 inflammasome in sciatic nerve and DRG, therefore it's probable that the primary source of released IL-1β is microglial (Jia et al., 2017; Peters et al., 2007).

Sex hormones can significantly affect the immune responses and drive pain and sensitization through different mechanisms (Jaillon et al., 2019). In a post-operative pain model, Cowie et al showed expression and activation of NLRP3 in neuronal cells contributes to pain sensation. In that regard, cell-specific knockout of NLRP3 could be investigated by creating and breeding NLRP3 conditional knockout mice ($NLRP3^{AdvCre+}$) to be expressed in glial or neuronal cells only. To explore possible sex hormones contributions, the experiment could be repeated with gonadectomized mice or mice supplemented with hormone replacement. This will provide more insight into cell-specific involvement role of NLRP3 in development of CIPN and a potential treatment target.

Our results indicate that oxaliplatin-induced mechanical hypersensitivity might be mediated by additional or other mechanisms than NLRP3 inflammasome-dependent maturation of IL-1β, as oxaliplatin-treated NLRP3 KO mice were not protected from developing OIPN. Assessment of levels of IL-1β and IL-18 in ASC KO and NLRP3 KO mice treated with oxaliplatin might provide important information on the proinflammatory cytokines profile in spinal cords, DRG or skin foot pads through the canonical NLRP3 inflammasome pathway. Further, changes in the peripheral intraepidermal nerve fibers density are a hallmark of CIPN. It might be informational to evaluate IENF of paw skin from NLRP3 KO and ASC KO mice treated with various doses of paclitaxel and oxaliplatin to assess changes in peripheral nerve fiber density whether in relation to a) the observed

mechanical and cold hypersensitivity, and b) observed sex differences of paclitaxel-induced mechanical hypersensitive in ASC KO and NLRP3 KO mice. IL-1B. In addition to sensory alterations, paclitaxel and oxaliplatin cause changes in affect-like behaviors in mice, while (Toma et al., 2017a; Warncke et al., 2021).

It is important to note that the NLRP3 inhibitor JC124 was effective at preventing development of CIPN when the low-dose paclitaxel regimen was used. The male mice treated with the mid-dose of Pac presented delayed onset of mechanical hypersensitivity. Future *in vivo* studies with NLRP3 inhibitors could evaluate their optimal treatment schedule and doses, and effectiveness at reversing CIPN. To add a translational value of JC124, it would be important to confirm that the NLRP3 inflammasome inhibitor will not promote tumor cell growth or attenuate the anti-neoplastic actions of chemotherapy via *in vitro* studies. For practical and ethical reasons, the vast majority of pre-clinical CIPN studies utilize cancer free animals (Gadgil et al., 2019). Exploring potential CIPN treatments in tumor-bearing animals comes with challenges such as accelerated neoplastic growth and tumor-induced changes such as onset of neuropathy (S. J.L. Flatters et al., 2017). In a murine breast carcinoma model of cancer-induced nociception, Balb/c female mice began to experience reduction in mechanical threshold on day 10 after inoculation with 4T1 cells. Mechanical hypersensitivity was observed on day 15 and lasted throughout the study until day 30 when the animals were sacrificed (de Almeida et al., 2019). Although most CIPN patients have or previously experienced cancer, chemotherapy is often administered after surgical removal of a tumor to eradicate possible micro-metastases. Therefore, modeling of chemotherapy-induced peripheral neuropathy via chemotherapy administration alone is an acceptable approach (S. J.L. Flatters et al., 2017).

LITERATURE CITED

Agnes, J. P., Santos, V. W. dos, das Neves, R. N., Gonçalves, R. M., Delgobo, M., Girardi, C. S., Lückemeyer, D. D., Ferreira, M. de A., Macedo-Júnior, S. J., Lopes, S. C., Spiller, F., Gelain, D. P., Moreira, J. C. F., Prediger, R. D., Ferreira, J., & Zanotto-Filho, A. (2021). Antioxidants Improve Oxaliplatin-Induced Peripheral Neuropathy in Tumor-Bearing Mice Model: Role of Spinal Cord Oxidative Stress and Inflammation. *Journal of Pain*, *22*(8). https://doi.org/10.1016/j.jpain.2021.03.142

Al-Mazidi, S., Alotaibi, M., Nedjadi, T., Chaudhary, A., Alzoghaibi, M., & Djouhri, L. (2018). Blocking of cytokines signalling attenuates evoked and spontaneous neuropathic pain behaviours in the paclitaxel rat model of chemotherapy-induced neuropathy. *European Journal of Pain (United Kingdom)*, *22*(4). https://doi.org/10.1002/ejp.1169

Alessandri-Haber, N., Dina, O. A., Yeh, J. J., Parada, C. A., Reichling, D. B., & Levine, J. D. (2004). Transient Receptor Potential Vanilloid 4 Is Essential in Chemotherapy-Induced Neuropathic Pain in the Rat. *Journal of Neuroscience*, *24*(18). https://doi.org/10.1523/JNEUROSCI.0242-04.2004

Allan, S. M., Tyrrell, P. J., & Rothwell, N. J. (2005). Interleukin-1 and neuronal injury. In *Nature Reviews Immunology* (Vol. 5, Issue 8). https://doi.org/10.1038/nri1664

Allchorne, A. J., Broom, D. C., & Woolf, C. J. (2005). Detection of cold pain, cold allodynia and cold hyperalgesia in freely behaving rats. *Molecular Pain*, *1*. https://doi.org/10.1186/1744-8069-1-36

Amraoui, F., Hassani Lahsinoui, H., Spijkers, L. J. A., Vogt, L., Peters, S. L. M., Wijesinghe, D. S., Warncke, U. O., Chalfant, C. E., Ris-Stalpers, C., van den Born, B.-J. H., & Afink, G. B. (2020). Plasma ceramide is increased and associated with proteinuria in women with pre-eclampsia and HELLP syndrome. *Pregnancy Hypertension*, *19*.

https://doi.org/10.1016/j.preghy.2019.12.006

Andoh, T., Fukutomi, D., Uta, D., & Kuraishi, Y. (2019). Prophylactic Repetitive Treatment with the Herbal Medicine Kei-kyoh-zoh-soh-oh-shin-bu-toh Attenuates Oxaliplatin-Induced Mechanical Allodynia by Decreasing Spinal Astrocytes. *Evidence-Based Complementary and Alternative Medicine*, *2019*. https://doi.org/10.1155/2019/4029694

Antonopoulos, C., El Sanadi, C., Kaiser, W. J., Mocarski, E. S., & Dubyak, G. R. (2013). Proapoptotic Chemotherapeutic Drugs Induce Noncanonical Processing and Release of IL-1β via Caspase-8 in Dendritic Cells. *The Journal of Immunology*, *191*(9). https://doi.org/10.4049/jimmunol.1300645

Arango, D., Wilson, A. J., Shi, Q., Corner, G. A., Arañes, M. J., Nicholas, C., Lesser, M., Mariadason, J. M., & Augenlicht, L. H. (2004). Molecular mechanisms of action and prediction of response to oxaliplatin in colorectal cancer cells. *British Journal of Cancer*, *91*(11). https://doi.org/10.1038/sj.bjc.6602215

Argyriou, A. A., Bruna, J., Marmiroli, P., & Cavaletti, G. (2012). Chemotherapy-induced peripheral neurotoxicity (CIPN): An update. In *Critical Reviews in Oncology/Hematology* (Vol. 82, Issue 1). https://doi.org/10.1016/j.critrevonc.2011.04.012

Argyriou, A. A., Cavaletti, G., Briani, C., Velasco, R., Bruna, J., Campagnolo, M., Alberti, P., Bergamo, F., Cortinovis, D., Cazzaniga, M., Santos, C., Papadimitriou, K., & Kalofonos, H. P. (2013). Clinical pattern and associations of oxaliplatin acute neurotoxicity: A prospective study in 170 patients with colorectal cancer. *Cancer*, *119*, 438–444. https://doi.org/10.1002/cncr.27732

Arnold, M., Rutherford, M. J., Bardot, A., Ferlay, J., Andersson, T. M. L., Myklebust, T. Å., Tervonen, H., Thursfield, V., Ransom, D., Shack, L., Woods, R. R., Turner, D., Leonfellner,

S., Ryan, S., Saint-Jacques, N., De, P., McClure, C., Ramanakumar, A. V., Stuart-Panko, H., … Bray, F. (2019). Progress in cancer survival, mortality, and incidence in seven high-income countries 1995–2014 (ICBP SURVMARK-2): a population-based study. *The Lancet Oncology*, *20*(11). https://doi.org/10.1016/S1470-2045(19)30456-5

Aschele, C., Friso, M. L., Pucciarelli, S., Lonardi, S., Sartor, L., Fabris, G., Urso, E. D. L., Del Bianco, P., Sotti, G., Lise, M., & Monfardini, S. (2005). A phase I-II study of weekly oxaliplatin, 5-fluorouracil continuous infusion and preoperative radiotherapy in locally advanced rectal cancer. *Annals of Oncology*, *16*, 1140–1146. https://doi.org/10.1093/annonc/mdi212

Atkins, P. C., von Allman, C., Valenzano, M., & Zweiman, B. (1993). The effects of gender on allergen-induced histamine release in ongoing allergic cutaneous reactions. *The Journal of Allergy and Clinical Immunology*, *91*(5). https://doi.org/10.1016/0091-6749(93)90216-3

Attal, N., Bouhassira, D., Gautron, M., Vaillant, J. N., Mitry, E., Lepère, C., Rougier, P., & Guirimand, F. (2009). Thermal hyperalgesia as a marker of oxaliplatin neurotoxicity: A prospective quantified sensory assessment study. *Pain*, *144*(3). https://doi.org/10.1016/j.pain.2009.03.024

Attal, Nadine, Lanteri-Minet, M., Laurent, B., Fermanian, J., & Bouhassira, D. (2011). The specific disease burden of neuropathic pain: Results of a French nationwide survey. *Pain*, *152*, 2836–2843. https://doi.org/10.1016/j.pain.2011.09.014

Avan, R., Janbabaei, G., Hendouei, N., Alipour, A., Borhani, S., Tabrizi, N., & Salehifar, E. (2018). The effect of pregabalin and duloxetine treatment on quality of life of breast cancer patients with taxane-induced sensory neuropathy: A randomized clinical trial. *Journal of Research in Medical Sciences*, *23*(1). https://doi.org/10.4103/jrms.JRMS_1068_17

Avraham, O., Feng, R., Ewan, E. E., Rustenhoven, J., Zhao, G., & Cavalli, V. (2021). Profiling sensory neuron microenvironment after peripheral and central axon injury reveals key pathways for neural repair. *ELife*, *10*. https://doi.org/10.7554/eLife.68457

Bae, J. Y., & Park, H. H. (2011). Crystal structure of NALP3 Protein Pyrin Domain (PYD) and its implications in inflammasome assembly. *Journal of Biological Chemistry*, *286*(45). https://doi.org/10.1074/jbc.M111.278812

Baecher-Allan, C., Kaskow, B. J., & Weiner, H. L. (2018). Multiple Sclerosis: Mechanisms and Immunotherapy. In *Neuron* (Vol. 97, Issue 4). https://doi.org/10.1016/j.neuron.2018.01.021

Bair, M. J., Robinson, R. L., Katon, W., & Kroenke, K. (2003). Depression and Pain Comorbidity: A Literature Review. *Archives of Internal Medicine*, *163*, 2433–2445. https://doi.org/10.1001/archinte.163.20.2433

Balayssac, D., Ferrier, J., Descoeur, J., Ling, B., Pezet, D., Eschalier, A., & Authier, N. (2011). Chemotherapy-induced peripheral neuropathies: From clinical relevance to preclinical evidence. In *Expert Opinion on Drug Safety* (Vol. 10, Issue 3). https://doi.org/10.1517/14740338.2011.543417

Banach, M., Juranek, J. K., & Zygulska, A. L. (2017). Chemotherapy-induced neuropathies—a growing problem for patients and health care providers. *Brain and Behavior*, *7*(1). https://doi.org/10.1002/brb3.558

Barajon, I., Bersani, M., Quartu, M., Del Fiacco, M., Cavaletti, G., Holst, J. J., & Tredici, G. (1996). Neuropeptides and morphological changes in cisplatin-induced dorsal root ganglion neuronopathy. *Experimental Neurology*, *138*(1). https://doi.org/10.1006/exnr.1996.0050

Baral, P., Udit, S., & Chiu, I. M. (2019). Pain and immunity: implications for host defence. In *Nature Reviews Immunology* (Vol. 19, Issue 7, pp. 433–447).

https://doi.org/10.1038/s41577-019-0147-2

Basu, S., & Sodhi, A. (1992). Increased release of interleukin-1 and tumour necrosis factor by interleukin-2-induced lymphokine-activated killer cells in the presence of cisplatin and FK-565. *Immunology and Cell Biology*, *70*(1), 15–24. https://doi.org/10.1111/j.1440-1711.1992.tb03554.x

Bauernfeind, F. G., Horvath, G., Stutz, A., Alnemri, E. S., MacDonald, K., Speert, D., Fernandes-Alnemri, T., Wu, J., Monks, B. G., Fitzgerald, K. A., Hornung, V., & Latz, E. (2009). Cutting Edge: NF-κB Activating Pattern Recognition and Cytokine Receptors License NLRP3 Inflammasome Activation by Regulating NLRP3 Expression. *The Journal of Immunology*, *183*(2). https://doi.org/10.4049/jimmunol.0901363

Beijers, A. J. M., Mols, F., & Vreugdenhil, G. (2014). A systematic review on chronic oxaliplatin-induced peripheral neuropathy and the relation with oxaliplatin administration. *Supportive Care in Cancer*, *22*, 1999–2007. https://doi.org/10.1007/s00520-014-2242-z

Bennett, B. K., Park, S. B., Lin, C. S. Y., Friedlander, M. L., Kiernan, M. C., & Goldstein, D. (2012). Impact of oxaliplatin-induced neuropathy: A patient perspective. *Supportive Care in Cancer*, *20*(11), 2959–2967. https://doi.org/10.1007/s00520-012-1428-5

Bennett, G. J., Liu, G. K., Xiao, W. H., Jin, H. W., & Siau, C. (2011). Terminal arbor degeneration - a novel lesion produced by the antineoplastic agent paclitaxel. *European Journal of Neuroscience*, *33*(9), 1667–1676. https://doi.org/10.1111/j.1460-9568.2011.07652.x

Binshtok AM, Wang H, Zimmermann K, Amaya F, Vardeh D, Shi L, Brenner GJ, Ji RR, Bean BP, Woolf CJ, & Samad TA. (2008). Nociceptors are interleukin-1beta sensors. *J Neurosci*, *28*(52).

Bobylev, I., Joshi, A. R., Barham, M., Ritter, C., Neiss, W. F., Höke, A., & Lehmann, H. C. (2015). Paclitaxel inhibits mRNA transport in axons. *Neurobiology of Disease*, *82*. https://doi.org/10.1016/j.nbd.2015.07.006

Bodnoff, S. R., Suranyi-Cadotte, B., Aitken, D. H., Quirion, R., & Meaney, M. J. (1988). The effects of chronic antidepressant treatment in an animal model of anxiety. *Psychopharmacology*, *95*(3). https://doi.org/10.1007/BF00181937

Boehmerle, W., Huehnchen, P., Lee, S. L. L., Harms, C., & Endres, M. (2018). TRPV4 inhibition prevents paclitaxel-induced neurotoxicity in preclinical models. *Experimental Neurology*, *306*. https://doi.org/10.1016/j.expneurol.2018.04.014

Boehmerle, W., Huehnchen, P., Peruzzaro, S., Balkaya, M., & Endres, M. (2014). Electrophysiological, behavioral and histological characterization of paclitaxel, cisplatin, vincristine and bortezomib-induced neuropathy in C57Bl/6 mice. *Scientific Reports*, *4*. https://doi.org/10.1038/srep06370

Bonhof, C. S., van de Poll-Franse, L. V., Vissers, P. A. J., Wasowicz, D. K., Wegdam, J. A., Révész, D., Vreugdenhil, G., & Mols, F. (2019). Anxiety and depression mediate the association between chemotherapy-induced peripheral neuropathy and fatigue: Results from the population-based PROFILES registry. *Psycho-Oncology*, *28*(9), 1926–1933. https://doi.org/10.1002/pon.5176

Boyette-Davis, J., & Dougherty, P. M. (2011). Protection against oxaliplatin-induced mechanical hyperalgesia and intraepidermal nerve fiber loss by minocycline. *Experimental Neurology*, *229*(2), 353–357. https://doi.org/10.1016/j.expneurol.2011.02.019

Brenner, D. S., Golden, J. P., & Gereau IV, R. W. (2012). A novel behavioral assay for measuring cold sensation in mice. *PLoS ONE*, *7*(6).

https://doi.org/10.1371/journal.pone.0039765

Broz, P., & Dixit, V. M. (2016). Inflammasomes: Mechanism of assembly, regulation and signalling. In *Nature Reviews Immunology* (Vol. 16, Issue 7). https://doi.org/10.1038/nri.2016.58

Broz, P., & Monack, D. M. (2013). Newly described pattern recognition receptors team up against intracellular pathogens. In *Nature Reviews Immunology* (Vol. 13, Issue 8). https://doi.org/10.1038/nri3479

Bruna, J., Alberti, P., Calls-Cobos, A., Caillaud, M., Damaj, M. I., & Navarro, X. (2020). Methods for in vivo studies in rodents of chemotherapy induced peripheral neuropathy. In *Experimental Neurology* (Vol. 325). Academic Press Inc. https://doi.org/10.1016/j.expneurol.2019.113154

Bruna, J., Udina, E., Alé, A., Vilches, J. J., Vynckier, A., Monbaliu, J., Silverman, L., & Navarro, X. (2010). Neurophysiological, histological and immunohistochemical characterization of bortezomib-induced neuropathy in mice. *Experimental Neurology*, *223*(2). https://doi.org/10.1016/j.expneurol.2010.02.006

Brushart, T. M. (2011). *Nerve Repair*. New York : Oxford University Press.

Bryant, C. D., Bagdas, D., Goldberg, L. R., Khalefa, T., Reed, E. R., Kirkpatrick, S. L., Kelliher, J. C., Chen, M. M., Johnson, W. E., Mulligan, M. K., & Imad Damaj, M. (2019). C57BL/6 substrain differences in inflammatory and neuropathic nociception and genetic mapping of a major quantitative trait locus underlying acute thermal nociception. *Molecular Pain*, *15*, 1–15. https://doi.org/10.1177/1744806918825046

Canta, A., Pozzi, E., & Carozzi, V. A. (2015). Mitochondrial dysfunction in chemotherapy-induced peripheral neuropathy (CIPN). In *Toxics* (Vol. 3, Issue 2, pp. 198–223).

https://doi.org/10.3390/toxics3020198

Carozzi, V. A., Canta, A., & Chiorazzi, A. (2015). Chemotherapy-induced peripheral neuropathy: What do we know about mechanisms? In *Neuroscience Letters* (Vol. 596, pp. 90–107). https://doi.org/10.1016/j.neulet.2014.10.014

Cavaletti, G., Cavalletti, E., Oggioni, N., Sottani, C., Minoia, C., D'Incalci, M., Zucchetti, M., Marmiroli, P., & Tredici, G. (2000). Distribution of paclitaxel within the nervous system of the rat after repeated intravenous administration. *NeuroToxicology*, *21*(3). https://doi.org/10.1046/j.1529-8027.2001.01008-5.x

Cavaletti, G., Cornblath, D. R., Merkies, I. S. J., Postma, T. J., Rossi, E., Frigeni, B., Alberti, P., Bruna, J., Velasco, R., Argyriou, A. A., Kalofonos, H. P., Psimaras, D., Ricard, D., Pace, A., Galiè, E., Briani, C., Dalla Torre, C., Faber, C. G., Lalisang, R. I., … Pessino, A. (2013). The chemotherapy-induced peripheral neuropathy outcome measures standardization study: From consensus to the first validity and reliability findings. *Annals of Oncology*, *24*(2). https://doi.org/10.1093/annonc/mds329

Chaplan, S. R., Bach, F. W., Pogrel, J. W., Chung, J. M., & Yaksh, T. L. (1994). Quantitative assessment of tactile allodynia in the rat paw. *Journal of Neuroscience Methods*, *53*(1), 55–63. https://doi.org/10.1016/0165-0270(94)90144-9

Chen, R., Yin, C., Fang, J., & Liu, B. (2021). The NLRP3 inflammasome: an emerging therapeutic target for chronic pain. In *Journal of Neuroinflammation* (Vol. 18, Issue 1). https://doi.org/10.1186/s12974-021-02131-0

Chen, Y., Yang, C., & Wang, Z. J. (2011). Proteinase-activated receptor 2 sensitizes transient receptor potential vanilloid 1, transient receptor potential vanilloid 4, and transient receptor potential ankyrin 1 in paclitaxel-induced neuropathic pain. *Neuroscience*, *193*.

https://doi.org/10.1016/j.neuroscience.2011.06.085

Cheng, C., Wu, H., Wang, M., Wang, L., Zou, H., Li, S., & Liu, R. (2019). Estrogen ameliorates allergic airway inflammation by regulating activation of NLRP3 in mice. *Bioscience Reports*, *39*(1). https://doi.org/10.1042/BSR20181117

Choleris, E., Thomas, A. W., Kavaliers, M., & Prato, F. S. (2001). A detailed ethological analysis of the mouse open field test: Effects of diazepam, chlordiazepoxide and an extremely low frequency pulsed magnetic field. *Neuroscience and Biobehavioral Reviews*, *25*(3). https://doi.org/10.1016/S0149-7634(01)00011-2

Chung, W. S., Allen, N. J., & Eroglu, C. (2015). Astrocytes control synapse formation, function, and elimination. *Cold Spring Harbor Perspectives in Biology*, *7*(9). https://doi.org/10.1101/cshperspect.a020370

Cliff, J., Jorgensen, A. L., Lord, R., Azam, F., Cossar, L., Carr, D. F., & Pirmohamed, M. (2017). The molecular genetics of chemotherapy–induced peripheral neuropathy: A systematic review and meta-analysis. *Critical Reviews in Oncology/Hematology*, *120*, 127–140. https://doi.org/10.1016/j.critrevonc.2017.09.009

Cobianchi, S., de Cruz, J., & Navarro, X. (2014). Assessment of sensory thresholds and nociceptive fiber growth after sciatic nerve injury reveals the differential contribution of collateral reinnervation and nerve regeneration to neuropathic pain. *Experimental Neurology*, *255*. https://doi.org/10.1016/j.expneurol.2014.02.008

Colburn, R. W., Lubin, M. Lou, Stone, D. J., Wang, Y., Lawrence, D., D'Andrea, M. R. R., Brandt, M. R., Liu, Y., Flores, C. M., & Qin, N. (2007). Attenuated Cold Sensitivity in TRPM8 Null Mice. *Neuron*, *54*(3). https://doi.org/10.1016/j.neuron.2007.04.017

Colloca, L., Ludman, T., Bouhassira, D., Baron, R., Dickenson, A. H., Yarnitsky, D., Freeman,

R., Truini, A., Attal, N., Finnerup, N. B., Eccleston, C., Kalso, E., Bennett, D. L., Dworkin, R. H., & Raja, S. N. (2017). Neuropathic pain. *Nature Reviews Disease Primers*, *3*. https://doi.org/10.1038/nrdp.2017.2

Cooper, J. A., Arulpragasam, A. R., & Treadway, M. T. (2018). Anhedonia in depression: biological mechanisms and computational models. In *Current Opinion in Behavioral Sciences* (Vol. 22). https://doi.org/10.1016/j.cobeha.2018.01.024

Cordero, M. D., Alcocer-Gómez, E., Culic, O., Carrión, A. M., De Miguel, M., Díaz-Parrado, E., Pérez-Villegas, E. M., Bullón, P., Battino, M., & Sánchez-Alcazar, J. A. (2014). NLRP3 inflammasome is activated in fibromyalgia: The effect of coenzyme Q10. In *Antioxidants and Redox Signaling* (Vol. 20, Issue 8). https://doi.org/10.1089/ars.2013.5198

Costa, R., Bicca, M. A., Manjavachi, M. N., Segat, G. C., Dias, F. C., Fernandes, E. S., & Calixto, J. B. (2018). Kinin Receptors Sensitize TRPV4 Channel and Induce Mechanical Hyperalgesia: Relevance to Paclitaxel-Induced Peripheral Neuropathy in Mice. *Molecular Neurobiology*, *55*(3). https://doi.org/10.1007/s12035-017-0475-9

Cowie, A. M., Menzel, A. D., O'Hara, C., Lawlor, M. W., & Stucky, C. L. (2019). NOD-like receptor protein 3 inflammasome drives postoperative mechanical pain in a sex-dependent manner. *Pain*, *160*(8). https://doi.org/10.1097/j.pain.0000000000001555

Crawley, J., & Goodwin, F. K. (1980). Preliminary report of a simple animal behavior model for the anxiolytic effects of benzodiazepines. *Pharmacology Biochemistry and Behavior*, *13*(2), 167–170. https://doi.org/10.1016/0091-3057(80)90067-2

Csordás, G., & Hajnóczky, G. (2009). SR/ER-mitochondrial local communication: Calcium and ROS. In *Biochimica et Biophysica Acta - Bioenergetics* (Vol. 1787, Issue 11). https://doi.org/10.1016/j.bbabio.2009.06.004

Currie, G. L., Angel-Scott, H. N., Colvin, L., Cramond, F., Hair, K., Khandoker, L., Liao, J., Macleod, M., McCann, S. K., Morland, R., Sherratt, N., Stewart, R., Tanriver-Ayder, E., Thomas, J., Wang, Q., Wodarski, R., Xiong, R., Rice, A. S. C., & Sena, E. S. (2019a). Animal models of chemotherapy-induced peripheral neuropathy: A machine-assisted systematic review and meta-analysis. *PLoS Biology*, *17*(5). https://doi.org/10.1371/journal.pbio.3000243

Currie, G. L., Angel-Scott, H. N., Colvin, L., Cramond, F., Hair, K., Khandoker, L., Liao, J., Macleod, M., McCann, S. K., Morland, R., Sherratt, N., Stewart, R., Tanriver-Ayder, E., Thomas, J., Wang, Q., Wodarski, R., Xiong, R., Rice, A. S. C., & Sena, E. S. (2019b). Animal models of chemotherapy-induced peripheral neuropathy: A machine-assisted systematic review and meta-analysis. *PLoS Biology*, *17*(5). https://doi.org/10.1371/journal.pbio.3000243

D'AMOUR, F. E., & SMITH, D. L. (1941). A METHOD FOR DETERMINING LOSS OF PAIN SENSATION. *The Journal of Pharmacology and Experimental Therapeutics*, *72*(1).

Dai, Y., Wang, H., Ogawa, A., Yamanaka, H., Obata, K., Tokunaga, A., & Noguchi, K. (2005). Ca2+/calmodulin-dependent protein kinase II in the spinal cord contributes to neuropathic pain in a rat model of mononeuropathy. *European Journal of Neuroscience*, *21*(9). https://doi.org/10.1111/j.1460-9568.2005.04091.x

Davis, B. K., Wen, H., & Ting, J. P. Y. (2011). The Inflammasome NLRs in immunity, inflammation, and associated diseases. *Annual Review of Immunology*, *29*. https://doi.org/10.1146/annurev-immunol-031210-101405

de Almeida, A. S., Rigo, F. K., De Prá, S. D. T., Milioli, A. M., Dalenogare, D. P., Pereira, G. C., Ritter, C. dos S., Peres, D. S., Antoniazzi, C. T. de D., Stein, C., Moresco, R. N., Oliveira, S.

M., & Trevisan, G. (2019). Characterization of Cancer-Induced Nociception in a Murine Model of Breast Carcinoma. *Cellular and Molecular Neurobiology*. https://doi.org/10.1007/s10571-019-00666-8

Decosterd, I., & Woolf, C. J. (2000). Spared nerve injury: An animal model of persistent peripheral neuropathic pain. *Pain*, *87*(2). https://doi.org/10.1016/S0304-3959(00)00276-1

Deng, L., Cornett, B. L., Mackie, K., & Hohmann, A. G. (2015). CB1 knockout mice unveil sustained CB2-mediated antiallodynic effects of the mixed CB1/CB2 agonist CP55,940 in a mouse model of paclitaxel-induced neuropathic pain. *Molecular Pharmacology*, *88*(1). https://doi.org/10.1124/mol.115.098483

Descoeur, J., Pereira, V., Pizzoccaro, A., Francois, A., Ling, B., Maffre, V., Couette, B., Busserolles, J., Courteix, C., Noel, J., Lazdunski, M., Eschalier, A., Authier, N., & Bourinet, E. (2011). Oxaliplatin-induced cold hypersensitivity is due to remodelling of ion channel expression in nociceptors. *EMBO Molecular Medicine*, *3*(5). https://doi.org/10.1002/emmm.201100134

Deuis, J. R., Dvorakova, L. S., & Vetter, I. (2017). Methods used to evaluate pain behaviors in rodents. *Frontiers in Molecular Neuroscience*, *10*. https://doi.org/10.3389/fnmol.2017.00284

Deuis, J. R., Lim, Y. L., De Sousa, S. R., Lewis, R. J., Alewood, P. F., Cabot, P. J., & Vetter, I. (2014). Analgesic effects of clinically used compounds in novel mouse models of polyneuropathy induced by oxaliplatin and cisplatin. *Neuro-Oncology*, *16*(10). https://doi.org/10.1093/neuonc/nou048

Deuis, J. R., Whately, E., Brust, A., Inserra, M. C., Asvadi, N. H., Lewis, R. J., Alewood, P. F., Cabot, P. J., & Vetter, I. (2015). Activation of κ Opioid Receptors in Cutaneous Nerve Endings by Conorphin-1, a Novel Subtype-Selective Conopeptide, Does Not Mediate

Peripheral Analgesia. *ACS Chemical Neuroscience*, *6*(10). https://doi.org/10.1021/acschemneuro.5b00113

Deuis, J. R., Zimmermann, K., Romanovsky, A. A., Possani, L. D., Cabot, P. J., Lewis, R. J., & Vetter, I. (2013). An animal model of oxaliplatin-induced cold allodynia reveals a crucial role for Nav1.6 in peripheral pain pathways. *Pain*, *154*(9). https://doi.org/10.1016/j.pain.2013.05.032

Devigili, G., Tugnoli, V., Penza, P., Camozzi, F., Lombardi, R., Melli, G., Broglio, L., Granieri, E., & Lauria, G. (2008). The diagnostic criteria for small fibre neuropathy: From symptoms to neuropathology. *Brain*, *131*(7), 1912–1925. https://doi.org/10.1093/brain/awn093

Di Cesare Mannelli, L., Zanardelli, M., Failli, P., & Ghelardini, C. (2012). Oxaliplatin-induced neuropathy: Oxidative Stress as Pathological Mechanism. Protective Effect of Silibinin. *Journal of Pain*, *13*(3). https://doi.org/10.1016/j.jpain.2011.11.009

Dieras, V., Bougnoux, P., Petit, T., Chollet, P., Beuzeboc, P., Borel, C., Husseini, F., Goupil, A., Kebrat, P., Misset, J. L., Bensmaïne, M. A., Tabah-Fisch, I., & Pouillart, P. (2002). Multicentre phase II study of oxaliplatin as a single-agent in cisplatin/carboplatin ± taxane-pretreated ovarian cancer patients. *Annals of Oncology*, *13*(2), 258–266. https://doi.org/10.1093/annonc/mdf018

Dinarello, C. A. (2009). Immunological and inflammatory functions of the interleukin-1 family. In *Annual Review of Immunology* (Vol. 27). https://doi.org/10.1146/annurev.immunol.021908.132612

Dixon, W. J. (1980). Efficient analysis of experimental observations. *Annual Review of Pharmacology and Toxicology*, *20*. https://doi.org/10.1146/annurev.pa.20.040180.002301

Donnelly, C. R., Chen, O., & Ji, R. R. (2020). How Do Sensory Neurons Sense Danger Signals?

In *Trends in Neurosciences* (Vol. 43, Issue 10). https://doi.org/10.1016/j.tins.2020.07.008

Duncan, J. A., Bergstralh, D. T., Wang, Y., Willingham, S. B., Ye, Z., Zimmermann, A. G., & Ting, J. P. Y. (2007). Cryopyrin/NALP3 binds ATP/dATP, is an ATPase, and requires ATP binding to mediate inflammatory signaling. *Proceedings of the National Academy of Sciences of the United States of America*, *104*(19). https://doi.org/10.1073/pnas.0611496104

EDDY, N. B., & LEIMBACH, D. (1953). Synthetic analgesics. II. Dithienylbutenyl- and dithienylbutylamines. *The Journal of Pharmacology and Experimental Therapeutics*, *107*(3).

Eldridge, S., Guo, L., & Hamre, J. (2020). A Comparative Review of Chemotherapy-Induced Peripheral Neuropathy in In Vivo and In Vitro Models. In *Toxicologic Pathology* (Vol. 48, Issue 1). https://doi.org/10.1177/0192623319861937

Ennaceur, A., & Chazot, P. L. (2016). Preclinical animal anxiety research – flaws and prejudices. *Pharmacology Research and Perspectives*, *4*(2), e00223. https://doi.org/10.1002/prp2.223

Evavold, C. L., Ruan, J., Tan, Y., Xia, S., Wu, H., & Kagan, J. C. (2018). The Pore-Forming Protein Gasdermin D Regulates Interleukin-1 Secretion from Living Macrophages. *Immunity*, *48*(1). https://doi.org/10.1016/j.immuni.2017.11.013

Everhardt Queen, A., Moerdyk-Schauwecker, M., McKee, L. M., Leamy, L. J., & Huet, Y. M. (2016). Differential expression of inflammatory cytokines and stress genes in male and female mice in response to a lipopolysaccharide challenge. *PLoS ONE*, *11*(4), e0152289. https://doi.org/10.1371/journal.pone.0152289

Feather, C. E., Lees, J. G., Makker, P. G. S., Goldstein, D., Kwok, J. B., Moalem-Taylor, G., & Polly, P. (2018). Oxaliplatin induces muscle loss and muscle-specific molecular changes in Mice. *Muscle and Nerve*, *57*(4), 650–658. https://doi.org/10.1002/mus.25966

Fernandes-Alnemri, T., Kang, S., Anderson, C., Sagara, J., Fitzgerald, K. A., & Alnemri, E. S. (2013). Cutting Edge: TLR Signaling Licenses IRAK1 for Rapid Activation of the NLRP3 Inflammasome. *The Journal of Immunology*, *191*(8). https://doi.org/10.4049/jimmunol.1301681

Ferrier, J., Pereira, V., Busserolles, J., Authier, N., & Balayssac, D. (2013). Emerging trends in understanding chemotherapy-induced peripheral neuropathy. *Current Pain and Headache Reports*, *17*(10). https://doi.org/10.1007/s11916-013-0364-5

Ferrini, F., Trang, T., Mattioli, T. A. M., Laffray, S., Del'Guidice, T., Lorenzo, L. E., Castonguay, A., Doyon, N., Zhang, W., Godin, A. G., Mohr, D., Beggs, S., Vandal, K., Beaulieu, J. M., Cahill, C. M., Salter, M. W., & De Koninck, Y. (2013). Morphine hyperalgesia gated through microglia-mediated disruption of neuronal Cl-homeostasis. *Nature Neuroscience*, *16*(2), 183–192. https://doi.org/10.1038/nn.3295

Fillingim, R. B., King, C. D., Ribeiro-Dasilva, M. C., Rahim-Williams, B., & Riley, J. L. (2009). Sex, Gender, and Pain: A Review of Recent Clinical and Experimental Findings. In *Journal of Pain* (Vol. 10, Issue 5). https://doi.org/10.1016/j.jpain.2008.12.001

Finnerup, N. B., Haroutounian, S., Kamerman, P., Baron, R., Bennett, D. L. H., Bouhassira, D., Cruccu, G., Freeman, R., Hansson, P., Nurmikko, T., Raja, S. N., Rice, A. S. C., Serra, J., Smith, B. H., Treede, R. D., & Jensen, T. S. (2016). Neuropathic pain: An updated grading system for research and clinical practice. *Pain*, *157*(8), 1599–1606. https://doi.org/10.1097/j.pain.0000000000000492

Fiore, N. T., & Austin, P. J. (2016). Are the emergence of affective disturbances in neuropathic pain states contingent on supraspinal neuroinflammation? *Brain, Behavior, and Immunity*, *56*, 397–411. https://doi.org/10.1016/j.bbi.2016.04.012

Flatters, S. J.L., Dougherty, P. M., & Colvin, L. A. (2017). Clinical and preclinical perspectives on Chemotherapy-Induced Peripheral Neuropathy (CIPN): A narrative review. In *British Journal of Anaesthesia* (Vol. 119, Issue 4). https://doi.org/10.1093/bja/aex229

Flatters, Sarah J.L., & Bennett, G. J. (2006). Studies of peripheral sensory nerves in paclitaxel-induced painful peripheral neuropathy: Evidence for mitochondrial dysfunction. *Pain*, *122*(3). https://doi.org/10.1016/j.pain.2006.01.037

Freeman, L., Guo, H., David, C. N., Brickey, W. J., Jha, S., & Ting, J. P. Y. (2017). NLR members NLRC4 and NLRP3 mediate sterile inflammasome activation in microglia and astrocytes. *Journal of Experimental Medicine*, *214*(5). https://doi.org/10.1084/jem.20150237

Freireich, E. J., Gehan, E. A., Rall, D. P., Schmidt, L. H., & Skipper, H. E. (1966). Quantitative comparison of toxicity of anticancer agents in mouse, rat, hamster, dog, monkey, and man. *Cancer Chemotherapy Reports*, *50*(4), 219–244.

Fumagalli, G., Monza, L., Cavaletti, G., Rigolio, R., & Meregalli, C. (2021). Neuroinflammatory Process Involved in Different Preclinical Models of Chemotherapy-Induced Peripheral Neuropathy. In *Frontiers in Immunology* (Vol. 11). https://doi.org/10.3389/fimmu.2020.626687

Gadgil, S., Ergün, M., van den Heuvel, S. A., van der Wal, S. E., Scheffer, G. J., & Hooijmans, C. R. (2019). A systematic summary and comparison of animal models for chemotherapy induced (peripheral) neuropathy (CIPN). *PLoS ONE*, *14*(8). https://doi.org/10.1371/journal.pone.0221787

Gaidt, M. M., Ebert, T. S., Chauhan, D., Schmidt, T., Schmid-Burgk, J. L., Rapino, F., Robertson, A. A. B., Cooper, M. A., Graf, T., & Hornung, V. (2016). Human Monocytes Engage an Alternative Inflammasome Pathway. *Immunity*, *44*(4).

https://doi.org/10.1016/j.immuni.2016.01.012

Gan, X. H., Jewett, A., & Bonavida, B. (1992). Activation of human peripheral-blood-derived monocytes by cis-diamminedichloroplatinum: Enhanced tumoricidal activity and secretion of tumor necrosis factor-alpha. *Natural Immunity*, *11*(3), 144–155.

Gebremedhn, E. G., Shortland, P. J., & Mahns, D. A. (2018). The incidence of acute oxaliplatin-induced neuropathy and its impact on treatment in the first cycle: A systematic review. *BMC Cancer*, *18*(1). https://doi.org/10.1186/s12885-018-4185-0

Gewandter, J. S., Kleckner, A. S., Marshall, J. H., Brown, J. S., Curtis, L. H., Bautista, J., Dworkin, R. H., Kleckner, I. R., Kolb, N., Mohile, S. G., & Mustian, K. M. (2020). Chemotherapy-induced peripheral neuropathy (CIPN) and its treatment: an NIH Collaboratory study of claims data. *Supportive Care in Cancer*, *28*(6). https://doi.org/10.1007/s00520-019-05063-x

Ghayur, T., Banerjee, S., Hugunin, M., Butler, D., Herzog, L., Carter, A., Quintal, L., Sekut, L., Talanian, R., Paskind, M., Wong, W., Kamen, R., Tracey, D., & Allen, H. (1997). Caspase-1 processes IFN-γ-inducing factor and regulates LPS-induced IFN-γ production. *Nature*, *386*(6625). https://doi.org/10.1038/386619a0

Ghiringhelli, F., Apetoh, L., Tesniere, A., Aymeric, L., Ma, Y., Ortiz, C., Vermaelen, K., Panaretakis, T., Mignot, G., Ullrich, E., Perfettini, J. L., Schlemmer, F., Tasdemir, E., Uhl, M., Génin, P., Civas, A., Ryffel, B., Kanellopoulos, J., Tschopp, J., … Zitvogel, L. (2009). Activation of the NLRP3 inflammasome in dendritic cells induces IL-1B-dependent adaptive immunity against tumors. *Nature Medicine*, *15*(10). https://doi.org/10.1038/nm.2028

Gitter, A. J., & Stolov, W. C. (1995). AAEM minimonograph #16: Instrumentation and

measurement in electrodiagnostic medicine–part I. *Muscle & Nerve*, *18*(8). https://doi.org/10.1002/mus.880180803

Glantz, M. J., Choy, H., Kearns, C. M., Mills, P. C., Wahlberg, L. U., Zuhowski, E. G., Calabresi, P., & Egorin, M. J. (1995). Paclitaxel disposition in plasma and central nervous systems of humans and rats with brain tumors. *Journal of the National Cancer Institute*, *87*(14). https://doi.org/10.1093/jnci/87.14.1077

Gómez, N., Cuadras, J., Butí, M., & Navarro, X. (1996). Histologic assessment of sciatic nerve regeneration following resection and graft or tube repair in the mouse. *Restorative Neurology and Neuroscience*, *10*(4). https://doi.org/10.3233/rnn-1996-10401

Gong, Z., Pan, J., Shen, Q., Li, M., & Peng, Y. (2018). Mitochondrial dysfunction induces NLRP3 inflammasome activation during cerebral ischemia/reperfusion injury. *Journal of Neuroinflammation*, *15*(1). https://doi.org/10.1186/s12974-018-1282-6

Govbakh, I. O., Zavodovskiy, D. O., Bulgakova, N. V., Sokołowska (Vereshchaka), I. V., Maznychenko, A. V., & Vasylenko, D. A. (2019). Nerve Conduction and Neuromuscular Transmission in C57Bl/6 Mice with Genetically Determined Peripheral Neuropathy. *Neurophysiology*, *51*(4). https://doi.org/10.1007/s11062-019-09817-5

Graeber, M. B. (2010). Changing face of microglia. In *Science* (Vol. 330, Issue 6005). https://doi.org/10.1126/science.1190929

Greten, F. R., & Grivennikov, S. I. (2019). Inflammation and Cancer: Triggers, Mechanisms, and Consequences. In *Immunity* (Vol. 51, Issue 1). https://doi.org/10.1016/j.immuni.2019.06.025

Grisold, W., Cavaletti, G., & Windebank, A. J. (2012). Peripheral neuropathies from chemotherapeutics and targeted agents: Diagnosis, treatment, and prevention. *Neuro-Oncology*, *14*(SUPPL.4). https://doi.org/10.1093/neuonc/nos203

Gustorff, B., Dorner, T., Likar, R., Grisold, W., Lawrence, K., Schwarz, F., & Rieder, A. (2008). Prevalence of self-reported neuropathic pain and impact on quality of life: A prospective representative survey. *Acta Anaesthesiologica Scandinavica*, *52*(1), 132–136. https://doi.org/10.1111/j.1399-6576.2007.01486.x

Hache, G., Guiard, B. P., Nguyen, T. H., Quesseveur, G., Gardier, A. M., Peters, D., Munro, G., & Coudoré, F. (2015). Antinociceptive activity of the new triple reuptake inhibitor NS18283 in a mouse model of chemotherapy-induced neuropathic pain. *European Journal of Pain (United Kingdom)*, *19*(3), 322–333. https://doi.org/10.1002/ejp.550

Hadzic, T., Aykin-Burns, N., Zhu, Y., Coleman, M. C., Leick, K., Jacobson, G. M., & Spitz, D. R. (2010). Paclitaxel combined with inhibitors of glucose and hydroperoxide metabolism enhances breast cancer cell killing via H2O2-mediated oxidative stress. *Free Radical Biology and Medicine*, *48*(8). https://doi.org/10.1016/j.freeradbiomed.2010.01.018

Hafner-Bratkovič, I., Sušjan, P., Lainšček, D., Tapia-Abellán, A., Cerović, K., Kadunc, L., Angosto-Bazarra, D., Pelegrín, P., & Jerala, R. (2018). NLRP3 lacking the leucine-rich repeat domain can be fully activated via the canonical inflammasome pathway. *Nature Communications*, *9*(1). https://doi.org/10.1038/s41467-018-07573-4

Hall, P. S., Swinson, D., Waters, J. S., Wadsley, J., Falk, S., Roy, R., Tillett, T., Nicoll, J., Cummings, S., Grumett, S. A., Kamposioras, K., Garcia, A., Allmark, C., Marshall, H., Ruddock, S., Katona, E., Velikova, G., Petty, R. D., Grabsch, H. I., & Seymour, M. T. (2019). Optimizing chemotherapy for frail and elderly patients (pts) with advanced gastroesophageal cancer (aGOAC): The GO2 phase III trial. *Journal of Clinical Oncology*, *37*(15_suppl). https://doi.org/10.1200/jco.2019.37.15_suppl.4006

Haller, D. G., Tabernero, J., Maroun, J., De Braud, F., Price, T., Van Cutsem, E., Hill, M.,

Gilberg, F., Rittweger, K., & Schmoll, H. J. (2011). Capecitabine plus oxaliplatin compared with fluorouracil and folinic acid as adjuvant therapy for stage III colon cancer. *Journal of Clinical Oncology*, *29*(11). https://doi.org/10.1200/JCO.2010.33.6297

Hara, T., Chiba, T., Abe, K., Makabe, A., Ikeno, S., Kawakami, K., Utsunomiya, I., Hama, T., & Taguchi, K. (2013). Effect of paclitaxel on transient receptor potential vanilloid 1 in rat dorsal root ganglion. *Pain*, *154*(6). https://doi.org/10.1016/j.pain.2013.02.023

Hargreaves, K., Dubner, R., Brown, F., Flores, C., & Joris, J. (1988). A new and sensitive method for measuring thermal nociception in cutaneous hyperalgesia. *Pain*, *32*(1). https://doi.org/10.1016/0304-3959(88)90026-7

Harkin, A., Houlihan, D. D., & Kelly, J. P. (2002). Reduction in preference for saccharin by repeated unpredictable stress in mice and its prevention by imipramine. *Journal of Psychopharmacology*, *16*(2), 115–123. https://doi.org/10.1177/026988110201600201

He, Y., Hara, H., & Núñez, G. (2016). Mechanism and Regulation of NLRP3 Inflammasome Activation. In *Trends in Biochemical Sciences* (Vol. 41, Issue 12). https://doi.org/10.1016/j.tibs.2016.09.002

He, Y., Zeng, M. Y., Yang, D., Motro, B., & Núñez, G. (2016). NEK7 is an essential mediator of NLRP3 activation downstream of potassium efflux. *Nature*, *530*(7590). https://doi.org/10.1038/nature16959

Heilig, R., & Broz, P. (2018). Function and mechanism of the pyrin inflammasome. In *European Journal of Immunology* (Vol. 48, Issue 2). https://doi.org/10.1002/eji.201746947

Helyes, Z., Tékus, V., Szentes, N., Pohóczky, K., Botz, B., Kiss, T., Kemény, Á., Környei, Z., Tóth, K., Lénárt, N., Ábrahám, H., Pinteaux, E., Francis, S., Sensi, S., Dénes, Á., & Goebel, A. (2019). Transfer of complex regional pain syndrome to mice via human autoantibodies is

mediated by interleukin-1–induced mechanisms. *Proceedings of the National Academy of Sciences of the United States of America*, *116*(26). https://doi.org/10.1073/pnas.1820168116

Hershman, D. L., Lacchetti, C., Dworkin, R. H., Lavoie Smith, E. M., Bleeker, J., Cavaletti, G., Chauhan, C., Gavin, P., Lavino, A., Lustberg, M. B., Paice, J., Schneider, B., Smith, M. Lou, Smith, T., Terstriep, S., Wagner-Johnston, N., Bak, K., & Loprinzi, C. L. (2014). Prevention and management of chemotherapy-induced peripheral neuropathy in survivors of adult cancers: American society of clinical oncology clinical practice guideline. In *Journal of Clinical Oncology* (Vol. 32, Issue 18). https://doi.org/10.1200/JCO.2013.54.0914

Hershman, D. L., Lacchetti, C., & Loprinzi, C. L. (2014). Prevention and management of chemotherapy-induced peripheral neuropathy in survivors of adult cancers: American Society of Clinical Oncology clinical practice guideline summary. In *Journal of Oncology Practice* (Vol. 10, Issue 6). https://doi.org/10.1200/JOP.2014.001776

Hershman, D. L., Weimer, L. H., Wang, A., Kranwinkel, G., Brafman, L., Fuentes, D., Awad, D., & Crew, K. D. (2011). Association between patient reported outcomes and quantitative sensory tests for measuring long-term neurotoxicity in breast cancer survivors treated with adjuvant paclitaxel chemotherapy. *Breast Cancer Research and Treatment*, *125*(3). https://doi.org/10.1007/s10549-010-1278-0

Hirayama, Y., Ishitani, K., Sato, Y., Iyama, S., Takada, K., Murase, K., Kuroda, H., Nagamachi, Y., Konuma, Y., Fujimi, A., Sagawa, T., Ono, K., Horiguchi, H., Terui, T., Koike, K., Kusakabe, T., Sato, T., Takimoto, R., Kobune, M., & Kato, J. (2015). Effect of duloxetine in Japanese patients with chemotherapy-induced peripheral neuropathy: a pilot randomized trial. *International Journal of Clinical Oncology*, *20*(5). https://doi.org/10.1007/s10147-015-0810-y

Höke, A. (2012). Animal Models of Peripheral Neuropathies. In *Neurotherapeutics* (Vol. 9, Issue 2). https://doi.org/10.1007/s13311-012-0116-y

Höke, A., & Ray, M. (2014). Rodent models of chemotherapy-induced peripheral neuropathy. *ILAR Journal*, *54*(3), 273–281. https://doi.org/10.1093/ilar/ilt053

Hong, Y. S., Kim, S. Y., Lee, J. S., Nam, B. H., Kim, K. pyo, Kim, J. E., Park, Y. S., Oh Park, J., Baek, J. Y., Kim, T. Y., Lee, K. W., Ahn, J. B., Lim, S. B., Yu, C. S., Kim, J. C., Yun, S. H., Kim, J. H., Park, J. hong, Park, H. C., … Kim, T. W. (2019). Oxaliplatin-based adjuvant chemotherapy for rectal cancer after preoperative chemoradiotherapy (ADORE): Long-term results of a randomized controlled trial. *Journal of Clinical Oncology*, *37*(33). https://doi.org/10.1200/JCO.19.00016

Hu, X., Jiang, Z., Teng, L., Yang, H., Hong, D., Zheng, D., & Zhao, Q. (2021). Platinum-Induced Peripheral Neuropathy (PIPN): ROS-Related Mechanism, Therapeutic Agents, and Nanosystems. In *Frontiers in Molecular Biosciences* (Vol. 8). https://doi.org/10.3389/fmolb.2021.770808

Hua Huang, Nora G. Smart, & B. Beutler. (2019). *Record for nd1, updated Jan 29, 2019*. MUTAGENETIX (TM), B. Beutler and Colleagues, Center for the Genetics of Host Defense, UT Southwestern Medical Center, Dallas, TX. URL: Mutagenetix.Utsouthwestern.Edu.

Hucho, T., & Levine, J. D. (2007). Signaling Pathways in Sensitization: Toward a Nociceptor Cell Biology. In *Neuron* (Vol. 55, Issue 3). https://doi.org/10.1016/j.neuron.2007.07.008

Humphries, F., Bergin, R., Jackson, R., Delagic, N., Wang, B., Yang, S., Dubois, A. V., Ingram, R. J., & Moynagh, P. N. (2018). The E3 ubiquitin ligase Pellino2 mediates priming of the NLRP3 inflammasome. *Nature Communications*, *9*(1). https://doi.org/10.1038/s41467-018-

03669-z

Imai, S., Koyanagi, M., Azimi, Z., Nakazato, Y., Matsumoto, M., Ogihara, T., Yonezawa, A., Omura, T., Nakagawa, S., Wakatsuki, S., Araki, T., Kaneko, S., Nakagawa, T., & Matsubara, K. (2017). Taxanes and platinum derivatives impair Schwann cells via distinct mechanisms. *Scientific Reports*, *7*(1). https://doi.org/10.1038/s41598-017-05784-1

Inoue, M., & Shinohara, M. L. (2013). NLRP3 inflammasome and MS/EAE. In *Autoimmune Diseases* (Vol. 2013). https://doi.org/10.1155/2013/859145

Jaillon, S., Berthenet, K., & Garlanda, C. (2019). Sexual Dimorphism in Innate Immunity. In *Clinical Reviews in Allergy and Immunology* (Vol. 56, Issue 3). https://doi.org/10.1007/s12016-017-8648-x

Jamieson, S. M. F., Liu, J., Connor, B., & McKeage, M. J. (2005). Oxaliplatin causes selective atrophy of a subpopulation of dorsal root ganglion neurons without inducing cell loss. *Cancer Chemotherapy and Pharmacology*, *56*(4), 391–399. https://doi.org/10.1007/s00280-004-0953-4

Janes, K., Little, J. W., Li, C., Bryant, L., Chen, C., Chen, Z., Kamocki, K., Doyle, T., Snider, A., Esposito, E., Cuzzocrea, S., Bieberich, E., Obeid, L., Petrache, I., Nicol, G., Neumann, W. L., & Salvemini, D. (2014). The development and maintenance of paclitaxel-induced neuropathic pain require activation of the sphingosine 1-phosphate receptor subtype 1. *Journal of Biological Chemistry*, *289*(30). https://doi.org/10.1074/jbc.M114.569574

Janes, K., Wahlman, C., Little, J. W., Doyle, T., Tosh, D. K., Jacobson, K. A., & Salvemini, D. (2015). Spinal neuroimmune activation is independent of T-cell infiltration and attenuated by A3 adenosine receptor agonists in a model of oxaliplatin-induced peripheral neuropathy. *Brain, Behavior, and Immunity*, *44*. https://doi.org/10.1016/j.bbi.2014.08.010

Jasmin, L., Kohan, L., Franssen, M., Janni, G., & Goff, J. R. (1998). The cold plate as a test of nociceptive behaviors: Description and application to the study of chronic neuropathic and inflammatory pain models. *Pain*, *75*(2–3). https://doi.org/10.1016/S0304-3959(98)00017-7

Jauhari, S., Singh, S., & Dash, A. K. (2008). Chapter 7 Paclitaxel. In *Profiles of Drug Substances, Excipients and Related Methodology* (Vol. 34). https://doi.org/10.1016/S1871-5125(09)34007-8

Javle, M., & Hsueh, C. T. (2010). Recent advances in gastrointestinal oncology - Updates and insights from the 2009 annual meeting of the American Society of Clinical Oncology. In *Journal of Hematology and Oncology* (Vol. 3, Issue 11). https://doi.org/10.1186/1756-8722-3-11

Jesse, C. R., Wilhelm, E. A., & Nogueira, C. W. (2010). Depression-like behavior and mechanical allodynia are reduced by bis selenide treatment in mice with chronic constriction injury: A comparison with fluoxetine, amitriptyline, and bupropion. *Psychopharmacology*, *212*(4), 513–522. https://doi.org/10.1007/s00213-010-1977-6

Jia, M., Wu, C., Gao, F., Xiang, H., Sun, N., Peng, P., Li, J., Yuan, X., Li, H., Meng, X., Tian, B., Shi, J., & Li, M. (2017). Activation of NLRP3 inflammasome in peripheral nerve contributes to paclitaxel-induced neuropathic pain. *Molecular Pain*, *13*. https://doi.org/10.1177/1744806917719804

Johnson, M. (2012). *Laboratory Mice and Rats*. Materials and Methods. https://doi.org/10.13070/mm.en.2.113

Jordan, M. A., Toso, R. J., Thrower, D., & Wilson, L. (1993). Mechanism of mitotic block and inhibition of cell proliferation by taxol at low concentrations. *Proceedings of the National Academy of Sciences of the United States of America*, *90*(20).

https://doi.org/10.1073/pnas.90.20.9552

Joseph, E. K., Chen, X., Bogen, O., & Levine, J. D. (2008). Oxaliplatin Acts on IB4-Positive Nociceptors to Induce an Oxidative Stress-Dependent Acute Painful Peripheral Neuropathy. *Journal of Pain*, *9*(5). https://doi.org/10.1016/j.jpain.2008.01.335

Juliana, C., Fernandes-Alnemri, T., Kang, S., Farias, A., Qin, F., & Alnemri, E. S. (2012). Non-transcriptional priming and deubiquitination regulate NLRP3 inflammasome activation. *Journal of Biological Chemistry*, *287*(43). https://doi.org/10.1074/jbc.M112.407130

Julius, D., & Basbaum, A. I. (2001). Molecular mechanisms of nociception. In *Nature* (Vol. 413, Issue 6852). https://doi.org/10.1038/35093019

Kanda, K., Fujimoto, K., & Kyota, A. (2017). Emotional responses to persistent chemotherapy-induced peripheral neuropathy experienced by patients with colorectal cancer in Japan. *Asia-Pacific Journal of Oncology Nursing*, *4*(3), 233–240. https://doi.org/10.4103/apjon.apjon_12_17

Kang, L., Tian, Y., Xu, S., & Chen, H. (2020). Oxaliplatin-induced peripheral neuropathy: clinical features, mechanisms, prevention and treatment. In *Journal of Neurology*. https://doi.org/10.1007/s00415-020-09942-w

Kasukurthi, R., Brenner, M. J., Moore, A. M., Moradzadeh, A., Ray, W. Z., Santosa, K. B., Mackinnon, S. E., & Hunter, D. A. (2009). Transcardial perfusion versus immersion fixation for assessment of peripheral nerve regeneration. *Journal of Neuroscience Methods*, *184*(2). https://doi.org/10.1016/j.jneumeth.2009.08.019

Kawana, N., Yamamoto, Y., Ishida, T., Saito, Y., Konno, H., Arima, K., & Satoh, J. I. (2013). Reactive astrocytes and perivascular macrophages express NLRP3 inflammasome in active demyelinating lesions of multiple sclerosis and necrotic lesions of neuromyelitis optica and

cerebral infarction. *Clinical and Experimental Neuroimmunology*, *4*(3). https://doi.org/10.1111/cen3.12068

Kawashiri, T., Egashira, N., Kurobe, K., Tsutsumi, K., Yamashita, Y., Ushio, S., Yano, T., & Oishi, R. (2012). L type Ca 2+channel blockers prevent oxaliplatin-induced cold hyperalgesia and TRPM8 overexpression in rats. *Molecular Pain*, *8*. https://doi.org/10.1186/1744-8069-8-7

Kayagaki, N., Stowe, I. B., Lee, B. L., O'Rourke, K., Anderson, K., Warming, S., Cuellar, T., Haley, B., Roose-Girma, M., Phung, Q. T., Liu, P. S., Lill, J. R., Li, H., Wu, J., Kummerfeld, S., Zhang, J., Lee, W. P., Snipas, S. J., Salvesen, G. S., … Dixit, V. M. (2015). Caspase-11 cleaves gasdermin D for non-canonical inflammasome signalling. *Nature*, *526*(7575). https://doi.org/10.1038/nature15541

Kayagaki, N., Warming, S., Lamkanfi, M., Walle, L. Vande, Louie, S., Dong, J., Newton, K., Qu, Y., Liu, J., Heldens, S., Zhang, J., Lee, W. P., Roose-Girma, M., & Dixit, V. M. (2011). Non-canonical inflammasome activation targets caspase-11. *Nature*, *479*(7371). https://doi.org/10.1038/nature10558

Kayagaki, N., Wong, M. T., Stowe, I. B., Ramani, S. R., Gonzalez, L. C., Akashi-Takamura, S., Miyake, K., Zhang, J., Lee, W. P., Muszyński, A., Forsberg, L. S., Carlson, R. W., & Dixit, V. M. (2013). Noncanonical inflammasome activation by intracellular LPS independent of TLR4. *Science*, *341*(6151). https://doi.org/10.1126/science.1240248

Kelley, N., Jeltema, D., Duan, Y., & He, Y. (2019). The NLRP3 inflammasome: An overview of mechanisms of activation and regulation. In *International Journal of Molecular Sciences* (Vol. 20, Issue 13). https://doi.org/10.3390/ijms20133328

Kennedy, W. R., & Wendelschafer-Crabb, G. (1993). The innervation of human epidermis.

Journal of the Neurological Sciences, *115*(2). https://doi.org/10.1016/0022-510X(93)90223-L

Kerckhove, N., Boudieu, L., Ourties, G., Bourdier, J., Daulhac, L., Eschalier, A., & Mallet, C. (2019). Ethosuximide improves chronic pain-induced anxiety- and depression-like behaviors. *European Neuropsychopharmacology*, *29*(12), 1419–1432. https://doi.org/10.1016/j.euroneuro.2019.10.012

Khan, N., Kuo, A., Brockman, D. A., Cooper, M. A., & Smith, M. T. (2018). Pharmacological inhibition of the NLRP3 inflammasome as a potential target for multiple sclerosis induced central neuropathic pain. *Inflammopharmacology*, *26*(1). https://doi.org/10.1007/s10787-017-0401-9

Kidd, J. F., Pilkington, M. F., Schell, M. J., Fogarty, K. E., Skepper, J. N., Taylor, C. W., & Thorn, P. (2002). Paclitaxel affects cytosolic calcium signals by opening the mitochondrial permeability transition pore. *Journal of Biological Chemistry*, *277*(8). https://doi.org/10.1074/jbc.M106802200

Kidwell, K. M., Yothers, G., Ganz, P. A., Land, S. R., Ko, C. Y., Cecchini, R. S., Kopec, J. A., & Wolmark, N. (2012). Long-term neurotoxicity effects of oxaliplatin added to fluorouracil and leucovorin as adjuvant therapy for colon cancer: Results from National Surgical Adjuvant Breast and Bowel Project trials C-07 and LTS-01. *Cancer*, *118*(22). https://doi.org/10.1002/cncr.27593

Kiselyov, K., & Muallem, S. (2016). ROS and intracellular ion channels. In *Cell Calcium* (Vol. 60, Issue 2). https://doi.org/10.1016/j.ceca.2016.03.004

Kokotis, P., Schmelz, M., Kostouros, E., Karandreas, N., & Dimopoulos, M. A. (2016). Oxaliplatin-Induced Neuropathy: A Long-Term Clinical and Neurophysiologic Follow-Up

Study. *Clinical Colorectal Cancer*, *15*(3). https://doi.org/10.1016/j.clcc.2016.02.009

Koonin, E. V., & Aravind, L. (2000). The NACHT family - A new group of predicted NTPases implicated in apoptosis and MHC transcription activation. In *Trends in Biochemical Sciences* (Vol. 25, Issue 5). https://doi.org/10.1016/S0968-0004(00)01577-2

Kuwar, R., Rolfe, A., Di, L., Xu, H., He, L., Jiang, Y., Zhang, S., & Sun, D. (2019). A novel small molecular NLRP3 inflammasome inhibitor alleviates neuroinflammatory response following traumatic brain injury. *Journal of Neuroinflammation*, *16*(1). https://doi.org/10.1186/s12974-019-1471-y

Kuyrukluyıldız, U., Küpeli, İ., Bedir, Z., Özmen, Ö., Onk, D., Süleyman, B., Mammadov, R., & Süleyman, H. (2016). The effect of anakinra on paclitaxel-induced peripheral neuropathic pain in rats. *Turk Anesteziyoloji ve Reanimasyon Dernegi Dergisi*, *44*(6). https://doi.org/10.5152/TJAR.2016.02212

Lacroix-Fralish, M. L., & Mogi, J. S. (2009). Progress in genetic studies of pain and analgesia. *Annual Review of Pharmacology and Toxicology*, *49*(1), 97–121. https://doi.org/10.1146/annurev-pharmtox-061008-103222

Langford, D. J., & Mogil, J. S. (2008). Pain Testing in the Laboratory Mouse. In *Anesthesia and Analgesia in Laboratory Animals*. https://doi.org/10.1016/B978-012373898-1.50027-9

Latremoliere, A., & Woolf, C. J. (2009). Central Sensitization: A Generator of Pain Hypersensitivity by Central Neural Plasticity. In *Journal of Pain* (Vol. 10, Issue 9). https://doi.org/10.1016/j.jpain.2009.06.012

Latz, E., Xiao, T. S., & Stutz, A. (2013). Activation and regulation of the inflammasomes. In *Nature Reviews Immunology* (Vol. 13, Issue 6). https://doi.org/10.1038/nri3452

Lauria, G., Hsieh, S. T., Johansson, O., Kennedy, W. R., Leger, J. M., Mellgren, S. I., Nolano,

M., Merkies, I. S. J., Polydefkis, M., Smith, A. G., Sommer, C., & Valls-Sole, J. (2010). European Federation of Neurological Societies/Peripheral Nerve Society guideline on the use of skin biopsy in the diagnosis of small fiber neuropathy. Report of a joint task force of the European Federation of Neurological Societies and the Peripheral Nerve Society. In *Journal of the Peripheral Nervous System* (Vol. 15, Issue 2). https://doi.org/10.1111/j.1529-8027.2010.00269.x

Le Bricon, T., Gugins, S., Cynober, L., & Baracos, V. E. (1995). Negative impact of cancer chemotherapy on protein metabolism in healthy and tumor-bearing rats. *Metabolism*, *44*(10), 1340–1348. https://doi.org/10.1016/0026-0495(95)90040-3

Leblanc, A. F., Sprowl, J. A., Alberti, P., Chiorazzi, A., David Arnold, W., Gibson, A. A., Hong, K. W., Pioso, M. S., Chen, M., Huang, K. M., Chodisetty, V., Costa, O., Florea, T., De Bruijn, P., Mathijssen, R. H., Reinbolt, R. E., Lustberg, M. B., Sucheston-Campbell, L. E., Cavaletti, G., … Hu, S. (2018). OATP1B2 deficiency protects against paclitaxel-induced neurotoxicity. *Journal of Clinical Investigation*, *128*(2). https://doi.org/10.1172/JCI96160

Ledeboer, A., Jekich, B. M., Sloane, E. M., Mahoney, J. H., Langer, S. J., Milligan, E. D., Martin, D., Maier, S. F., Johnson, K. W., Leinwand, L. A., Chavez, R. A., & Watkins, L. R. (2007). Intrathecal interleukin-10 gene therapy attenuates paclitaxel-induced mechanical allodynia and proinflammatory cytokine expression in dorsal root ganglia in rats. *Brain, Behavior, and Immunity*, *21*(5). https://doi.org/10.1016/j.bbi.2006.10.012

Lee, K. H., Chang, H. J., Han, S. W., Oh, D. Y., Im, S. A., Bang, Y. J., Kim, S. Y., Lee, K. W., Kim, J. H., Hong, Y. S., Kim, T. W., Park, Y. S., Kang, W. K., Shin, S. J., Ahn, J. B., Kang, G. H., Jeong, S. Y., Park, K. J., Park, J. G., & Kim, T. Y. (2013). Pharmacogenetic analysis of adjuvant FOLFOX for Korean patients with colon cancer. *Cancer Chemotherapy and*

Pharmacology, *71*(4), 843–851. https://doi.org/10.1007/s00280-013-2075-3

Leith, J. L., Koutsikou, S., Lumb, B. M., & Apps, R. (2010). Spinal processing of noxious and innocuous cold information: Differential modulation by the periaqueductal gray. *Journal of Neuroscience*, *30*(14). https://doi.org/10.1523/JNEUROSCI.0122-10.2010

Lemmers, B., Salmena, L., Bidère, N., Su, H., Matysiak-Zablocki, E., Murakami, K., Ohashi, P. S., Jurisicova, A., Lenardo, M., Hakem, R., & Hakem, A. (2007). Essential role for caspase-8 in toll-like receptors and NFκB signaling. *Journal of Biological Chemistry*, *282*(10). https://doi.org/10.1074/jbc.M606721200

Leo, M., Schmitt, L. I., Küsterarent, P., Kutritz, A., Rassaf, T., Kleinschnitz, C., Hendgen-Cotta, U. B., & Hagenacker, T. (2020). Platinum-based drugs cause mitochondrial dysfunction in cultured dorsal root ganglion neurons. *International Journal of Molecular Sciences*, *21*(22). https://doi.org/10.3390/ijms21228636

Li, L., Li, J., Zuo, Y., Dang, D., Frost, J. A., & Yang, Q. (2019). Activation of KCNQ Channels Prevents Paclitaxel-Induced Peripheral Neuropathy and Associated Neuropathic Pain. *Journal of Pain*, *20*(5). https://doi.org/10.1016/j.jpain.2018.11.001

Li, P., Allen, H., Banerjee, S., Franklin, S., Herzog, L., Johnston, C., McDowell, J., Paskind, M., Rodman, L., Salfeld, J., Towne, E., Tracey, D., Wardwell, S., Wei, F. Y., Wong, W., Kamen, R., & Seshadri, T. (1995). Mice deficient in IL-1β-converting enzyme are defective in production of mature IL-1β and resistant to endotoxic shock. *Cell*, *80*(3). https://doi.org/10.1016/0092-8674(95)90490-5

Li, Q., & Barres, B. A. (2018). Microglia and macrophages in brain homeostasis and disease. In *Nature Reviews Immunology* (Vol. 18, Issue 4). https://doi.org/10.1038/nri.2017.125

Liem, K. F., Loeb, G. E., & Gans, C. (1987). Electromyography for Experimentalists. *Copeia*,

1987(4). https://doi.org/10.2307/1445582

Lindsey, A. E., Loverso, R. L., Tovar, C. A., Hill, C. E., Beattie, M. S., & Bresnahan, J. C. (2000). An Analysis of Changes in Sensory Thresholds to Mild Tactile and Cold Stimuli after Experimental Spinal Cord Injury in the Rat. *Neurorehabilitation and Neural Repair*, *14*(4). https://doi.org/10.1177/154596830001400405

Liston, D. R., & Davis, M. (2017). Clinically relevant concentrations of anticancer drugs: A guide for nonclinical studies. *Clinical Cancer Research*, *23*(14). https://doi.org/10.1158/1078-0432.CCR-16-3083

Liu, C. C., Huang, Z. X., Li, X., Shen, K. F., Liu, M., Ouyang, H. D., Zhang, S. B., Ruan, Y. T., Zhang, X. L., Wu, S. L., Xin, W. J., & Ma, C. (2018). Upregulation of NLRP3 via STAT3-dependent histone acetylation contributes to painful neuropathy induced by bortezomib. *Experimental Neurology*, *302*. https://doi.org/10.1016/j.expneurol.2018.01.011

Løseth, S., Stålberg, E., Jorde, R., & Mellgren, S. I. (2008). Early diabetic neuropathy: Thermal thresholds and intraepidermal nerve fibre density in patients with normal nerve conduction studies. *Journal of Neurology*, *255*(8), 1197–1202. https://doi.org/10.1007/s00415-008-0872-0

Lu, A., Li, Y., Schmidt, F. I., Yin, Q., Chen, S., Fu, T. M., Tong, A. B., Ploegh, H. L., Mao, Y., & Wu, H. (2016). Molecular basis of caspase-1 polymerization and its inhibition by a new capping mechanism. *Nature Structural and Molecular Biology*, *23*(5). https://doi.org/10.1038/nsmb.3199

Lu, A., Magupalli, V. G., Ruan, J., Yin, Q., Atianand, M. K., Vos, M. R., Schröder, G. F., Fitzgerald, K. A., Wu, H., & Egelman, E. H. (2014). Unified polymerization mechanism for the assembly of asc-dependent inflammasomes. *Cell*, *156*(6).

https://doi.org/10.1016/j.cell.2014.02.008

Lu, F., Lan, Z., Xin, Z., He, C., Guo, Z., Xia, X., & Hu, T. (2020). Emerging insights into molecular mechanisms underlying pyroptosis and functions of inflammasomes in diseases. In *Journal of Cellular Physiology* (Vol. 235, Issue 4). https://doi.org/10.1002/jcp.29268

Luedtke, K., Bouchard, S. M., Woller, S. A., Funk, M. K., Aceves, M., & Hook, M. A. (2014). Assessment of depression in a rodent model of spinal cord injury. *Journal of Neurotrauma*, *31*(12), 1107–1121. https://doi.org/10.1089/neu.2013.3204

Luo, F., Yang, C., Chen, Y., Shukla, P., Tang, L., Wang, L. X., & Zaijie, J. W. (2008). Reversal of chronic inflammatory pain by acute inhibition of Ca 2+/calmodulin-dependent protein kinase II. *Journal of Pharmacology and Experimental Therapeutics*, *325*(1). https://doi.org/10.1124/jpet.107.132167

Luo, H., Liu, H. Z., Zhang, W. W., Matsuda, M., Lv, N., Chen, G., Xu, Z. Z., & Zhang, Y. Q. (2019). Interleukin-17 Regulates Neuron-Glial Communications, Synaptic Transmission, and Neuropathic Pain after Chemotherapy. *Cell Reports*, *29*(8). https://doi.org/10.1016/j.celrep.2019.10.085

Macht, V. A. (2016). Neuro-immune interactions across development: A look at glutamate in the prefrontal cortex. In *Neuroscience and Biobehavioral Reviews* (Vol. 71). https://doi.org/10.1016/j.neubiorev.2016.08.039

Madison, R. D., Archibald, S. J., & Brushart, T. M. (1996). Reinnervation accuracy of the rat femoral nerve by motor and sensory neurons. *Journal of Neuroscience*, *16*(18). https://doi.org/10.1523/jneurosci.16-18-05698.1996

Majithia, N., Temkin, S. M., Ruddy, K. J., Beutler, A. S., Hershman, D. L., & Loprinzi, C. L. (2016). National Cancer Institute-supported chemotherapy-induced peripheral neuropathy

trials: outcomes and lessons. In *Supportive Care in Cancer* (Vol. 24, Issue 3). https://doi.org/10.1007/s00520-015-3063-4

Mamik, M. K., & Power, C. (2017). Inflammasomes in neurological diseases: Emerging pathogenic and therapeutic concepts. *Brain*, *140*(9). https://doi.org/10.1093/brain/awx133

Mariathasan, S., Hewton, K., Monack, D. M., Vucic, D., French, D. M., Lee, W. P., Roose-Girma, M., Erickson, S., & Dixit, V. M. (2004). Differential activation of the inflammasome by caspase-1 adaptors ASC and Ipaf. *Nature*, *430*(6996). https://doi.org/10.1038/nature02664

Marmiroli, P., Riva, B., Pozzi, E., Ballarini, E., Lim, D., Chiorazzi, A., Meregalli, C., Distasi, C., Renn, C. L., Semperboni, S., Morosi, L., Ruffinatti, F. A., Zucchetti, M., Dorsey, S. G., Cavaletti, G., Genazzani, A., & Carozzi, V. A. (2017a). Susceptibility of different mouse strains to oxaliplatin peripheral neurotoxicity: Phenotypic and genotypic insights. *PLoS ONE*, *12*(10), e0186250. https://doi.org/10.1371/journal.pone.0186250

Marmiroli, P., Riva, B., Pozzi, E., Ballarini, E., Lim, D., Chiorazzi, A., Meregalli, C., Distasi, C., Renn, C. L., Semperboni, S., Morosi, L., Ruffinatti, F. A., Zucchetti, M., Dorsey, S. G., Cavaletti, G., Genazzani, A., & Carozzi, V. A. (2017b). Susceptibility of different mouse strains to oxaliplatin peripheral neurotoxicity: Phenotypic and genotypic insights. *PLoS ONE*, *12*(10). https://doi.org/10.1371/journal.pone.0186250

Martinez, F. O., & Gordon, S. (2014). The M1 and M2 paradigm of macrophage activation: Time for reassessment. *F1000Prime Reports*, *6*. https://doi.org/10.12703/P6-13

Martinon, F. (2008). Detection of immune danger signals by NALP3. *Journal of Leukocyte Biology*, *83*(3). https://doi.org/10.1189/jlb.0607362

Martinon, F., Burns, K., & Tschopp, J. (2002). The Inflammasome: A molecular platform

triggering activation of inflammatory caspases and processing of proIL-β. *Molecular Cell*, *10*(2). https://doi.org/10.1016/S1097-2765(02)00599-3

Mascarenhas, L., Malogolowkin, M., Armenian, S. H., Sposto, R., & Venkatramani, R. (2013). A phase I study of oxaliplatin and doxorubicin in pediatric patients with relapsed or refractory extracranial non-hematopoietic solid tumors. *Pediatric Blood and Cancer*, *60*(7), 1103–1107. https://doi.org/10.1002/pbc.24471

Massie, M. J. (2004). Prevalence of depression in patients with cancer. In *Journal of the National Cancer Institute. Monographs* (Issue 32, pp. 57–71). https://doi.org/10.1093/jncimonographs/lgh014

McKenzie, B. A., Mamik, M. K., Saito, L. B., Boghozian, R., Monaco, M. C., Major, E. O., Lu, J. Q., Branton, W. G., & Power, C. (2018). Caspase-1 inhibition prevents glial inflammasome activation and pyroptosis in models of multiple sclerosis. *Proceedings of the National Academy of Sciences of the United States of America*, *115*(26). https://doi.org/10.1073/pnas.1722041115

McLean, I. W., & Nakane, P. K. (1974). Periodate lysine paraformaldehyde fixative. A new fixative for immunoelectron microscopy. *Journal of Histochemistry and Cytochemistry*, *22*(12), 1077–1083. https://doi.org/10.1177/22.12.1077

Meade, J. A., Alkhlaif, Y., Contreras, K. M., Obeng, S., Toma, W., Sim-Selley, L. J., Selley, D. E., & Damaj, M. I. (2020). Kappa opioid receptors mediate an initial aversive component of paclitaxel-induced neuropathy. *Psychopharmacology*, *237*(9), 2777–2793. https://doi.org/10.1007/s00213-020-05572-2

Meade, J. A., Fowlkes, A. N., Wood, M. J., Kurtz, M. C., May, M. M., Toma, W. B., Warncke, U. O., Mann, J., Mustafa, M., Lichtman, A. H., & Damaj, M. I. (2021). Effects of

Chemotherapy on Operant Responding for Palatable Food in Male and Female Mice. *Behavioural Pharmacology*. in press

Mehnert, A., Brähler, E., Faller, H., Härter, M., Keller, M., Schulz, H., Wegscheider, K., Weis, J., Boehncke, A., Hund, B., Reuter, K., Richard, M., Sehner, S., Sommerfeldt, S., Szalai, C., Wittchen, H. U., & Koch, U. (2014). Four-week prevalence of mental disorders in patients with cancer across major tumor entities. *Journal of Clinical Oncology*, *32*(31), 3540–3546. https://doi.org/10.1200/JCO.2014.56.0086

Mekhail, T. M., & Markman, M. (2002). Paclitaxel in cancer therapy. In *Expert Opinion on Pharmacotherapy* (Vol. 3, Issue 6). https://doi.org/10.1517/14656566.3.6.755

Meyer, L., Patte-Mensah, C., Taleb, O., & Mensah-Nyagan, A. G. (2011). Allopregnanolone prevents and suppresses oxaliplatin-evoked painful neuropathy: Multi-parametric assessment and direct evidence. *Pain*, *152*(1), 170–181. https://doi.org/10.1016/j.pain.2010.10.015

Miaskowski, C., Mastick, J., Paul, S. M., Topp, K., Smoot, B., Abrams, G., Chen, L. M., Kober, K. M., Conley, Y. P., Chesney, M., Bolla, K., Mausisa, G., Mazor, M., Wong, M., Schumacher, M., & Levine, J. D. (2017). Chemotherapy-Induced Neuropathy in Cancer Survivors. *Journal of Pain and Symptom Management*, *54*(2). https://doi.org/10.1016/j.jpainsymman.2016.12.342

Michaelides, A., & Zis, P. (2019). Depression, anxiety and acute pain: links and management challenges. *Postgraduate Medicine*, *131*(7), 438–444. https://doi.org/10.1080/00325481.2019.1663705

Micov, A. M., Tomić, M. A., Todorović, M. B., Vuković, M. J., Pecikoza, U. B., Jasnic, N. I., Djordjevic, J. D., & Stepanović-Petrović, R. M. (2020). Vortioxetine reduces pain

hypersensitivity and associated depression-like behavior in mice with oxaliplatin-induced neuropathy. *Progress in Neuro-Psychopharmacology and Biological Psychiatry*, *103*. https://doi.org/10.1016/j.pnpbp.2020.109975

Miguel, C. A., Raggio, M. C., Villar, M. J., Gonzalez, S. L., & Coronel, M. F. (2019). Anti-allodynic and anti-inflammatory effects of 17α-hydroxyprogesterone caproate in oxaliplatin-induced peripheral neuropathy. *Journal of the Peripheral Nervous System*, *24*(1). https://doi.org/10.1111/jns.12307

Mihara, Y., Egashira, N., Sada, H., Kawashiri, T., Ushio, S., Yano, T., Ikesue, H., & Oishi, R. (2011). Involvement of spinal NR2B-containing NMDA receptors in oxaliplatin-induced mechanical allodynia in rats. *Molecular Pain*, *7*. https://doi.org/10.1186/1744-8069-7-8

Minett, M. S., Quick, K., & Wood, J. N. (2011). Behavioral Measures of Pain Thresholds. *Current Protocols in Mouse Biology*, *1*(3). https://doi.org/10.1002/9780470942390.mo110116

Misawa, T., Takahama, M., Kozaki, T., Lee, H., Zou, J., Saitoh, T., & Akira, S. (2013). Microtubule-driven spatial arrangement of mitochondria promotes activation of the NLRP3 inflammasome. *Nature Immunology*, *14*(5). https://doi.org/10.1038/ni.2550

Miyake, T., Nakamura, S., Zhao, M., So, K., Inoue, K., Numata, T., Takahashi, N., Shirakawa, H., Mori, Y., Nakagawa, T., & Kaneko, S. (2016). Cold sensitivity of TRPA1 is unveiled by the prolyl hydroxylation blockade-induced sensitization to ROS. *Nature Communications*, *7*. https://doi.org/10.1038/ncomms12840

Molassiotis, A., Cheng, H. L., Leung, K. T., Li, Y. C., Wong, K. H., Au, J. S. K., Sundar, R., Chan, A., Ng, T. R. De, Suen, L. K. P., Chan, C. W., Yorke, J., & Lopez, V. (2019). Risk factors for chemotherapy-induced peripheral neuropathy in patients receiving taxane- and

platinum-based chemotherapy. *Brain and Behavior*, *9*(6). https://doi.org/10.1002/brb3.1312

Mols, F., Beijers, T., Vreugdenhil, G., & Van De Poll-Franse, L. (2014). Chemotherapy-induced peripheral neuropathy and its association with quality of life: A systematic review. In *Supportive Care in Cancer* (Vol. 22, Issue 8). https://doi.org/10.1007/s00520-014-2255-7

Mulvihill, E., Sborgi, L., Mari, S. A., Pfreundschuh, M., Hiller, S., & Müller, D. J. (2018). Mechanism of membrane pore formation by human gasdermin-D. *The EMBO Journal*, *37*(14). https://doi.org/10.15252/embj.201798321

Myers, R. R., Campana, W. M., & Shubayev, V. I. (2006). The role of neuroinflammation in neuropathic pain: Mechanisms and therapeutic targets. In *Drug Discovery Today* (Vol. 11, Issues 1–2). https://doi.org/10.1016/S1359-6446(05)03637-8

Naji-Esfahani, H., Vaseghi, G., Safaeian, L., Pilehvarian, A. A., Abed, A., & Rafieian-Kopaei, M. (2016). Gender differences in a mouse model of chemotherapy-induced neuropathic pain. *Laboratory Animals*, *50*(1), 15–20. https://doi.org/10.1177/0023677215575863

Nakagawa, T., & Kaneko, S. (2017). Roles of transient receptor potential ankyrin 1 in oxaliplatin-induced peripheral neuropathy. *Biological and Pharmaceutical Bulletin*, *40*(7), 947–953. https://doi.org/10.1248/bpb.b17-00243

Nassini, R., Gees, M., Harrison, S., De Siena, G., Materazzi, S., Moretto, N., Failli, P., Preti, D., Marchetti, N., Cavazzini, A., Mancini, F., Pedretti, P., Nilius, B., Patacchini, R., & Geppetti, P. (2011). Oxaliplatin elicits mechanical and cold allodynia in rodents via TRPA1 receptor stimulation. *Pain*, *152*(7), 1621–1631. https://doi.org/10.1016/j.pain.2011.02.051

Navarro, X., Verdú, E., Wendelschafer-Crabb, G., & Kennedy, W. R. (1995). Innervation of cutaneous structures in the mouse hind paw: A confocal microscopy immunohistochemical study. *Journal of Neuroscience Research*, *41*(1). https://doi.org/10.1002/jnr.490410113

Navarro, Xavier, & Udina, E. (2009). Chapter 6 Methods and Protocols in Peripheral Nerve Regeneration Experimental Research. Part III-Electrophysiological Evaluation. In *International Review of Neurobiology* (Vol. 87, Issue C). https://doi.org/10.1016/S0074-7742(09)87006-2

Negus, S. S., Neddenriep, B., Altarifi, A. A., Carroll, F. I., Leitl, M. D., & Miller, L. L. (2015). Effects of ketoprofen, morphine, and kappa opioids on pain-related depression of nesting in mice. *Pain*, *156*(6). https://doi.org/10.1097/j.pain.0000000000000171

Ni, W., Zheng, X., Hu, L., Kong, C., & Xu, Q. (2020). Preventing oxaliplatin-induced neuropathic pain: Using berberine to inhibit the activation of NF-κB and release of pro-inflammatory cytokines in dorsal root ganglions in rats. *Experimental and Therapeutic Medicine*, *21*(2). https://doi.org/10.3892/etm.2020.9567

Nimmerjahn, A., Kirchhoff, F., & Helmchen, F. (2005). Neuroscience: Resting microglial cells are highly dynamic surveillants of brain parenchyma in vivo. *Science*, *308*(5726). https://doi.org/10.1126/science.1110647

Niu, T., De Rosny, C., Chautard, S., Rey, A., Patoli, D., Groslambert, M., Cosson, C., Lagrange, B., Zhang, Z., Visvikis, O., Hacot, S., Hologne, M., Walker, O., Wong, J., Wang, P., Ricci, R., Henry, T., Boyer, L., Petrilli, V., & Py, B. F. (2021). NLRP3 phosphorylation in its LRR domain critically regulates inflammasome assembly. *Nature Communications*, *12*(1). https://doi.org/10.1038/s41467-021-26142-w

O'Brien, B. J., Drummond, M. F., Labelle, R. J., & Willan, A. (1994). In search of power and significance: issues in the design and analysis of stochastic cost-effectiveness studies in health care. *Medical Care*, *32*(2), 150–163. http://www.ncbi.nlm.nih.gov/pubmed/8302107

Oh, P. J., & Cho, J. R. (2020). Changes in Fatigue, Psychological Distress, and Quality of Life

after Chemotherapy in Women with Breast Cancer: A Prospective Study. *Cancer Nursing*, *43*(1). https://doi.org/10.1097/NCC.0000000000000689

Ohtori, S., Takahashi, K., Moriya, H., & Myers, R. R. (2004). TNF-α and TNF-α receptor type 1 upregulation in glia and neurons after peripheral nerve injury: Studies in murine DRG and spinal cord. *Spine*, *29*(10). https://doi.org/10.1097/00007632-200405150-00006

Okun, A., McKinzie, D. L., Witkin, J. M., Remeniuk, B., Husein, O., Gleason, S. D., Oyarzo, J., Navratilova, E., McElroy, B., Cowen, S., Kennedy, J. D., & Porreca, F. (2016). Hedonic and motivational responses to food reward are unchanged in rats with neuropathic pain. *Pain*, *157*(12), 2731–2738. https://doi.org/10.1097/j.pain.0000000000000695

Oliver, V. L., Thurston, S. E., & Lofgren, J. L. (2018). Using cageside measures to evaluate analgesic efficacy in mice (Mus Musculus) after surgery. *Journal of the American Association for Laboratory Animal Science*, *57*(2), 186–201.

Oroz, J., Barrera-Vilarmau, S., Alfonso, C., Rivas, G., & De Alba, E. (2016). ASC pyrin domain self-associates and binds NLRP3 protein using equivalent binding interfaces∗. *Journal of Biological Chemistry*, *291*(37). https://doi.org/10.1074/jbc.M116.741082

Osuchowski, M. F., Teener, J., & Remick, D. G. (2009). Noninvasive model of sciatic nerve conduction in healthy and septic mice: Reliability and normative data. *Muscle and Nerve*, *40*(4). https://doi.org/10.1002/mus.21284

Otake, A., Yoshino, K., Ueda, Y., Sawada, K., Mabuchi, S., Kimura, T., Kobayashi, E., Isobe, A., Egawa-Takata, T., Matsuzaki, S., Fujita, M., & Kimura, T. (2015). Usefulness of duloxetine for paclitaxel-induced peripheral neuropathy treatment in gynecological cancer patients. *Anticancer Research*, *35*(1).

Pachman, D. R., Qin, R., Seisler, D., Smith, E. M. L., Kaggal, S., Novotny, P., Ruddy, K. J.,

Lafky, J. M., Ta, L. E., Beutler, A. S., Wagner-Johnston, N. D., Staff, N. P., Grothey, A., Dougherty, P. M., Cavaletti, G., & Loprinzi, C. L. (2016). Comparison of oxaliplatin and paclitaxel-induced neuropathy (Alliance A151505). *Supportive Care in Cancer*, *24*(12), 5059–5068. https://doi.org/10.1007/s00520-016-3373-1

Panis, C., Lemos, L. G. T., Victorino, V. J., Herrera, A. C. S. A., Campos, F. C., Colado Simão, A. N., Pinge-Filho, P., Cecchini, A. L., & Cecchini, R. (2012). Immunological effects of Taxol and Adryamicin in breast cancer patients. *Cancer Immunology, Immunotherapy*, *61*(4). https://doi.org/10.1007/s00262-011-1117-0

Park, S. B., Goldstein, D., Krishnan, A. V., Lin, C. S.-Y., Friedlander, M. L., Cassidy, J., Koltzenburg, M., & Kiernan, M. C. (2013). Chemotherapy-induced peripheral neurotoxicity: A critical analysis. *CA: A Cancer Journal for Clinicians*, *63*(6). https://doi.org/10.3322/caac.21204

Park, S. B., & Koltzenburg, M. (2012a). Longitudinal assessment of oxaliplatin-induced neuropathy. In *Neurology* (Vol. 78, Issue 2, p. 152). https://doi.org/10.1212/01.wnl.0000410913.88642.bf

Park, S. B., & Koltzenburg, M. (2012b). Longitudinal assessment of oxaliplatin-induced neuropathy. In *Neurology* (Vol. 78, Issue 2, p. 152). Lippincott Williams and Wilkins. https://doi.org/10.1212/01.wnl.0000410913.88642.bf

Park, S. B., Lin, C. S. Y., Krishnan, A. V., Goldstein, D., Friedlander, M. L., & Kiernan, M. C. (2011). Long-Term Neuropathy After Oxaliplatin Treatment: Challenging the Dictum of Reversibility. *The Oncologist*, *16*(5). https://doi.org/10.1634/theoncologist.2010-0248

Paton, K. F., Luo, D., La Flamme, A. C., Prisinzano, T. E., & Kivell, B. M. (2022). Sex Differences in Kappa Opioid Receptor Agonist Mediated Attenuation of Chemotherapy-

Induced Neuropathic Pain in Mice. *Frontiers in Pharmacology*, *13*. https://doi.org/10.3389/fphar.2022.813562

Pease-Raissi, S. E., Pazyra-Murphy, M. F., Li, Y., Wachter, F., Fukuda, Y., Fenstermacher, S. J., Barclay, L. A., Bird, G. H., Walensky, L. D., & Segal, R. A. (2017). Paclitaxel Reduces Axonal Bclw to Initiate IP3R1-Dependent Axon Degeneration. *Neuron*, *96*(2). https://doi.org/10.1016/j.neuron.2017.09.034

Pestieau, S. R., Belliveau, J. F., Griffin, H., Anthony Stuart, O., & Sugarbaker, P. H. (2001). Pharmacokinetics of intraperitoneal oxaliplatin: Experimental studies. *Journal of Surgical Oncology*, *76*(2), 106–114. https://doi.org/10.1002/1096-9098(200102)76:2<106::AID-JSO1020>3.0.CO;2-E

Peters, C. M., Jimenez-Andrade, J. M., Jonas, B. M., Sevcik, M. A., Koewler, N. J., Ghilardi, J. R., Wong, G. Y., & Mantyh, P. W. (2007). Intravenous paclitaxel administration in the rat induces a peripheral sensory neuropathy characterized by macrophage infiltration and injury to sensory neurons and their supporting cells. *Experimental Neurology*, *203*(1). https://doi.org/10.1016/j.expneurol.2006.07.022

Pétrilli, V., Papin, S., Dostert, C., Mayor, A., Martinon, F., & Tschopp, J. (2007). Activation of the NALP3 inflammasome is triggered by low intracellular potassium concentration. *Cell Death and Differentiation*, *14*(9). https://doi.org/10.1038/sj.cdd.4402195

Polomano, R. C., Mannes, A. J., Clark, U. S., & Bennett, G. J. (2001). A painful peripheral neuropathy in the rat produced by the chemotherapeutic drug, paclitaxel. *Pain*, *94*(3), 293–304. https://doi.org/10.1016/S0304-3959(01)00363-3

Poupon, L., Kerckhove, N., Vein, J., Lamoine, S., Authier, N., Busserolles, J., & Balayssac, D. (2015). Minimizing chemotherapy-induced peripheral neuropathy: Preclinical and clinical

development of new perspectives. In *Expert Opinion on Drug Safety* (Vol. 14, Issue 8). https://doi.org/10.1517/14740338.2015.1056777

Pover, C. M., & Coggeshall, R. E. (1991). Verification of the disector method for counting neurons, with comments on the empirical method. *The Anatomical Record*, *231*(4). https://doi.org/10.1002/ar.1092310419

Pozzi, E., Fumagalli, G., Chiorazzi, A., Canta, A., Meregalli, C., Monza, L., Carozzi, V. A., Oggioni, N., Rodriguez-Menendez, V., Cavaletti, G., & Marmiroli, P. (2020). The relevance of multimodal assessment in experimental oxaliplatin-induced peripheral neurotoxicity. *Experimental Neurology*, *334*. https://doi.org/10.1016/j.expneurol.2020.113458

Py, B. F., Kim, M. S., Vakifahmetoglu-Norberg, H., & Yuan, J. (2013). Deubiquitination of NLRP3 by BRCC3 Critically Regulates Inflammasome Activity. *Molecular Cell*, *49*(2). https://doi.org/10.1016/j.molcel.2012.11.009

Qian, J., Zhu, W., Lu, M., Ni, B., & Yang, J. (2017). D-β-hydroxybutyrate promotes functional recovery and relieves pain hypersensitivity in mice with spinal cord injury. *British Journal of Pharmacology*, *174*(13). https://doi.org/10.1111/bph.13788

Radaelli, E., Santagostino, S. F., Sellers, R. S., & Brayton, C. F. (2018). Immune Relevant and Immune Deficient Mice: Options and Opportunities in Translational Research. In *ILAR Journal* (Vol. 59, Issue 3). https://doi.org/10.1093/ilar/ily026

Raja, S. N., Carr, D. B., Cohen, M., Finnerup, N. B., Flor, H., Gibson, S., Keefe, F. J., Mogil, J. S., Ringkamp, M., Sluka, K. A., Song, X. J., Stevens, B., Sullivan, M. D., Tutelman, P. R., Ushida, T., & Vader, K. (2020). The revised International Association for the Study of Pain definition of pain: concepts, challenges, and compromises. *Pain*, *161*(9), 1976–1982. https://doi.org/10.1097/j.pain.0000000000001939

Ramnarine, S., Williams, L. J., Dougherty, P. M., & Fallon, M. T. (2016). A comparison of chemotherapy-induced peripheral neuropathy assessment tools in patients receiving neurotoxic chemotherapy. *Journal of Clinical Oncology*, *34*(3_suppl). https://doi.org/10.1200/jco.2016.34.3_suppl.132

RANDALL, L. O., & SELITTO, J. J. (1957). A method for measurement of analgesic activity on inflamed tissue. *Archives Internationales de Pharmacodynamie et de Thérapie*, *111*(4).

Rao, S., Krauss, N. E., Heerding, J. M., Swindell, C. S., Ringel, I., Orr, G. A., & Horwitz, S. B. (1994). 3'-(p-Azidobenzamido)taxol photolabels the N-terminal 31 amino acids of β-tubulin. *Journal of Biological Chemistry*, *269*(5). https://doi.org/10.1016/s0021-9258(17)41836-9

Rathinam, V. A. K., & Fitzgerald, K. A. (2016). Inflammasome Complexes: Emerging Mechanisms and Effector Functions. In *Cell* (Vol. 165, Issue 4). https://doi.org/10.1016/j.cell.2016.03.046

Ray, B., Gupta, B., & Mehrotra, R. (2019). Binding of platinum derivative, oxaliplatin to deoxyribonucleic acid: structural insight into antitumor action. *Journal of Biomolecular Structure and Dynamics*, *37*(14). https://doi.org/10.1080/07391102.2018.1531059

Raymond, E., Faivre, S., Woynarowski, J. M., & Chaney, S. G. (1998). Oxaliplatin: Mechanism of action and antineoplastic activity. In *Seminars in Oncology* (Vol. 25, Issue 2 SUPPL. 5).

Reeves, B. N., Dakhil, S. R., Sloan, J. A., Wolf, S. L., Burger, K. N., Kamal, A., Le-Lindqwister, N. A., Soori, G. S., Jaslowski, A. J., Kelaghan, J., Novotny, P. J., Lachance, D. H., & Loprinzi, C. L. (2012). Further data supporting that paclitaxel-associated acute pain syndrome is associated with development of peripheral neuropathy: North Central Cancer Treatment Group trial N08C1. *Cancer*, *118*(20), 5171–5178. https://doi.org/10.1002/cncr.27489

Reis, A. S., Paltian, J. J., Domingues, W. B., Costa, G. P., Alves, D., Giongo, J. L., Campos, V. F., Luchese, C., & Wilhelm, E. A. (2020). Pharmacological modulation of Na+, K+-ATPase as a potential target for OXA-induced neurotoxicity: Correlation between anxiety and cognitive decline and beneficial effects of 7-chloro-4-(phenylselanyl) quinoline. *Brain Research Bulletin*, *162*, 282–290. https://doi.org/10.1016/j.brainresbull.2020.06.021

Renn, C. L., Carozzi, V. A., Rhee, P., Gallop, D., Dorsey, S. G., & Cavaletti, G. (2011). Multimodal assessment of painful peripheral neuropathy induced by chronic oxaliplatin-based chemotherapy in mice. *Molecular Pain*, *7*(29). https://doi.org/10.1186/1744-8069-7-29

Resta, F., Micheli, L., Laurino, A., Spinelli, V., Mello, T., Sartiani, L., Di Cesare Mannelli, L., Cerbai, E., Ghelardini, C., Romanelli, M. N., Mannaioni, G., & Masi, A. (2018). Selective HCN1 block as a strategy to control oxaliplatin-induced neuropathy. *Neuropharmacology*, *131*. https://doi.org/10.1016/j.neuropharm.2018.01.014

Riddell, I. A. (2018). Cisplatin and Oxaliplatin: Our Current Understanding of Their Actions. In *Metal ions in life sciences* (Vol. 18). https://doi.org/10.1515/9783110470734-007

Riva, B., Dionisi, M., Potenzieri, A., Chiorazzi, A., Cordero-Sanchez, C., Rigolio, R., Carozzi, V. A., Lim, D., Cavaletti, G., Marmiroli, P., Distasi, C., & Genazzani, A. A. (2018). Oxaliplatin induces pH acidification in dorsal root ganglia neurons. *Scientific Reports*, *8*(1). https://doi.org/10.1038/s41598-018-33508-6

Ruzzo, A., Graziano, F., Galli, F., Galli, F., Rulli, E., Lonardi, S., Ronzoni, M., Massidda, B., Zagonel, V., Pella, N., Mucciarini, C., Labianca, R., Ionta, M. T., Bagaloni, I., Veltri, E., Sozzi, P., Barni, S., Ricci, V., Foltran, L., … Magnani, M. (2019). Sex-Related Differences in Impact on Safety of Pharmacogenetic Profile for Colon Cancer Patients Treated with

FOLFOX-4 or XELOX Adjuvant Chemotherapy. *Scientific Reports*, *9*(1), 1–9. https://doi.org/10.1038/s41598-019-47627-1

Saibil, S., Fitzgerald, B., Freedman, O. C., Amir, E., Napolskikh, J., Salvo, N., Dranitsaris, G., & Clemons, M. (2010). Incidence of taxane-induced pain and distress in patients receiving chemotherapy for early-stage breast cancer: A retrospective, outcomes-based survey. *Current Oncology*, *17*(4). https://doi.org/10.3747/co.v17i4.562

Sakurai, M., Egashira, N., Kawashiri, T., Yano, T., Ikesue, H., & Oishi, R. (2009). Oxaliplatin-induced neuropathy in the rat: Involvement of oxalate in cold hyperalgesia but not mechanical allodynia. *Pain*, *147*(1–3). https://doi.org/10.1016/j.pain.2009.09.003

Saltz, L. B., Clarke, S., Díaz-Rubio, E., Scheithauer, W., Figer, A., Wong, R., Koski, S., Lichinitser, M., Yang, T. S., Rivera, F., Couture, F., Sirzén, F., & Cassidy, J. (2008). Bevacizumab in combination with oxaliplatin-based chemotherapy as first-line therapy in metastatic colorectal cancer: A randomized phase III study. *Journal of Clinical Oncology*, *26*(12), 2013–2019. https://doi.org/10.1200/JCO.2007.14.9930

Salvemini, D., Doyle, T., Chen, Z., Muscoli, C., Bryant, L., Esposito, E., Cuzzocrea, S., Dagostino, C., Ryerse, J., Rausaria, S., Kamadulski, A., & Neumann, W. L. (2012). Targeting the overproduction of peroxynitrite for the prevention and reversal of paclitaxel-induced neuropathic pain. *Journal of Neuroscience*, *32*(18). https://doi.org/10.1523/JNEUROSCI.6343-11.2012

Sarlus, H., & Heneka, M. T. (2017). Microglia in Alzheimer's disease. *Journal of Clinical Investigation*, *127*(9), 3240–3249. https://doi.org/10.1172/JCI90606

Schmidt, F. I., Lu, A., Chen, J. W., Ruan, J., Tang, C., Wu, H., & Ploegh, H. L. (2016). A single domain antibody fragment that recognizes the adaptor ASC defines the role of ASC domains

in inflammasome assembly. *Journal of Experimental Medicine*, *213*(5). https://doi.org/10.1084/jem.20151790

Scholz, J., Broom, D. C., Youn, D. H., Mills, C. D., Kohno, T., Suter, M. R., Moore, K. A., Decosterd, I., Coggeshall, R. E., & Woolf, C. J. (2005). Blocking caspase activity prevents transsynaptic neuronal apoptosis and the loss of inhibition in lamina II of the dorsal horn after peripheral nerve injury. *Journal of Neuroscience*, *25*(32). https://doi.org/10.1523/JNEUROSCI.1526-05.2005

Schroder, K., & Tschopp, J. (2010). The Inflammasomes. In *Cell* (Vol. 140, Issue 6). https://doi.org/10.1016/j.cell.2010.01.040

Seibenhener, M. L., & Wooten, M. C. (2015). Use of the open field maze to measure locomotor and anxiety-like behavior in mice. *Journal of Visualized Experiments*, *96*. https://doi.org/10.3791/52434

Selvy, M., Pereira, B., Kerckhove, N., Busserolles, J., Farsi, F., Guastella, V., Merle, P., Pezet, D., & Balayssac, D. (2021). Prevention, diagnosis and management of chemotherapy-induced peripheral neuropathy: a cross-sectional study of French oncologists' professional practices. *Supportive Care in Cancer*. https://doi.org/10.1007/s00520-020-05928-6

Seok, J. K., Kang, H. C., Cho, Y. Y., Lee, H. S., & Lee, J. Y. (2021). Regulation of the NLRP3 Inflammasome by Post-Translational Modifications and Small Molecules. In *Frontiers in Immunology* (Vol. 11). https://doi.org/10.3389/fimmu.2020.618231

Seretny, M., Currie, G. L., Sena, E. S., Ramnarine, S., Grant, R., Macleod, M. R., Colvin, L. A., & Fallon, M. (2014). Incidence, prevalence, and predictors of chemotherapy-induced peripheral neuropathy: A systematic review and meta-analysis. In *Pain* (Vol. 155, Issue 12). https://doi.org/10.1016/j.pain.2014.09.020

Sharif, H., Wang, L., Wang, W. L., Magupalli, V. G., Andreeva, L., Qiao, Q., Hauenstein, A. V., Wu, Z., Núñez, G., Mao, Y., & Wu, H. (2019). Structural mechanism for NEK7-licensed activation of NLRP3 inflammasome. *Nature*, *570*(7761). https://doi.org/10.1038/s41586-019-1295-z

Sherwin, C. M., Haug, E., Terkelsen, N., & Vadgama, M. (2004). Studies on the motivation for burrowing by laboratory mice. *Applied Animal Behaviour Science*, *88*, 343–358. https://doi.org/10.1016/j.applanim.2004.03.009

Shi, J., Zhao, Y., Wang, Y., Gao, W., Ding, J., Li, P., Hu, L., & Shao, F. (2014). Inflammatory caspases are innate immune receptors for intracellular LPS. *Nature*, *514*(7521). https://doi.org/10.1038/nature13683

Shiohara, M., Taniguchi, S., Masumoto, J., Yasui, K., Koike, K., Komiyama, A., & Sagara, J. (2002). ASC, which is composed of a PYD and a CARD, is up-regulated by inflammation and apoptosis in human neutrophils. *Biochemical and Biophysical Research Communications*, *293*(5). https://doi.org/10.1016/S0006-291X(02)00384-4

Shirahama, M., Ushio, S., Egashira, N., Yamamoto, S., Sada, H., Masuguchi, K., Kawashiri, T., & Oishi, R. (2012). Inhibition of Ca 2+/Calmodulin-dependent protein kinase II reverses oxaliplatin-induced mechanical allodynia in Rats. *Molecular Pain*, *8*. https://doi.org/10.1186/1744-8069-8-26

Sieberg, C. B., Taras, C., Gomaa, A., Nickerson, C., Wong, C., Ward, C., Baskozos, G., Bennett, D. L. H., Ramirez, J. D., Themistocleous, A. C., Rice, A. S. C., Shillo, P. R., Tesfaye, S., Edwards, R. R., Andrews, N. A., Berde, C., & Costigan, M. (2018). Neuropathic pain drives anxiety behavior in mice, results consistent with anxiety levels in diabetic neuropathy patients. *Pain Reports*, *3*(3), e651. https://doi.org/10.1097/PR9.0000000000000651

Simpson, D., Dunn, C., Curran, M., & Goa, K. L. (2003). Oxaliplatin: A review of its use in combination therapy for advanced metastatic colorectal cancer. In *Drugs* (Vol. 63, Issue 19). https://doi.org/10.2165/00003495-200363190-00013

Sisignano, M., Angioni, C., Park, C. K., Santos, S. M. Dos, Jordan, H., Kuzikov, M., Liu, D., Zinn, S., Hohman, S. W., Schreiber, Y., Zimmer, B., Schmidt, M., Lu, R., Suo, J., Zhang, D. D., Schäfer, S. M. G., Hofmann, M., Yekkirala, A. S., De Bruin, N., … Geisslinger, G. (2016). Targeting CYP2J to reduce paclitaxel-induced peripheral neuropathic pain. *Proceedings of the National Academy of Sciences of the United States of America*, *113*(44). https://doi.org/10.1073/pnas.1613246113

Sleigh, J. N., Weir, G. A., & Schiavo, G. (2016). A simple, step-by-step dissection protocol for the rapid isolation of mouse dorsal root ganglia. *BMC Research Notes*, *9*(1). https://doi.org/10.1186/s13104-016-1915-8

Slivicki, R. A., Ali, Y. O., Lu, H. C., & Hohmann, A. G. (2016). Impact of genetic reduction of NMNAT2 on chemotherapy-induced losses in cell viability in vitro and peripheral neuropathy in vivo. *PLoS ONE*, *11*(1). https://doi.org/10.1371/journal.pone.0147620

Son, S., Shim, D. W., Hwang, I., Park, J. H., & Yu, J. W. (2019). Chemotherapeutic agent paclitaxel mediates priming of NLRP3 inflammasome activation. *Frontiers in Immunology*, *10*(MAY). https://doi.org/10.3389/fimmu.2019.01108

Sorensen, J. C., Petersen, A. C., Timpani, C. A., Campelj, D. G., Cook, J., Trewin, A. J., Stojanovska, V., Stewart, M., Hayes, A., & Rybalka, E. (2017). BGP-15 protects against oxaliplatin-induced skeletal myopathy and mitochondrial reactive oxygen species production in mice. *Frontiers in Pharmacology*, *8*(137). https://doi.org/10.3389/fphar.2017.00137

Sorge, R. E., LaCroix-Fralish, M. L., Tuttle, A. H., Sotocinal, S. G., Austin, J. S., Ritchie, J.,

Chanda, M. L., Graham, A. C., Topham, L., Beggs, S., Salter, M. W., & Mogil, J. S. (2011). Spinal cord toll-like receptor 4 mediates inflammatory and neuropathic hypersensitivity in male but not female mice. *Journal of Neuroscience*, *31*(43). https://doi.org/10.1523/JNEUROSCI.3859-11.2011

Sorge, R. E., Mapplebeck, J. C. S., Rosen, S., Beggs, S., Taves, S., Alexander, J. K., Martin, L. J., Austin, J. S., Sotocinal, S. G., Chen, D., Yang, M., Shi, X. Q., Huang, H., Pillon, N. J., Bilan, P. J., Tu, Y., Klip, A., Ji, R. R., Zhang, J., … Mogil, J. S. (2015). Different immune cells mediate mechanical pain hypersensitivity in male and female mice. *Nature Neuroscience*, *18*(8). https://doi.org/10.1038/nn.4053

Spalinger, M. R., Kasper, S., Gottier, C., Lang, S., Atrott, K., Vavricka, S. R., Scharl, S., Gutte, P. M., Grütter, M. G., Beer, H. D., Contassot, E., Chan, A. C., Dai, X., Rawlings, D. J., Mair, F., Becher, B., Falk, W., Fried, M., Rogler, G., & Scharl, M. (2016). NLRP3 tyrosine phosphorylation is controlled by protein tyrosine phosphatase PTPN22. *Journal of Clinical Investigation*, *126*(5). https://doi.org/10.1172/JCI83669

Spittau, B. (2017). Aging microglia-phenotypes, functions and implications for age-related neurodegenerative diseases. *Frontiers in Aging Neuroscience*, *9*(JUN). https://doi.org/10.3389/fnagi.2017.00194

Sprowl, J. A., Ciarimboli, G., Lancaster, C. S., Giovinazzo, H., Gibson, A. A., Du, G., Janke, L. J., Cavaletti, G., Shields, A. F., & Sparreboom, A. (2013). Oxaliplatin-induced neurotoxicity is dependent on the organic cation transporter OCT2. *Proceedings of the National Academy of Sciences of the United States of America*, *110*(27). https://doi.org/10.1073/pnas.1305321110

Staff, N. P., Grisold, A., Grisold, W., & Windebank, A. J. (2017). Chemotherapy-induced

peripheral neuropathy: A current review. In *Annals of Neurology* (Vol. 81, Issue 6). https://doi.org/10.1002/ana.24951

Starobova, H., Monteleone, M., Adolphe, C., Batoon, L., Sandrock, C. J., Tay, B., Deuis, J. R., Smith, A. V., Mueller, A., Nadar, E. I., Lawrence, G. P., Mayor, A., Tolson, E., Levesque, J. P., Pettit, A. R., Wainwright, B. J., Schroder, K., & Vetter, I. (2021). Vincristine-induced peripheral neuropathy is driven by canonical NLRP3 activation and IL-1β release. *Journal of Experimental Medicine*, *218*(5). https://doi.org/10.1084/JEM.20201452

Starobova, H., Mueller, A., Deuis, J. R., Carter, D. A., & Vetter, I. (2020). Inflammatory and Neuropathic Gene Expression Signatures of Chemotherapy-Induced Neuropathy Induced by Vincristine, Cisplatin, and Oxaliplatin in C57BL/6J Mice. *Journal of Pain*, *21*(1–2). https://doi.org/10.1016/j.jpain.2019.06.008

Starobova, H., Nadar, E. I., & Vetter, I. (2020). The NLRP3 Inflammasome: Role and Therapeutic Potential in Pain Treatment. In *Frontiers in Physiology* (Vol. 11). Frontiers Media S.A. https://doi.org/10.3389/fphys.2020.01016

Stehlik, C. (2009). Multiple interleukin-1β-converting enzymes contribute to inflammatory arthritis. In *Arthritis and Rheumatism* (Vol. 60, Issue 12). https://doi.org/10.1002/art.24961

Stojanovska, V., Prakash, M., McQuade, R., Fraser, S., Apostolopoulos, V., Sakkal, S., & Nurgali, K. (2019). Oxaliplatin Treatment Alters Systemic Immune Responses. *BioMed Research International*, *2019*. https://doi.org/10.1155/2019/4650695

Streit, W. J. (2002). Microglia as neuroprotective, immunocompetent cells of the CNS. In *GLIA* (Vol. 40, Issue 2). https://doi.org/10.1002/glia.10154

Sumner, C. J., Sheth, S., Griffin, J. W., Cornblath, D. R., & Polydefkis, M. (2003). The spectrum of neuropathy in diabetes and impaired glucose tolerance. *Neurology*, *60*(1), 108–111.

https://doi.org/10.1212/WNL.60.1.108

Sutterwala, F. S., Haasken, S., & Cassel, S. L. (2014). Mechanism of NLRP3 inflammasome activation. *Annals of the New York Academy of Sciences*, *1319*(1). https://doi.org/10.1111/nyas.12458

Ta, L. E., Low, P. A., & Windebank, A. J. (2009a). Mice with cisplatin and oxaliplatin-induced painful neuropathy develop distinct early responses to thermal stimuli. *Molecular Pain*, *5*(9). https://doi.org/10.1186/1744-8069-5-9

Ta, L. E., Low, P. A., & Windebank, A. J. (2009b). Mice with cisplatin and oxaliplatin-induced painful neuropathy develop distinct early responses to thermal stimuli. *Molecular Pain*, *5*. https://doi.org/10.1186/1744-8069-5-9

Taylor, B. A. (1972). Genetic relationships between inbred strains of mice. *Journal of Heredity*, *63*(2), 83–86. https://doi.org/10.1093/oxfordjournals.jhered.a108235

Tesniere, A., Schlemmer, F., Boige, V., Kepp, O., Martins, I., Ghiringhelli, F., Aymeric, L., Michaud, M., Apetoh, L., Barault, L., Mendiboure, J., Pignon, J. P., Jooste, V., Van Endert, P., Ducreux, M., Zitvogel, L., Piard, F., & Kroemer, G. (2010). Immunogenic death of colon cancer cells treated with oxaliplatin. *Oncogene*, *29*(4). https://doi.org/10.1038/onc.2009.356

Thompson, R. D., & Grant, C. V. (1971). AUTOMATED PREFERENCE TESTING APPARATUS FOR RATING PALATABILITY OF FOODS 1. *Journal of the Experimental Analysis of Behavior*, *15*(2), 215–220. https://doi.org/10.1901/jeab.1971.15-215

Tofthagen, C. (2010). Surviving chemotherapy for colon cancer and living with the consequences. *Journal of Palliative Medicine*, *13*(11), 1389–1391. https://doi.org/10.1089/jpm.2010.0124

Toldo, S., Mauro, A. G., Cutter, Z., Van Tassell, B. W., Mezzaroma, E., Del Buono, M. G.,

Prestamburgo, A., Potere, N., & Abbate, A. (2019). The NLRP3 Inflammasome Inhibitor, OLT1177 (Dapansutrile), Reduces Infarct Size and Preserves Contractile Function after Ischemia Reperfusion Injury in the Mouse. *Journal of Cardiovascular Pharmacology*, *73*(4). https://doi.org/10.1097/FJC.0000000000000658

Toma, W., Kyte, S. L., Bagdas, D., Alkhlaif, Y., Alsharari, S. D., Lichtman, A. H., Chen, Z. J., Del Fabbro, E., Bigbee, J. W., Gewirtz, D. A., & Damaj, M. I. (2017a). Effects of paclitaxel on the development of neuropathy and affective behaviors in the mouse. *Neuropharmacology*, *117*, 305–315. https://doi.org/10.1016/j.neuropharm.2017.02.020

Toma, W., Kyte, S. L., Bagdas, D., Alkhlaif, Y., Alsharari, S. D., Lichtman, A. H., Chen, Z. J., Del Fabbro, E., Bigbee, J. W., Gewirtz, D. A., & Damaj, M. I. (2017b). Effects of paclitaxel on the development of neuropathy and affective behaviors in the mouse. *Neuropharmacology*, *117*, 305–315. https://doi.org/10.1016/j.neuropharm.2017.02.020

Tonkin, R. S., Bowles, C., Perera, C. J., Keating, B. A., Makker, P. G. S., Duffy, S. S., Lees, J. G., Tran, C., Don, A. S., Fath, T., Liu, L., O'Carroll, S. J., Nicholson, L. F. B., Green, C. R., Gorrie, C., & Moalem-Taylor, G. (2018). Attenuation of mechanical pain hypersensitivity by treatment with Peptide5, a connexin-43 mimetic peptide, involves inhibition of NLRP3 inflammasome in nerve-injured mice. *Experimental Neurology*, *300*. https://doi.org/10.1016/j.expneurol.2017.10.016

Topp, K. S., Tanner, K. D., & Levine, J. D. (2000). Damage to the cytoskeleton of large diameter sensory neurons and myelinated axons in vincristine-induced painful peripheral neuropathy in the rat. *Journal of Comparative Neurology*, *424*(4), 563–576. https://doi.org/10.1002/1096-9861(20000904)424:4<563::AID-CNE1>3.0.CO;2-U

U. S. Food and Drug Administration, & Center for Drug Evaluation and Research. (2005).

Guidance for Industry: Estimating the Maximum Safe Starting Dose in Initial Clinical Trials for Therapeutics in Adult Healthy Volunteers. In *US Department of Health and Human Services* (Issue July). Food and Drug Administration. https://www.fda.gov/media/72309/download

Uchida, H., Nagai, J., & Ueda, H. (2014). Lysophosphatidic acid and its receptors LPA1 and LPA3 mediate paclitaxel-induced neuropathic pain in mice. *Molecular Pain*, *10*. https://doi.org/10.1186/1744-8069-10-71

Ulker, E., Caillaud, M., Patel, T., White, A., Rashid, D., Alqasem, M., Lichtman, A. H., Bryant, C. D., & Damaj, M. I. (2020). C57BL/6 substrain differences in formalin-induced pain-like behavioral responses. *Behavioural Brain Research*, *390*. https://doi.org/10.1016/j.bbr.2020.112698

Urits, I., Shen, A. H., Jones, M. R., Viswanath, O., & Kaye, A. D. (2018). Complex Regional Pain Syndrome, Current Concepts and Treatment Options. In *Current Pain and Headache Reports* (Vol. 22, Issue 2). https://doi.org/10.1007/s11916-018-0667-7

Valenstein, E. S., Kakolewski, J. W., & Cox, V. C. (1967). Sex differences in taste preference for glucose and saccharin solutions. *Science*, *156*(3777), 942–943. https://doi.org/10.1126/science.156.3777.942

Vanitallie, T. B. (2010). Gout: Epitome of painful arthritis. In *Metabolism: Clinical and Experimental* (Vol. 59, Issue SUPPL. 1). https://doi.org/10.1016/j.metabol.2010.07.009

Velasco, R., & Bruna, J. (2010). Chemotherapy-induced peripheral neuropathy: An unresolved issue. *Neurología (English Edition)*, *25*(2), 116–131. https://doi.org/10.1016/s2173-5808(10)70022-5

Velasco, Roser, & Bruna, J. (2015). Taxane-induced peripheral neurotoxicity. In *Toxics* (Vol. 3,

Issue 2, pp. 152–169). https://doi.org/10.3390/toxics3020152

Vichaya, E. G., Chiu, G. S., Krukowski, K., Lacourt, T. E., Kavelaars, A., Dantzer, R., Heijnen, C. J., & Walker, A. K. (2015). Mechanisms of chemotherapy-induced behavioral toxicities. In *Frontiers in Neuroscience* (Vol. 9, Issue APR). https://doi.org/10.3389/fnins.2015.00131

Vladimer, G. I., Marty-Roix, R., Ghosh, S., Weng, D., & Lien, E. (2013). Inflammasomes and host defenses against bacterial infections. In *Current Opinion in Microbiology* (Vol. 16, Issue 1). https://doi.org/10.1016/j.mib.2012.11.008

Voet, S., Srinivasan, S., Lamkanfi, M., & Loo, G. (2019). Inflammasomes in neuroinflammatory and neurodegenerative diseases. *EMBO Molecular Medicine*, *11*(6). https://doi.org/10.15252/emmm.201810248

Wahlman, C., Doyle, T. M., Little, J. W., Luongo, L., Janes, K., Chen, Z., Esposito, E., Tosh, D. K., Cuzzocre, S., Jacobson, K. A., & Salvemini, D. (2018). Chemotherapy-induced pain is promoted by enhanced spinal adenosine kinase levels through astrocyte-dependent mechanisms. *Pain*, *159*(6). https://doi.org/10.1097/j.pain.0000000000001177

Wang, Li, & Hauenstein, A. V. (2020). The NLRP3 inflammasome: Mechanism of action, role in disease and therapies. In *Molecular Aspects of Medicine* (Vol. 76). https://doi.org/10.1016/j.mam.2020.100889

Wang, Luqiao, Fu, H., Nanayakkara, G., Li, Y., Shao, Y., Johnson, C., Cheng, J., Yang, W. Y., Yang, F., Lavallee, M., Xu, Y., Cheng, X., Xi, H., Yi, J., Yu, J., Choi, E. T., Wang, H., & Yang, X. (2016). Novel extracellular and nuclear caspase-1 and inflammasomes propagate inflammation and regulate gene expression: a comprehensive database mining study. *Journal of Hematology and Oncology*, *9*(1). https://doi.org/10.1186/s13045-016-0351-5

Wang, X., Loram, L. C., Ramos, K., De Jesus, A. J., Thomas, J., Cheng, K., Reddy, A., Somogyi,

A. A., Hutchinson, M. R., Watkins, L. R., & Yin, H. (2012). Morphine activates neuroinflammation in a manner parallel to endotoxin. *Proceedings of the National Academy of Sciences of the United States of America*, *109*(16), 6325–6330. https://doi.org/10.1073/pnas.1200130109

Wang, X. M., Lehky, T. J., Brell, J. M., & Dorsey, S. G. (2012). Discovering cytokines as targets for chemotherapy-induced painful peripheral neuropathy. In *Cytokine* (Vol. 59, Issue 1). https://doi.org/10.1016/j.cyto.2012.03.027

Warncke, U. O., Toma, W., Meade, J. A., Park, A. J., Thompson, D. C., Caillaud, M., Bigbee, J. W., Bryant, C. D., & Damaj, M. I. (2021). Impact of Dose, Sex, and Strain on Oxaliplatin-Induced Peripheral Neuropathy in Mice. *Frontiers in Pain Research*, *2*. https://doi.org/10.3389/fpain.2021.683168

Warwick, R. A., & Hanani, M. (2013). The contribution of satellite glial cells to chemotherapy-induced neuropathic pain. *European Journal of Pain (United Kingdom)*, *17*(4). https://doi.org/10.1002/j.1532-2149.2012.00219.x

Watanabe, H., Numata, K., Ito, T., Takagi, K., & Matsukawa, A. (2004). Innate immune response in Th1- and Th2-dominant mouse strains. *Shock*, *22*(5), 460–466. https://doi.org/10.1097/01.shk.0000142249.08135.e9

Watkins, L. R., Milligan, E. D., & Maier, S. F. (2001). Glial activation: A driving force for pathological pain. In *Trends in Neurosciences* (Vol. 24, Issue 8). https://doi.org/10.1016/S0166-2236(00)01854-3

Williams, L. S., Jones, W. J., Shen, J., Robinson, R. L., Weinberger, M., & Kroenke, K. (2003). Prevalence and impact of depression and pain in neurology outpatients. *Journal of Neurology, Neurosurgery and Psychiatry*, *74*(11), 1587–1589.

https://doi.org/10.1136/jnnp.74.11.1587

Willner, P., Muscat, R., & Papp, M. (1992). Chronic mild stress-induced anhedonia: A realistic animal model of depression. *Neuroscience and Biobehavioral Reviews*, *16*(4), 525–534. https://doi.org/10.1016/S0149-7634(05)80194-0

World Health Organization. (2017). WHO Model List of Essential Medicines: 20th list. *WHO Medicines*, *March*.

Wotton, J. M., Peterson, E., Anderson, L., Murray, S. A., Braun, R. E., Chesler, E. J., White, J. K., & Kumar, V. (2020). Machine learning-based automated phenotyping of inflammatory nocifensive behavior in mice. *Molecular Pain*, *16*, 1–16. https://doi.org/10.1177/1744806920958596

Wozniak, K. M., Nomoto, K., Lapidus, R. G., Wu, Y., Carozzi, V., Cavaletti, G., Hayakawa, K., Hosokawa, S., Towle, M. J., Littlefield, B. A., & Slusher, B. S. (2011). Comparison of neuropathy-inducing effects of eribulin mesylate, paclitaxel, and ixabepilone in mice. *Cancer Research*, *71*(11), 3952–3962. https://doi.org/10.1158/0008-5472.CAN-10-4184

Wozniak, K. M., Vornov, J. J., Wu, Y., Nomoto, K., Littlefield, B. A., DesJardins, C., Yu, Y., Lai, G., Reyderman, L., Wong, N., & Slusher, B. S. (2016). Sustained accumulation of microtubule-binding chemotherapy drugs in the peripheral nervous system: Correlations with time course and neurotoxic severity. *Cancer Research*, *76*(11), 3332–3339. https://doi.org/10.1158/0008-5472.CAN-15-2525

Xiao, W. H., Zheng, H., Zheng, F. Y., Nuydens, R., Meert, T. F., & Bennett, G. J. (2011). Mitochondrial abnormality in sensory, but not motor, axons in paclitaxel-evoked painful peripheral neuropathy in the rat. *Neuroscience*, *199*. https://doi.org/10.1016/j.neuroscience.2011.10.010

Xiao, Wen Hua, & Bennett, G. J. (2012). Effects of mitochondrial poisons on the neuropathic pain produced by the chemotherapeutic agents, paclitaxel and oxaliplatin. *Pain*, *153*(3), 704–709. https://doi.org/10.1016/j.pain.2011.12.011

Yamamoto, S., & Egashira, N. (2021). Drug Repositioning for the Prevention and Treatment of Chemotherapy-Induced Peripheral Neuropathy: A Mechanism- and Screening-Based Strategy. In *Frontiers in Pharmacology* (Vol. 11). https://doi.org/10.3389/fphar.2020.607780

Yamamoto, S., Ushio, S., Egashira, N., Kawashiri, T., Mitsuyasu, S., Higuchi, H., Ozawa, N., Masuguchi, K., Ono, Y., & Masuda, S. (2017). Excessive spinal glutamate transmission is involved in oxaliplatin-induced mechanical allodynia: A possibility for riluzole as a prophylactic drug. *Scientific Reports*, *7*(1). https://doi.org/10.1038/s41598-017-08891-1

Yan, X., Maixner, D. W., Yadav, R., Gao, M., Li, P., Bartlett, M. G., & Weng, H. R. (2015). Paclitaxel Induces Acute Pain via Directly Activating Toll like Receptor 4. *Molecular Pain*, *11*. https://doi.org/10.1186/s12990-015-0005-6

Yang, J., Liu, Z., Wang, C., Yang, R., Rathkey, J. K., Pinkard, O. W., Shi, W., Chen, Y., Dubyak, G. R., Abbott, D. W., & Xiao, T. S. (2018). Mechanism of gasdermin D recognition by inflammatory caspases and their inhibition by a gasdermin D-derived peptide inhibitor. *Proceedings of the National Academy of Sciences of the United States of America*, *115*(26). https://doi.org/10.1073/pnas.1800562115

Ye, Z., & Ting, J. P. Y. (2008). NLR, the nucleotide-binding domain leucine-rich repeat containing gene family. In *Current Opinion in Immunology* (Vol. 20, Issue 1). https://doi.org/10.1016/j.coi.2008.01.003

Yoshida, S., Hagiwara, Y., Tsuchiya, M., Shinoda, M., Koide, M., Hatakeyama, H.,

Chaweewannakorn, C., Suzuki, K., Yano, T., Sogi, Y., Itaya, N., Sekiguchi, T., Yabe, Y., Sasaki, K., Kanzaki, M., & Itoi, E. (2019). Involvement of inflammasome activation via elevation of uric acid level in nociception in a mouse model of muscle pain. *Molecular Pain*, *15*. https://doi.org/10.1177/1744806919858797

Youm, Y. H., Nguyen, K. Y., Grant, R. W., Goldberg, E. L., Bodogai, M., Kim, D., D'Agostino, D., Planavsky, N., Lupfer, C., Kanneganti, T. D., Kang, S., Horvath, T. L., Fahmy, T. M., Crawford, P. A., Biragyn, A., Alnemri, E., & Dixit, V. D. (2015). The ketone metabolite β-hydroxybutyrate blocks NLRP3 inflammasome-mediated inflammatory disease. *Nature Medicine*, *21*(3). https://doi.org/10.1038/nm.3804

Yvon, A. M. C., Wadsworth, P., & Jordan, M. A. (1999). Taxol suppresses dynamics of individual microtubules in living human tumor cells. *Molecular Biology of the Cell*, *10*(4). https://doi.org/10.1091/mbc.10.4.947

Zajaczkowską, R., Kocot-Kępska, M., Leppert, W., Wrzosek, A., Mika, J., & Wordliczek, J. (2019). Mechanisms of chemotherapy-induced peripheral neuropathy. In *International Journal of Molecular Sciences* (Vol. 20, Issue 6). MDPI AG. https://doi.org/10.3390/ijms20061451

Zeng, Q. zhen, Yang, F., Li, C. guang, Xu, L. hui, He, X. hui, Mai, F. yi, Zeng, C. ying, Zhang, C. cheng, Zha, Q. bing, & Ouyang, D. yun. (2019). Paclitaxel enhances the innate immunity by promoting NLRP3 inflammasome activation in macrophages. *Frontiers in Immunology*, *10*(JAN). https://doi.org/10.3389/fimmu.2019.00072

Zhang, D., Yang, R., Wang, S., & Dong, Z. (2014). Paclitaxel: New uses for an old drug. *Drug Design, Development and Therapy*, *8*. https://doi.org/10.2147/DDDT.S56801

Zhang, H., Boyette-Davis, J. A., Kosturakis, A. K., Li, Y., Yoon, S. Y., Walters, E. T., &

Dougherty, P. M. (2013). Induction of monocyte chemoattractant protein-1 (mcp-1) and its receptor ccr2 in primary sensory neurons contributes to paclitaxel-induced peripheral neuropathy. *Journal of Pain*, *14*(10), 1031–1044. https://doi.org/10.1016/j.jpain.2013.03.012

Zheng, H., Xiao, W. H., & Bennett, G. J. (2012). Mitotoxicity and bortezomib-induced chronic painful peripheral neuropathy. *Experimental Neurology*, *238*(2), 225–234. https://doi.org/10.1016/j.expneurol.2012.08.023

Zheng, Huaien, Xiao, W. H., & Bennett, G. J. (2011). Functional deficits in peripheral nerve mitochondria in rats with paclitaxel- and oxaliplatin-evoked painful peripheral neuropathy. *Experimental Neurology*, *232*(2). https://doi.org/10.1016/j.expneurol.2011.08.016

Zhou, R., Yazdi, A. S., Menu, P., & Tschopp, J. (2011). A role for mitochondria in NLRP3 inflammasome activation. *Nature*, *469*(7329). https://doi.org/10.1038/nature09663

Zhou, X., Huang, Z., Zhang, J., Chen, J. L., Yao, P. W., Mai, C. L., Mai, J. Z., Zhang, H., & Liu, X. G. (2020). Chronic Oral Administration of Magnesium-L-Threonate Prevents Oxaliplatin-Induced Memory and Emotional Deficits by Normalization of TNF-α/NF-κB Signaling in Rats. *Neuroscience Bulletin*, *37*, 55–69. https://doi.org/10.1007/s12264-020-00563-x

Zimmermann, K., Deuis, J. R., Inserra, M. C., Collins, L. S., Namer, B., Cabot, P. J., Reeh, P. W., Lewis, R. J., & Vetter, I. (2013). Analgesic treatment of ciguatoxin-induced cold allodynia. *Pain*, *154*(10). https://doi.org/10.1016/j.pain.2013.06.015

VITA

Urszula “Ula” Osińska Warncke was born and raised in small town, Ciechanowiec, Poland. She came to the United State of America after finishing high school in 2006 as an Au Pair in a cultural exchange program. In 2010, Ula received an Associate of Art from Sinclair Community College in 2010 and completed a Bachelor’s Degree in Biology at Wright State University in 2012, in Dayton, Ohio. In 2013, she started a Master’s Degree in Biochemistry and Molecular Biology at Wright State University, Dayton Ohio, and completed it in 2015. Ula enrolled in the Clinical and Translational Sciences, Concentration in Cancer and Molecular Medicine Doctoral Program at Virginia Commonwealth University in August 2015. She was the first person in her family to receive a college degree.

CURICULUM VITA

URSZULA OSINSKA WARNCKE
ULAOSINSKA@HOTMAIL.COM

Ph.D. in Clinical and Translational Siences with over 11 years of experience in independent bench work, 9 publications, posters at two national meetings. Open to new challenges and opportunities. Enthusiastic willingness to learn.

- Molecular Techniques
- Teaching/Mentoring
- Interpersonal Skills
- Teambuilding
- Project Management
- Organizational Skills
- Problem Solving
- Data Analysis & Presentation
- Microsoft Office
- GraphPad Prism Statistical Analysis
- Experimental Design
- Protocol Optimization

ACADEMIC/ PROFESSIONAL WORK EXPERIENCE

Bioanalytical Scientist 1, May 2021 – Present
Meso Scale Diagnostics LLC, Rockville, MD

- Plan and oversee experiments performed in the bioanalytical laboratory utilizing appropriate protocols
- Ensure resources (reagents, materials, equipment) are available and appropriate for intended use by lab personnel
- Review documentation associated with executed projects including data capture, forms logbooks, and inventory batch records
- Writing and executing analytical method validation
- Assist team members with interpreting results and troubleshooting technical issues
- Verify the accuracy and validity of data; correct errors
- Ensure that out-of-specification results or deviations from protocol are properly documented
- Present laboratory management with summaries of troubleshooting efforts and conclusions
- Direct efforts supporting qualification of materials and lot concordance, lot bridging studies, and transfer of newly developed assays/platforms for routine testing in a regulated environment
- Ensure that general lab maintenance initiatives are being performed and meet documented requirements
- Verify electronic inventory databases, physical inventory and records of processing/aliquoting/vialing/labeling materials are accurate and up-to-date
- Utilize self-reliance in understanding and adhering to laboratory safety precautions and proper use of personal protective equipment
- Handling BSL-2 samples and working in a Biological Safety Cabinet
- Responsible for supporting, mentoring and documenting performance evaluation of supervisee
- Responsible for training and development of laboratory personnel

Research Assistant, February 2018 – May 2021
Virginia Commonwealth University, Richmond, VA

- Lab Maintenance and organization, proactive, results-oriented, self-motivated team player with growing leadership skill
- Overseeing lab safety and healthy environment by complying with safety policies and procedures
- Responsible for organizational communications with lab members, presenting data at lab meetings and conferences
- Reduced time needed to perform western blots implementing new methods and new equipment
- Established protocol for nerve conduction on mice
- Consultant on hiring and other staff related matters
- Performing behavioral testing on mice: mechanical hypersensitivity, anxiety behavior, depression-like behavior, cold sensitivity, motivation, tactile hyposensitivity, anhedonia
- Anesthesia and administration of intraperitoneal and subcutaneous injections
- Troubleshooting and optimization of immunohistochemistry techniques
- Designing, planning, and executing experiments
- Collaborating with lab members on their projects
- Characterization of chemotherapy-induced peripheral neuropathy (CIPN) in various nociceptive and affective pain-like behaviors in mouse model
- Molecular (western blot, qPCR, IHC) and behavioral analyses of NLRP3 inflammasomes molecular mechanism
- Optimization of protocols for immunohistochemical analysis of nervous tissue in rodent models of neuropathy

Research Assistant, October 2015 – March 2018
Virginia Commonwealth University, Richmond, VA

- Performed targeted and untargeted lipidomic analyses via Liquid Chromatography Mass Spectrometry: sample extraction, operation of a mass spectrometer, method troubleshooting and data analysis
- Created metabolomics pathways using Cytoscape and Inkscape
- Interpreted and analyzed quantitative and qualitative results
- Fast learner: in two weeks learned new software and produced publishable figures
- Developed new mass spectroscopy method for detecting presence of anticoagulants in blood with a 98% accuracy
- Contributed to development of mass spectroscopy method for detection of 50 commonly used medications for collaborative project on medication reconciliation
- Created a library of over 100 lipids and their metabolites and improved LC-MS/MS detection method for lipid analysis, design and development of analytical methods involving separation and analysis of biomolecules
- Beta-tested new LC-MS/MS method and system for SCIEX Instruments

Laboratory Assistant, September 2010 – June 2011
Wright State University, Dayton, OH

- Acknowledged and praised for practicing sterile laboratory techniques, maintained cultures and made stocks of various cell types

- Harvested and cultured murine macrophages, extracted and purified DNA and RNA, performed gel electrophoresis
- Contributed to publication of Kaitsuka T, Katagiri C, Beesetty P, Nakamura K, Hourani S, Tomizawa K, Kozak JA, Matsushita M. *Inactivation of TRPM7 kinase activity does not impair its channel function in mice*. Sci Rep. (2014)

Administrative Assistant, February 2012- April 2013, July 2014- July 2015
Bellbrook Family Practice**,** Centerville, OH

- Maintained patient accounts by obtaining, recording, and updating personal and financial information
- Coordinated appointment schedules and answer incoming calls from patients, hospital, and other third-party medical facilities
- Helped implement new patient medical records system

State Certified Nurse Aide, September 2010– February 2012
Bethany Lutheran Village**,** Dayton, OH

- Assisted with direct patient care and daily activities
- Promptly responded, within scope, to needs and concerns of residents and family members including call lights
- Ensured residents' comfort while assisting them in achieving their highest practicable level of functioning and privacy

EDUCATION

Doctor of Philosophy in Clinical and Translational Sciences, August 2022
Concentration in Cancer and Molecular Medicine
Virginia Commonwealth University, Richmond, VA, GPA 3.54
Dissertation Title: The Role of NLRP3 Inflammasome in Mouse Models of Chemotherapy-Induced Peripheral Neuropathy

Master of Science in Biochemistry and Molecular Biology, August 2015
Wright State University, Dayton, OH, GPA 3.8
Thesis: Profiling Fatty Acid Composition of Brown Adipose Tissue, White Adipose Tissues and Bone Marrow Adipose of Healthy and Diet-Induced Obese Mice
Profiling composition of adipose tissues of mice via [1H], [13C], and [31P] NMR analyses of lipid and aqueous extracts.

Bachelor of Science in Biology, May 2012
Wright State University, Dayton, OH, GPA 3.3

Associate of Arts in Science, May 2010
Sinclair Community College, Dayton, OH, GPA 3.7

AWARDS/HONORS

- Travel award: Chemistry and Pharmacology of Drug Abuse conference, Northeastern University, Boston, MA (2018)
- Undergraduate Research Support Grant, Wright State University, Dayton, OH (2011)

- Awarded a $2,000 Rike Transfer Student Scholarship for completing a two-year associate degree with a GPA higher than 3.5, Wright State University, Dayton, OH (2010, 2011)

SCIENTIFIC OUTREACH ACTIVITIES

- *Girl Scout Science Day*, Virginia Commonwealth University, Richmond, VA (2018, 2019)
- *Christ Chapel Academy field trip.* Hosted a group of high school students, gave a tour of laboratory, coordinated scientific demonstrations with lab mates. Richmond, VA (March 2019)
- *STEM Fair.* Helped with organization and demonstrated scientific experiments to students and parents. *St.* Francis Elementary School Richmond, VA (2018)
- *Liquid Chromatography Mass Spectrometry*. Taught new LC-MS/MS techniques and methods to post-doctoral fellows in laboratory of Professor Nancy Denslow, Universioty of Florida, Gainesville, FL (2017, 2018)
- *The Math Science Innovation Center (MSiC) Richmond Metro STEM fair*. Judged Junior Division Medicine and Health projects. Richmond, VA (2017)

PUBLICATIONS

Toma W, Paris JJ, **Warncke UO**, Nass SR, Caillaud M, Bigbee JW, Knapp PE, Hauser KF, Damaj MI. Persistent Sensory Changes and Sex Differences in Transgenic Mice Conditionally Expressing HIC-1Tat Regulatory Protein. *In Preparation*

Warncke UO, Toma WB, Meade JA, Park AJ, Thompson DC, Caillaud M, Bigbee JW, Bryant CD, M. Damaj MI. Impact of Dose, Sex, and Strain on Oxaliplatin-Induced Peripheral Neuropathy in Mice. Frontiers in Pain Research, 2021.683168

Meade JA, Fowlkes AN, Wood MJ, Kurtz MC, May MM, Toma WT, Warncke UO, jared Mann J, Mustafa M, Lichtman AH, Damaj MI. Effects of Chemotherapy on Operant Responding for Palatable Food in Male and Female Mice. Behav Pharmacol. 2021;32(5):422-434.

Caillaud M, Aung Myo YP, McKiver BD, Warncke UO, Thompson D, Mann J, Del Fabbro E, Desmoulière A, Billet F, Damaj MI. Key Developments in the Potential of Curcumin for the Treatment of Peripheral Neuropathies. Antioxidants (Basel). 2020 Oct 2;9(10).

Amraoui F, Hassani Lahsinoui H, Spijkers LJA, Vogt L, Peters SLM, Wijesinghe DS, **Warncke UO**, Chalfant CE, Ris-Stalpers C, van den Born BH, Afink GB. Plasma ceramide is increased and associated with proteinuria in women with pre-eclampsia and HELLP syndrome. Pregnancy Hypertens. 2020 Jan;19:100-105.

Jayaraman SP, Anand RJ, DeAntonio JH, Mangino M, Aboutanos MB, Kasirajan V, Ivatury RR, Valadka AB, Glushakova O, Hayes RL, Bachmann LM, Brophy GM, Contaifer D, **Warncke UO**, Brophy DF, Wijesinghe DS. Metabolomics and Precision Medicine in Trauma: The State of the Field. Shock. 2018 Jul;50(1):5-13.

Mohammed BM, Sanford KW, Fisher BJ, Martin EJ, Contaifer D Jr, **Warncke UO**, Wijesinghe DS, Chalfant CE, Brophy DF, Fowler Iii AA, Natarajan R. Impact of high dose vitamin C on platelet function. World J Crit Care Med. 2017 Feb 4;6(1):37-47.

Contaifer D Jr, Carl DE, **Warncke UO**, Martin EJ, Mohammed BM, Van Tassell B, Brophy DF, Chalfant CE, Wijesinghe DS. Unsupervised analysis of combined lipid and coagulation data reveals coagulopathy subtypes among dialysis patients. J Lipid Res. 2017 Mar;58(3):586-599.

Wijesinghe DS, **Warncke UO**, Diegelmann RF. Human as the Ultimate Wound Healing Model: Strategies for Studies Investigating the Dermal Lipidome. Curr Dermatol Rep. 2016 Dec;5(4):244-251.

Asgharpour A, Cazanave SC, Pacana T, Seneshaw M, Vincent R, Banini BA, Kumar DP, Daita K, Min HK, Mirshahi F, Bedossa P, Sun X, Hoshida Y, Koduru SV, Contaifer D Jr, **Warncke UO**, Wijesinghe DS, Sanyal AJ. A diet-induced animal model of non-alcoholic fatty liver disease and hepatocellular cancer. J Hepatol. 2016 Sep;65(3):579-88.

POSTER PRESENTATION AND CONFERENCES

NIH Workshop: A Critical Evaluation of Animal Pain Models. January 30-31,2019. National Institutes of Health (NIH), Bethesda, MD.

U. O. Warncke, W. Toma, S. L. Kyte, T. Tran, D.A. Gewirtz S. Zhang, P-L Li1, and M.I. Damaj "NLRP3 Inflammasome ss a Target for the Treatment of Chemotherapy-Induced Peripheral Neuropathy (CIPN): Studies in Animal Models", Chemistry and Pharmacology of Drug Abuse, Boston, MA (2018)

U. O. Warncke, D. Contaifer Jr., M. A. Peberdy, D. S. Wijesinghe. "Determination of Metabolomic Profile Changes for Prediction of Mortality in Cardiac Arrest Patients After Induced Hypothermia", ASMS Conference on Mass Spectrometry and Allied Topics, Indianapolis, IN (2017)

K. Amarasinghe, **U. O. Warncke**, M. Manic, D. S. Wijesinghe, "Artificial Neural Networks Based Visual Data Mining for Clinical and Metabolomic Data", ASMS Conference on Mass Spectrometry and Allied Topics, Indianapolis, IN (2017)

Spectrometry and Allied Topics, Indianapolis, IN (2017)